SIEMENS Healthineers

Imaging Life

Your Resource for Molecular Imaging Innovation

Issue 11 | siemens.com/imaginglife

Follow us!

@SiemensHealth

#ImagingLife

Big differences start small… together, as technology providers and care providers, we can all contribute to the advancement and growth of molecular imaging.

Mario Zeiss
Vice President
Global Marketing and Sales
Molecular Imaging
Siemens Healthcare

Dear Reader,

In healthcare, it is often the smallest details that create the greatest value over time. This is no more apparent than when I talk with our customers and walk through our factories. I see our teams taking your input and designing it into our technologies, growing detector crystals, building collimators, and assembling and testing our scanners—each conversation, idea, person and process adds up to a greater whole.

We are the only molecular imaging company that owns the entire value chain. Every step in our development and manufacturing process is managed in-house to ensure we deliver quality and performance without compromise. This approach also gives us the ability to adapt and innovate based on your needs, so you can continue setting new standards in healthcare delivery and improving patient outcomes.

Our collaboration and dialogue with you is an essential component of the ongoing evolution of this value chain. With your input, we are better. Your work inspires our innovation, and our innovation contributes to your inspiring work.

As you read this issue of *Imaging Life*, you will see healthcare providers, physicians and researchers who leverage our technology and their expertise to go beyond best practices and establish new ones. You will see how an improved image can lead to an earlier diagnosis. An earlier diagnosis can lead to more effective treatment strategies. And effective treatment strategies can lead to the best possible patient care.

Big differences start small. And working together, as technology providers and care providers, we can all contribute to the advancement and growth of molecular imaging.

Enjoy reading,

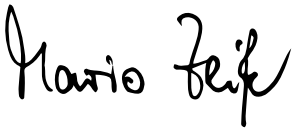

Mario Zeiss
Vice President, Global Marketing and Sales
Molecular Imaging, Siemens Healthcare

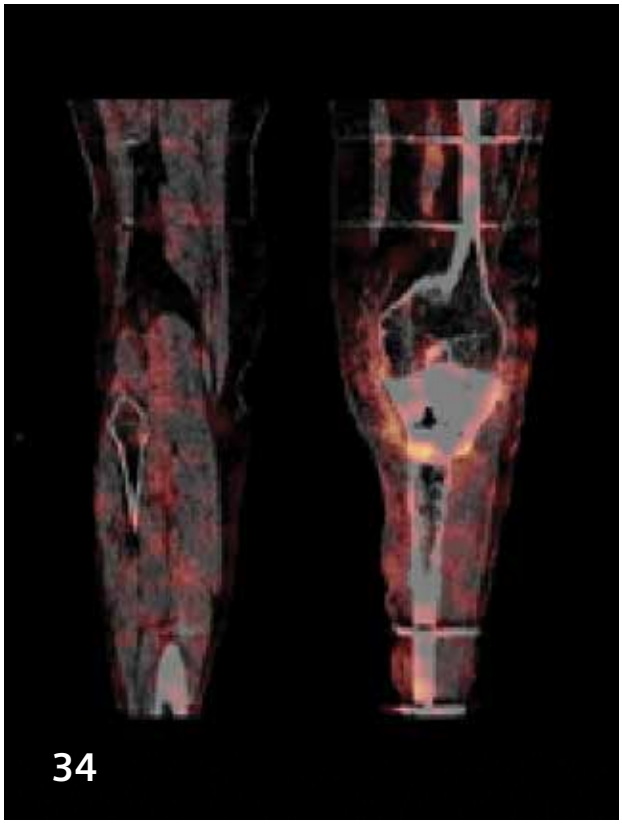

Table of Contents

Features

Outcomes

Science

Clinical Results

Two Imaging Specialists Join Forces for Better Patient Management

After spending time at Vienna University Hospital's nuclear medicine department in Austria, radiologist Philipp Peloschek, MD, realized many pathologies are simply invisible to radiology. In 2014, he teamed up with nuclear medicine specialist Martha Hoffmann, MD, to establish the private Radiology Center next door to the university. Together, the two successfully deliver a full spectrum of diagnostic imaging services. And their collaborative approach to patient management offers a glimpse into what the future of imaging could be.

By Philipp Grätzel von Grätz

Doctors who have spent years of their working life at a university hospital often experience an unexpected amount of solitude when they decide to go private. "In the university setting, we are trained to discuss every image we acquire with our colleagues. There is always interaction, and you learn new things every day," said Philipp Peloschek, MD, radiologist by training and a specialist in bone imaging on CT and MRI. Once in a private practice, this much-valued interaction often diminishes. "This is something I absolutely wanted to avoid. And that's why we decided, in 2014, to build the Radiology Center in direct proximity to the referring doctors."

The Radiology Center in Vienna is not only close to several private clinics with surgeons, oncologists and cardiologists in constant need of state-of-the-art imaging. It also has a distinct architecture: Upon entering, the Radiology Center feels bright and open, with the imaging workstations located right in the middle of the facility, surrounded by glass, rather than locked away in dark rooms—a set-up that suggests a clear intention to interact. And it works: "This is really the imaging center I had always dreamt of," said Peloschek. "The location is ideal. The referring physicians come over to discuss the images. We get feedback on which therapies are chosen and whether they are successful. It is great."

The Additional Benefit of Molecular Imaging

The main business partner of the Radiology Center is the Vienna Private Clinic (Wiener Privatklinik) located next door. Apart from its collaborative philosophy, another notable difference about the Radiology Center is that it is not only about radiology, but also nuclear medicine. This is where Martha Hoffmann, MD, comes into play, a nuclear medicine specialist with extensive experience in the field of oncological molecular imaging. She is medical director of the molecular imaging facility, and as such, respon-sible for the first-ever PET/CT owned by a private imaging center in Austria, a Biograph™ PET/CT* system. But they are also intrigued by the utility and future potential of their Symbia™ SPECT/CT*.

That a radiologist and a nuclear medicine specialist join forces in this way remains uncommon in the imaging world. But it makes perfect sense, said Hoffmann: "Our position is at the end of the diagnostic pathway. Referring doctors expect us to make precise interpretations, and by combining our expertise, we can give very straight-forward recommendations most of the time." The experts also advise referring doctors on which imaging modality is best used in certain cases, another reason why the Radiology Center established itself so quickly: "Virtually from day one, we've had a high volume of patients. We accomplished this without any advertising or other gimmicks. We simply offer good medicine."

Good medicine can take time. Peloschek and Hoffmann regularly discuss a case for 15 to 20 minutes before they close it: "Sometimes the morphological findings don't align with the molecular findings, and then we have to sort that out," said Peloschek.

"Referring doctors expect us to make precise interpretations, and by combining our expertise [radiology and nuclear medicine], we can give very straight-forward recommendations..."

Martha Hoffmann, MD
Nuclear Medicine Specialist
Radiology Center, Vienna, Austria

Complementing each other's specialties, radiologist Philip Peloscheck, MD, and Martha Hoffman, MD, a nuclear medicine specialist, discuss cases performed on the Radiology Center's hybrid scanners.

"We could help more patients if SPECT/CT was used more broadly in oncology and if more oncological SPECT tracers were available."

Philipp Peloschek, MD
Radiology Specialist
Radiology Center, Vienna, Austria

Although he comes from radiology, Peloschek is impressed by what molecular imaging can offer on top of the morphological information that comes through conventional radiology, CT and MRI: "I was lucky enough to spend time in the nuclear medicine department at Vienna University Hospital, and I realized that many pathologies are simply invisible to radiologists. True, we can increasingly depict molecular features with MRI, too. Metabolic imaging has been scientifically proven for decades, and you don't need a 3 or 7 Tesla MRI machine."

A Powerful Tool for Lower Back Pain Patients

As a specialist in musculoskeletal imaging, Peloschek continues to be amazed at how molecular imaging can add to radiological bone imaging. Patients with chronic lower back pain or patients after spine fusion surgery can benefit greatly from molecular imaging," he said. "In such a patient, MRI might show some distorted nerves, but no real compression. There might be some inflammation in the intervertebral discs, and some sign of edema in the small vertebral joints."

These findings are all real, but often it is not specific enough. SPECT/CT, in contrary, might show that there is increased metabolic activity in a clearly defined region of a specific intervertebral disc, or it might hint to increased osteoplastic activity in one of several somewhat inflamed small intervertebral joints. "SPECT/CT tells us exactly which joint has to be treated by the interventional radiologist, and this will lead to good therapy results for the patient in the end. SPECT/CT in chronic lower back pain is a powerful method to find the source of the problem."

Older patients with peripheral bone problems are good candidates for SPECT/CT too, for example diabetics with suspected osteomyelitis or patients with pain after the implantation of an orthopedic prosthesis. "As a radiologist I know that MRI is a great modality for these patients, and we use it regularly, of course. But the signs of altered bone metabolism that we see on MRI sometimes don't tell the whole story. And there are also less movement artifacts on SPECT/CT," said Peloschek. He recalled an elderly diabetic patient with a cardiac pacemaker with pain in the forefoot. SPECT/CT depicted an osteomyelitis in the distal phalange of one of the toes. "We saw it

glowing. It was really fascinating. And for the patient, this was important news because we were able to tell the surgeon exactly where the problem was. He knew immediately what he had to do to help this patient."

Another Work-horse for Oncology Imaging?

Apart from patients with musculoskeletal diseases, patients with oncological diseases are the second largest group of customers who keep the PET/CT and SPECT/CT systems of the Radiology Center busy. The majority of PET/CT cases, in particular, are in oncology, explained Hoffmann: "Lung cancer staging prior to surgery is a big area, and diagnostic lung cancer imaging in patients with suspicious nodules. We also regularly examine patients with lymphoma, melanoma, and colorectal or esophageal carcinoma."

SPECT/CT is also regularly used for oncology at the Radiology Center, and not only for bone, thyroid, and cardiac ischemia imaging. Since the PET tracer ^{68}Ga-DOTATOC** is not readily available in Austria, Hoffmann and Peloschek perform ^{99m}Tc-labelled octreotide** SPECT/CT studies in patients with neuroendocrine tumors. "I was surprised by the quality of this method."

Peloschek agreed: "The images are fantastic. You can clearly see a 3 mm lymph node right under the diaphragm. It is really impressive."

Hoffmann and Peloschek see a need for many more SPECT tracers and predict that SPECT/CT will have a bright future in oncology. "SPECT/CT is flexible. It has a low price point, which makes it more accessible," said Hoffmann. While she agrees that PET/CT is recognized as the high-end method for molecular oncological imaging, she is convinced that having more SPECT/CTs and oncological SPECT tracers would markedly improve the access to molecular imaging for many oncological patients.

"We satisfied our controller"

Looking back at two years of their "radiology meets nuclear medicine" joint venture, both Peloschek and Hoffmann say it was worth all the effort. They not only receive excellent feedback from their colleagues on the quality of their diagnostics, but have also managed to perform financially: "After the first full year, our external controller was satisfied," Peloschek smiled.

The use of multi-modality imaging equipment had its share in this success. "We have a lot of imaging hardware, but we don't have a CT system. We do all of our routine CTs on either the SPECT/CT or the PET/CT," explained the radiologist. This has several advantages. It saves space, as there is no need for an additional exam room and the associated radiation shielding. "It is inefficient to buy imaging technology that can only perform one kind of examination. Our SPECT/CT is very cost efficient."

Although there is no separate CT system at the Radiology Center, Peloschek said that thanks to the Siemens PET/CT and SPECT/CT scanners, he is not compromising on the quality of CT diagnostics. "Our scanners have full diagnostic CT capabilities. This makes the systems the ideal choice not only for a nuclear medicine specialist, but also for a radiologist." ■

Philipp Grätzel von Grätz is a medical doctor turned freelance writer and book author based in Berlin, Germany. His focus is on biomedicine, medical technology, health IT, and health policy.

* The products mentioned herein are not commercially available in all countries. Due to regulatory reasons, their future availability cannot be guaranteed. Please contact your local Siemens organization for further details.

** ^{68}Ga-DOTATOC and ^{99m}Tc-labelled octreotide referenced herein are not currently recognized by the US FDA as being safe and effective, and Siemens does not make any claims regarding its use.

The statements by Siemens customers described herein are based on results that were achieved in the customer's unique setting. Since there is no "typical" hospital and many variables exist (e.g., hospital size, case mix, level of IT adoption), there can be no guarantee that other customers will achieve the same results.

Mobilizing the Standard of Care

Alliance HealthCare Services is the first provider to deploy the Biograph mCT Flow™* PET/CT scanner in mobile units. Rich Jones, President of Alliance HealthCare Radiology, and Dale Hockel, Chief Operating Officer, talk about their experience.

By Martin Suter

Rich Jones, President
Alliance HealthCare Radiology

Alliance HealthCare Radiology is a leading provider of radiology services to over 1,000 hospitals and clinics in the US. Can you tell us about the volume of your radiology business?

Rich Jones: With revenue of 350 million US dollars, Alliance HealthCare Radiology is the largest division of Alliance HealthCare Services. We perform roughly 50,000 radiology procedures a month. Our customers are spread pretty evenly across the country. We own and operate nearly 500 MRI, CT and PET/CT scanners, most of which are mobile on trucks.

Why do hospitals and Integrated Delivery Networks (IDNs) choose mobile imaging services?

Rich Jones: Customers use supplemental services for a couple of reasons. One reason is to test a market where they want to develop new services. Another reason is to evaluate their full market capacity. We often start by testing the market with mobile services, and over time we transition our customer's business to a fixed location.

Some customers stay with mobile solutions—why?

Rich Jones: Many customers have only a handful of patients a week that fit the criteria, especially for PET/CT. So, the volume does not justify the burden of owning a full-time PET/CT scanner. In contrast, using assets one or two days a week to care for patients right at the hospital makes a lot of sense. It is very cost-effective for the hospital.

How big is your market share?

Rich Jones: We perform about ten percent of all PET/CT procedures in the US. We run a fleet of about 150 PET/CT units and operate twelve fixed PET/CT sites.

Are there any industry-wide trends pushing mobile solutions?

Rich Jones: A mobile solution aligns with many pressures hospitals face these days. Mobile solutions allow the hospital to offer their patients imaging exams in a timely and cost-effective manner, balanced with careful capital expenditure management.

What payment structures do you offer your customers?

Rich Jones: Payment structures can be fee-per-procedure, a monthly rate, a daily rate or even a joint venture arrangement. It all depends on the strategic needs of the hospital.

Logistically, what is the best use of the trucks?

Rich Jones: Trucks are assigned specific routes to go from one hospital to the next. They typically move at night and are set up and ready for the next day of service. Most of our mobile units are busy five to six days a week.

Do technologists travel with the trucks?

Rich Jones: Our technologists are based in the area where the service is provided. We ensure that we have the right technologist with the right license and experience to serve our clients.

Does access to the latest technology keep technologists at Alliance HealthCare Radiology?

Dale Hockel: Technologists are always interested in working with the latest technology. So that does help us from a recruiting standpoint. Shorter scan times allow technologists to move patients through quickly and avoid backlog, which is always a challenge in a large system.

How many mobile Biograph mCT Flow units does Alliance HealthCare Radiology have?

Rich Jones: Over the last quarter, we put four Biograph mCT Flow units into operation. We have another three on order that will be in operation by June 2016. So we will have seven Biograph mCT Flow trucks in operation with our large IDN clients. As far as I know, we are the only company currently using this system in a mobile capacity (March 2016).

What advantages are there to mobilizing Biograph mCT Flow?

Dale Hockel: Standardization of care was critical, especially for our IDN clients with multiple locations. Other reasons include patient comfort and controlling the dose of the radioactive tracers. Biograph mCT Flow offers low-dose options, which is where the market is headed. And the technology has been significantly easier for our technologists to use.

How would you describe your experience with Biograph mCT Flow so far?

Rich Jones: The feedback has been extremely positive from our clients as well as from our technologists using

Dale Hockel, Chief Operating Officer Alliance HealthCare Radiology

Three Ways Hospitals Incorporate Mobile PET/CT Services

As consolidation continues to take place, healthcare providers are incorporating mobile scanners to deliver cost-efficient, high-quality care across the entire network. In the experience of Alliance HealthCare Radiology, here are three benefits to using mobile PET/CT services.

Integrate new technology
Test the market with the latest technology to develop new services without a significant investment.

Operate based on true consumption
Provide operational capacities that meet the needs of a location's patient volume.

Provide standardized care
Balance the need to achieve a reliable, consistent level of quality patient outcomes with careful capital expenditure across the network.

the equipment. Patients appreciate the fast scan times. PET/CT patients often go through a very stressful time obtaining their diagnosis. It helps minimize the time required for imaging. The bore size is large, making exams easy for larger or bariatric patients.

What about the clinical feedback?

Rich Jones: From a clinical standpoint, we have seen increased accuracy compared to older imaging technologies with the high resolution feature. From an operational perspective, we have seen a significant improvement in scan time and image uniformity, compared to conventional step-and-shoot methods. Our technical teams are extremely happy with the exam quality.

How have the new trucks impacted the general perception of mobile scanners?

Dale Hockel: Historically, people have viewed mobile MRI and mobile PET/CT as lower-end services. Biograph mCT Flow, with the quality and the patient satisfaction that comes from that technology, will help us improve the perception.

How do you make mobile scanners more inviting for patients?

Rich Jones: We work with the hospital to ensure the surroundings are as calming as possible. Our teams do a phenomenal job of making the patients comfortable. As a company, we do patient surveys, and patient satisfaction runs at about 95 percent across the board nationally.

Healthcare consolidation is a big trend. How does this impact Alliance HealthCare Radiology?

Rich Jones: I think it has a positive impact. We currently operate in 45 states, and we provide a wide variety of services. Hospitals that consolidate can turn to us for solutions for their whole network, whether it is fixed multi-modality centers, mobile PET/CT, mobile MRI or even leasing an asset. For us, consolidation is an opportunity to do a good job for all these systems.

As organizations grow larger, do they consider providing these services themselves?

Rich Jones: We work with customers to take that on for them, because we have the infrastructure to do that. We can show that Alliance HealthCare Radiology can bring a lower cost-per-interaction than hospitals can do themselves, whether it is mobile or fixed. In particular, Biograph mCT Flow, if used correctly, ends up being a cost reducer. ■

Martin Suter is reporting about technology, healthcare, business and politics for various European publications. He is based in New York.

* Biograph mCT Flow is not commercially available in all countries. Due to regulatory reasons its future availability cannot be guaranteed. Please contact your local Siemens organization for further details.

The statements by Siemens customers described herein are based on results that were achieved in the customer's unique setting. Since there is no "typical" hospital and many variables exist (e.g., hospital size, case mix, level of IT adoption), there can be no guarantee that other customers will achieve the same results.

How to Get the Most from Advanced PET Scanners: Harmonizing Quantitative PET Data

Nicolas Aide, MD, PhD, a professor of nuclear medicine and nuclear medicine physician at Caen University Hospital and François Baclesse Cancer Centre, Caen, France, and colleagues* proved that PET data could be harmonized, regardless of the scanner generation or reconstruction method. Since then, his research has led to the creation of a software solution that automates harmonization across scanner manufacture and makes it practical in routine clinical use.

By Greg Freiherr

As technology advances, sensitivity increases. Under most circumstances, the net effect is positive—but not when making quantitative PET measurements to assess the effect of therapy.

With more sensitive detectors and advanced reconstruction techniques, the latest PET/CT systems make lesions easier to see, but they also produce higher standard uptake values (SUVs). The clinical meaning of these SUVs can be skewed by this improved technology.

This is especially so in oncology, where high SUVs typically correlate with tumor growth. If SUVs recorded on advanced PET/CTs are compared to those made on equipment of older design, clinicians may conclude that the cancer appears to have metabolic growth when, in fact, the higher values are due to the increased sensitivity of the machine measuring them.

This is where EQ•PET comes in.

"EQ•PET is an efficient tool to get rid of reconstruction variability in quantitative data."

Nicolas Aide, MD, PhD
Professor of Nuclear Medicine and Nuclear Medicine Physician
Caen University Hospital and François Baclesse Cancer Centre, Caen, France

EQ•PET software, developed by Siemens Healthcare and independently validated in clinical studies under a research grant, harmonizes quantitative measurements made on old- and new-generation scanners. The harmonized result is an accurate assessment of patient response to therapy determined by correctly comparing pre- and post-therapy quantitative PET measurements.

Clinical research, published in peer-reviewed journals, indicate that EQ•PET is valid across all types of solid tumors, regardless of tumor size, shape, or location in the body or in the field-of-view of the scanner, according to Nicolas Aide, MD, PhD, who spearheaded the research.

"By validating EQ•PET over a very large series of patients, and by focusing on several types of cancers, we have proved that it works and it works well," Aide said. "EQ•PET is an efficient tool to get rid of reconstruction variability in quantitative data."

Aide cautions, however, that while EQ•PET is very good at what it does, various sources of error can still skew the interpretation of SUVs. All who use this proprietary software should follow internationally accepted guidelines for the acquisition of PET data, he said.

"It is important to emphasize that this tool needs to be used within the framework of harmonization programs, which usually give the user all the steps needed to make standard uptake values as accurate as possible," he said.

If the sources of error are controlled and EQ•PET is correctly calibrated, the software is able to harmonize data obtained on equipment of different generations. This capability should be able to transcend not only the generation, but the make of the equipment. Thus far, however, clinical research performed by Aide has validated the software only on Siemens PET/CT scanners.

"We have validated the capability of EQ•PET to harmonize SUVs within different Siemens PET/CT systems," Aide said.

The ability to harmonize quantitative PET/CT data promises to impact the management of individual patient therapy; the worldwide use of PET/CT in therapy assessment; and the conduct of multi-center research projects aimed at determining either the utility of PET/CT or the effectiveness of cancer treatment. By harmonizing the quantitative data and leaving it intact, EQ•PET preserves the sensitivity of high-resolution PET/CT images.

"You get the best of the two worlds," he said. "You get the optimum diagnostic information from the image, because you have selected your reconstruction parameters to achieve the highest lesion detectability possible. And you get harmonized quantitative data [for comparison to previously obtained data]."

Harmonization using EQ•PET is remarkably accurate, according to Aide, who has compared the performance of this software to what can otherwise only be obtained through time-consuming means.

"When applying EQ•PET, the difference is less than 2 percent," he said.**

Getting as close to perfect is important, he said, because in oncology SUVs are often used to evaluate patient response to therapy. These SUVs are mapped against PERCIST (PET Response Criteria in Solid Tumors) thresholds. An increase of 30 percent or more above the PERCIST threshold suggests the therapy is not effective against the patient's solid tumor and should be changed. An SUV decline of 30 percent or more indicates the therapy is likely having a positive effect and should be continued.

Aide first proved that PET data could be harmonized three years ago. Using a NEMA (National Electrical Manufacturers Association) IEC PET Body phantom, he and his colleagues developed a mathematical formula that translated quantitative measurements obtained using different reconstruction algorithms into comparable data sets. They proved that this formula could be applied to evaluate data obtained during pre- and post-therapy evaluations of patients with non-small cell lung cancer.[1]

When preliminary data from the research was presented at a scientific meeting in 2013, it caught the eye of Jerome Declerck, PhD, who was a director of science and technology at Siemens Healthcare's molecular imaging business line at that time. Declerck, who is today a senior advisor for clinical innovations with the company, had been leading the development of software to harmonize PET quantitative data. The software was based on the same concept as the mathematical formula developed by Aide and his colleagues, but it was automated, turning what was essentially an academic exercise into a practical one.[2]

"Dr. Aide was the right partner for us because we understood what we both wanted to achieve, and our objectives were very much aligned," Declerck said. "We needed to extend the results obtained on a handful of in-house image data to a proper trial with a vast patient cohort."

Aide and his colleagues did exactly that over the coming two years, harmonizing data that covered a range of solid tumors, including breast cancer, non-small cell lung cancer, and melanoma and liver metastases from colorectal cancer. Aide chose these tumors because they are widely representative of the kinds of tumors seen in routine oncology.

"The idea was to validate EQ•PET across a very large series of lesions, covering all the locations that will be faced in real life," he said.

The researchers most recently validated EQ•PET in 517 oncology patients examined at multiple locations in France and Australia. The research harmonized data from 1380 lesions, using point-spread function (PSF); PSF plus Time-of-Flight (ToF); and an earlier reconstruction algorithm, called OSEM (ordered subsets expectation maximization).[3]

"We proved that you get the same results with EQ•PET when it is applied to each of these reconstruction methods," he said. "That means that EQ•PET

"Dr. Aide was the right partner for us because we understood what we both wanted to achieve, and our objectives were very much aligned."

Jerome Declerck, PhD
Senior Advisor for Clinical Innovations
Siemens Healthcare

can harmonize SUV data from new-generation and former-generation PET/CT systems."

Today EQ•PET is commercially available around the world as part of the multimodality oncology application built into *syngo*®.via*** for Molecular Imaging, a software platform designed for advanced data processing and communication.

Once calibrated, the lesion is outlined on the PET/CT image; the area clicked; and the data automatically harmonized with those indicated on an earlier scan. In this way, SUVs from baseline and post-treatment scans can be compared quickly and efficiently.

Calibration is relatively simple. It is achieved by first outlining a region of interest, such as a lung lesion in a baseline PET image. Next the region of interest in a post-treatment image is outlined. The appropriate filter is chosen from EQ•PET, and the software does the rest. From then on, data obtained using new and earlier generation PET scanners are automatically harmonized using the chosen filter, according to Declerck.

"Whenever a new patient comes in, and you want to compare old and new scan data, you don't have to reenter this filter," Declerck said. "EQ•PET will remember it."

Declerck describes a software that is becoming practical in routine use. Toward that end, according to Aide, EQ•PET is a fast, user-friendly and accurate method for harmonizing quantitative PET data. ■

References:

[1] Lasnon C, Desmonts C, Quak E, et.al. Harmonizing SUVs in multicentre trials when using different generation PET systems: prospective validation in non-small cell lung cancer patients. *Eur J Nucl Med Mol Imaging*. 2013 Jul;40(7):985-96.

[2] Kelly M, Declerck J. "SUVref: reducing reconstruction-dependent variation in PET SUV." *Eur J Nucl Med Mol Imaging Research*. 2011; 1(1):1-16.

[3] Quak E, Le Roux PY, Hofman MS, et. al. Harmonizing FDG PET quantification while maintaining optimal lesion detection: prospective multicentre validation in 517 oncology patients. *Eur J Nucl Med Mol Imaging*. 2015 Dec; 42(13):2072-82. http://link.springer.com/article/10.1007%2Fs00259-015-3128-0.

* In addition to the colleagues at Caen University Hospital and François Baclesse Cancer Centre in Caen, France, researchers who participated in the validation of EQ•PET software include Michael S. Hofman, Jason Callahan, David Binns and Rodney J. Hicks from Peter MacCallum Cancer Centre, Melbourne, Australia; and Pierre-Yves Le Roux, Philippe Robin, David Bourhis and Pierre-Yves Salaun from Brest University Hospital, Brest, France.

** The statements by Siemens customers described herein are based on results that were achieved in the customer's unique setting. Since there is no "typical" hospital and many variables exist (e.g., hospital size, case mix, level of IT adoption) there can be no guarantee that other customers will achieve the same results.

*** *syngo*.via can be used as a standalone device or together with a variety of *syngo*.via-based software options, which are medical devices in their own right. *syngo*.via and the *syngo*.via-based software options are not commercially available in all countries. Due to regulatory reasons its future availability cannot be guaranteed. Please contact your local Siemens organization for further details.

At Halifax Health, SPECT/CT Protocol Helps to Improve Patient Care and Reduce Costs

More effective care—delivered faster and at a lower cost—is possible. The users of SPECT/CT at Halifax Health in Florida, USA, are proving it.

By Greg Freiherr

Diabetics who seek emergency care for painful foot infection at Halifax Health hospitals are benefiting from a streamlined protocol that has cut the time in half from "door to diagnosis" for patients suspected of having osteomyelitis, a bone infection that often requires surgery.

The protocol, which leverages the specificity and localizing capabilities of SPECT/CT, may serve as a model for future efforts to make healthcare better and less expensive. Its development illustrates how technology providers and care providers can work together to promote this.

Pioneering this technique is podiatrist and wound care expert Eric M. Goldenberg, DPM. Working with the Halifax nuclear medicine coordinator, Andrea Huffman, RT(N), Goldenberg is proving the potential of this hybrid modality in quickly and definitively diagnosing osteomyelitis.

SPECT/CT helps accelerate the diagnosis and, therefore, the treatment of patients found to have this bone infection. The sooner the diagnosis, the better the chance of reducing the spread of infection through the patient's body, he said. Simultaneously, it spares those without the disease from unnecessary hospitalization—or worse.

"The last thing I want to do is take a patient to the operating room and find out on the pathology report that it was negative," Goldenberg said. "It has never happened, and I never want it to happen."

The specificity of SPECT, achieved by visualizing the patient's radiolabeled white blood cells, combined with CT localization allows physicians to determine—without a doubt—if there is an infection and where it is.

Goldenberg and Huffman contend that by working smarter rather than harder, their SPECT/CT protocol both improves clinical outcomes and reduces cost for diabetics suspected of osteomyelitis. Earlier diagnosis leads to faster treatment and, ultimately, quicker discharge of patients, while shifting care from the inpatient to the outpatient environment.

The conventional diagnostic process requires up to six days. Within that time, X-ray, MRI and SPECT-only scans are performed and interpreted, as listed in the American College of Radiology (ACR) appropriateness criteria. The shortened

SPECT/CT helps accelerate the diagnosis and, therefore, the treatment of patients found to have this bone infection. The sooner the diagnosis, the better the chance of reducing the spread of infection through the patient's body. Simultaneously, it spares those without the disease from unnecessary hospitalization.

Eric M. Goldenberg, DPM
Clinical Director of Wound Care
Halifax Health, Florida, USA

protocol streamlines the process, according to Goldenberg. Now, the patient undergoes X-ray and SPECT/CT. This streamlined process can save up to three or even four days, all or several of which would be spent in the hospital.

"Halifax Health is always looking for opportunities to improve outcomes while at the same time gaining efficiencies within the healthcare system," said Matthew Petkus, MBA, RT(R)(CV), Halifax Health service line administrator for Clinical Ancillary Services. "With the new age of healthcare reform, being able to achieve the best possible outcome in a condensed time frame is very important to healthcare's future success."

Better Care at Less Cost

The significance for public health is staggering. About one in 10 people in the U.S. have diabetes.[1] More than 60 percent of non-traumatic lower leg amputations occur in diabetic patients, according to the American Diabetes Association.[1]

Improving patient outcomes is the prime consideration behind using the new protocol, but cost savings are important, as well. So far, Huffman has documented only time savings from using the protocol. The organization is now building metrics to track the monetary savings.

Getting a handle on cost has been a recent priority, as the healthcare community edges closer to value-based medicine and away from traditional fee-for-service. A new cost consciousness is pervading local and national thinking about healthcare. The U.S. annually spends more than any other developed nation, according to the Organization for Economic Co-operation and Development.[2] The annual cost comes out to $8,713 USD per person.[2]

But value-based medicine is about more than just reducing cost. Its goal is to lower healthcare costs while improving quality and outcomes,[3] delivering greater benefit to the patient for the expense of less money and time. As applied at Halifax Health, SPECT/CT achieves this.

This opportunity arose when Halifax Health purchased five Siemens Symbia™ scanners, four in 2010, at the flagship hospital in Daytona Beach, the other in 2012, at the medical center in Port Orange. Soon after these systems became operational, the Siemens product sales executive, working with Huffman, began looking for clinical opportunities unique to the new scanners. Goldenberg was receptive to SPECT/CT and recognized early the potential to improve and shorten the diagnostic process associated with osteomyelitis.

Before the Symbia SPECT/CTs arrived, emergency physicians followed the ACR protocol under which X-rays of the foot were ordered, followed by MRI, and then a nuclear medicine scan, usually involving white blood cells (WBC), drawn from the patient, labeled with radioisotopes and injected back into the patient.

Increasingly, over the past six months, Halifax emergency physicians have gone straight from doing X-rays to nuclear scans. WBC SPECT/CT, performed on their Siemens scanners, determines whether infection is present, if it is in the bone and, if so, exactly where.

MRI was removed from the protocol because it is not as specific, which can lead to inconclusive results, according to Goldenberg. For example, MRI has been inconclusive in cases when SPECT/CT definitively showed

Impact of SPECT/CT

On diagnosis of osteomyelitis at Halifax Health

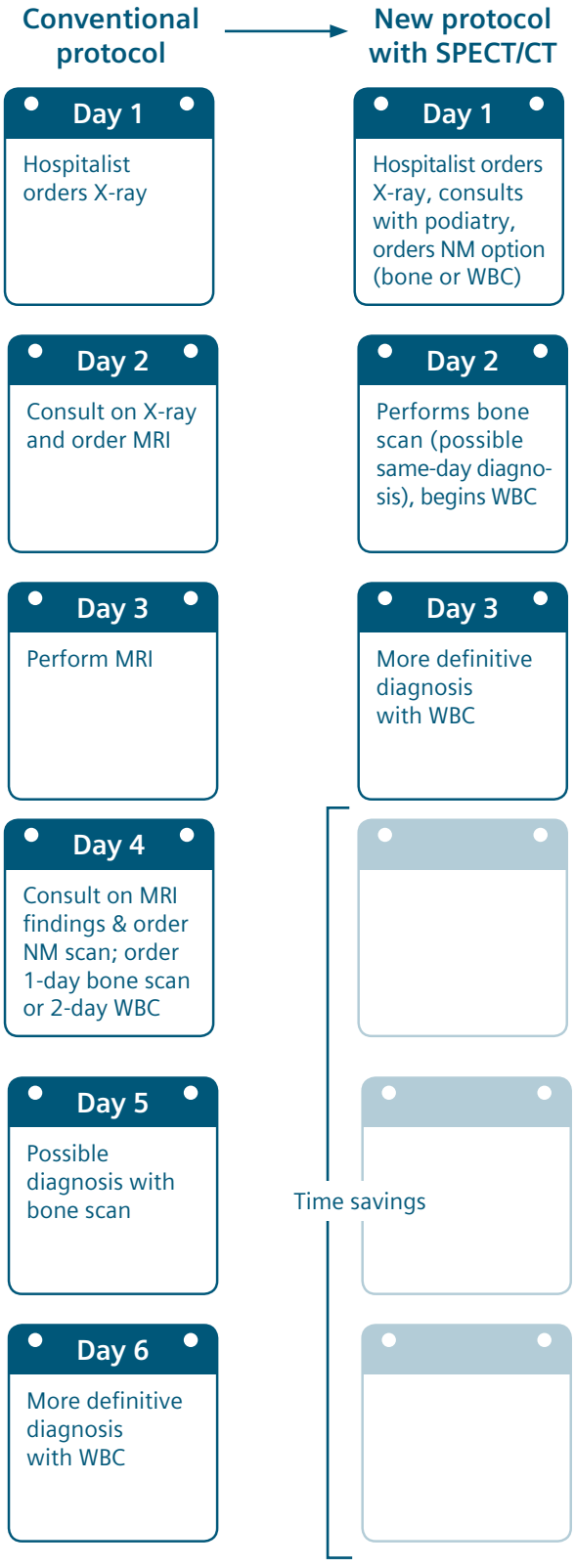

its presence. Conversely, MRI has been positive for osteomyelitis, only to be contradicted by SPECT/CT.

This is illustrated by a recent case in which MRI demonstrated "extensive destruction of the first metatarsophalangeal joint... and basically all of the proximal phalanx consistent with osteomyelitis and septic arthritis," according to the radiology report. The SPECT/CT study, however, identified only soft tissue swelling "that does not involve any of the adjacent bones," the nuclear medicine report stated.

Rather than taking the patient to the operating room, as would have happened if the MRI were the only modality used, "we sent the patient home with visits to our outpatient clinic for wound care," Goldenberg said. "With antibiotics, the patient did very well—and we saved a tremendous amount of healthcare dollars."

A New Workflow

Under the revised protocol, on the first day, the hospitalist orders the X-ray, consulting on the results with a specialist of podiatry or infectious disease. The decision is then made whether to order a two-day WBC scan. If ordered before 3:00 pm, SPECT/CT results can be in hand before close of the second day. If ordered after 3:00 pm, the process takes an additional day, bringing the total to three days—half the norm.

"The radiology department's initiative with SPECT/CT for osteomyelitis was unique in that it considered an inefficient process for the diagnosis and management of a condition and proactively sought how to improve the time from diagnosis to treatment of a patient," Petkus said. "This ultimately leads to better patient care, improved clinician satisfaction, reduced length of stay and overall a more efficient episode of care. Instead of being just diagnosticians, it turns the nuclear medicine department into the driver of an advanced care pathway."

Goldenberg has personally championed this change, rallying colleagues to the cause with clinical presentations, one delivered to emergency room doctors and staff at 7:00 am. Working in concert with Goldenberg, Huffman—with assistance from Siemens—has spread the word about the benefits of the new protocol among ordering physicians. Huffman's efforts have also led to administrative approval to alter radiopharmacy hours to accommodate weekend and late orders for radiolabeled WBCs, so the SPECT/CT protocol could be used throughout the week.

With faster diagnosis and more effective treatment has come increased patient satisfaction, according to Huffman. This translates into better HCAHP (Hospital Con-

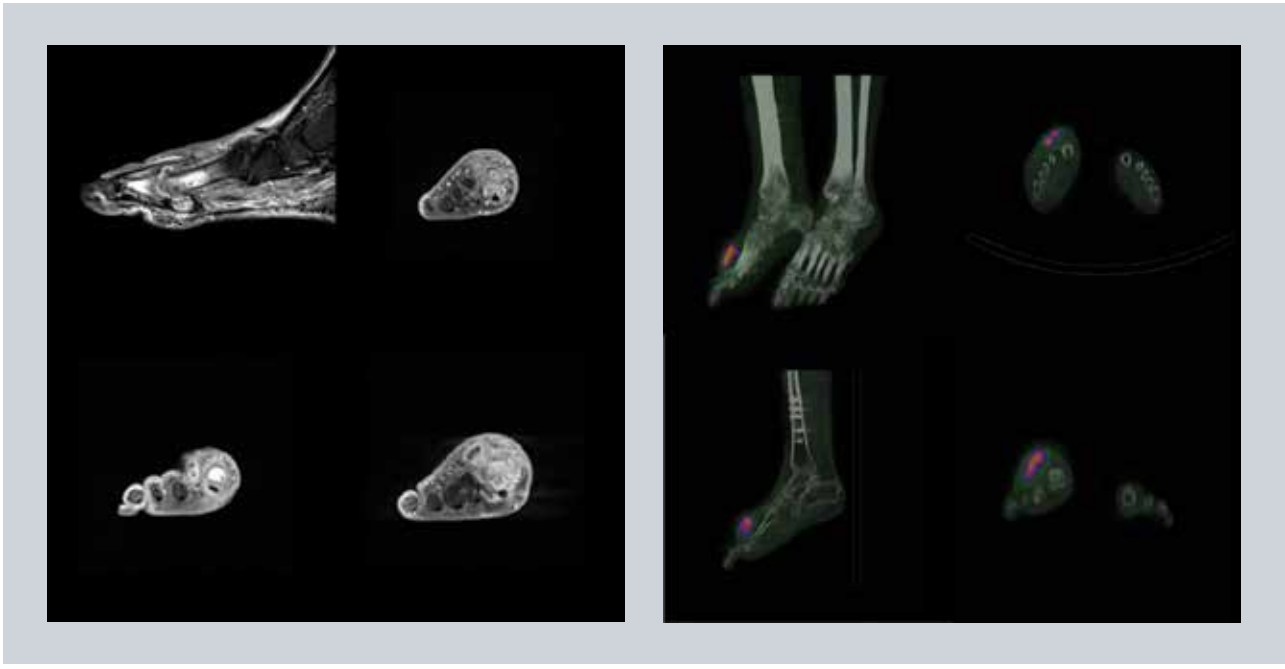

A comparison between MRI (*left*) and SPECT/CT (*right*) imaging demonstrates that, in the same patient, the MRI is positive for osteomyelitis, but the SPECT/CT WBC imaging came back negative. As such, the patient's care pathway was adjusted according to the diagnosis obtained from SPECT/CT, which avoided sending the patient to the operating room and the associated healthcare dollars. Data courtesy of Halifax Health, Florida, USA.

sumer Assessment of Healthcare Providers and Systems) scores, she said. These scores, obtained from patient surveys about the care they receive, are becoming increasingly important.

"HCAHP factors heavily into how we get reimbursed in today's value-driven healthcare," Huffman said.

The increased profile of nuclear medicine in the management of patients suspected of osteomyelitis validates efforts by Halifax Health to acquire the SPECT/CT scanners. The recent success with the systems may prompt the development of other cost-saving protocols involving bone disease, according to Huffman. In the immediate future, however, she and her colleagues are focusing on the formalization of the protocol for osteomyelitis.

Although this shortened protocol has not been formalized, more and more physicians at Halifax are using SPECT/CT to more quickly assess patients suspected of the bone infection.

"Finding clinical pathways to decrease length of stay and readmissions is the focus of our organization," said Alberto Tineo, Halifax vice president of operations. "In the long run, it is better patient care to have patients in their correct setting. And [it] is more cost effective."

Tineo has requested a detailed accounting of how exactly the revised protocol affects healthcare costs. A key element of that assessment will likely address whether and to what extent the use of SPECT/CT to diagnose osteomyelitis impacts patient length of stay in the hospital. Huffman and her staff are now gathering the data.

The need for cost-effective healthcare will grow in the coming years with the rise of value-based medicine. The extended reliance on SPECT/CT to evaluate osteomyelitis patients may help illuminate the road to meeting that need. ■

References:
[1] "Statistic About Diabetes." American Diabetes Association. Accessed on April 18, 2016.
[2] "OECD Health Statistics 2015." Organization for Economic Co-operation and Development. Accessed on April 18, 2016.
[3] Cosgrove T. "Value-Based Health Care Is Inevitable and That's Good." Harvard Business Review. September 24, 2013.

Time-of-Flight Paves the Way to Faster Scans and Lower Radiation Dose

Researchers at Central Manchester University Hospital in the United Kingdom conducted a study to optimize their Time-of-Flight-equipped PET/CT scanner. As a result, the institution adopted a new protocol that has led to reduced radiation exposure to patients and staff, and has provided the flexibility to perform more PET/CT scans per year.

By John C. Hayes

The growing demand for PET/CT in oncology poses a challenge for Central Manchester University Hospital, with a projected 14 percent annual increase on scanning numbers. Its use of F 18 Fludeoxyglucose (^{18}F-FDG)* in oncology produced reliable results, but there was a clear need to increase efficiency to accommodate this increasing demand.

Additionally, the departmental physicists are always looking for ways to reduce radiation exposures while maintaining the same high quality results. Both staff and patients, some of them relatively young, were being exposed to relatively high levels of ionizing radiation during PET/CT scans.

New technology offered a possible solution.

Central Manchester researchers found their solution in a Siemens Biograph™ mCT PET/CT scanner, equipped with TrueV and Time-of-Flight (ToF) technology. By measuring the actual time difference between the detection of each coincidence photon, ToF can localize the event within a small range along each line of response. This increases signal-to-noise ratio (SNR), enabling faster scans, lower injected dose and improved image quality.[1, 2]

Though studies have shown that ToF improves both SNR and definition of small lesions, Manchester researchers had a more involved question: Could ToF help them develop a protocol that could reduce radiation exposure, while increasing flexibility in scheduling to handle the approximately 3,300 annual patient scans. Of that 3,300, about half of the annual scans are ^{18}F-FDG related, the other being for ^{82}RB cardiac PET.

Therefore, the Manchester team conducted two studies, examining different times for bed positions and doses. The team used a strategy of trimming photon counts with ToF reconstructions to simulate shorter bed times

* Indications and important safety information on Fludeoxyglucose F 18 injection can be found on page 25. The full prescribing information can be found on page 62-64.

and less ^{18}F-FDG administration. Today, they use a protocol based on the weight of the patient that has reduced bed times and ^{18}F-FDG administration. They estimate that the changes have reduced radiation exposure for both patients and staff by up to 30 percent and have increased annual throughput by 100 scans.[3, 4]

Before, most UK institutions had been using a protocol from a government advisory committee (ARSAC, the Administration of Radioactive Substances Advisory Committee) with two prescribed ^{18}F-FDG dose levels (350 MBq and 400 MBq, based on weight), and a bed position segment time (2.5 minutes) that failed to reflect advances in PET detector technology and reconstruction algorithms. Central Manchester University Hospital was among those using the ARSAC guidelines.

"We followed the standard practice, and I always said, given our state-of-the art equipment, surely we can do better," said Ian S. Armstrong, principal physicist at the department, who spearheaded the research and was lead author on a publication of results.

To explore the possibilities of ToF, the Manchester team developed a strategy: Run patients through the scanner, and reconstruct the data without ToF. After that, the researchers used list-mode data to reduce photon counts and reconstruct the data again using ToF. Scan quality was evaluated by measuring SNR in the liver, standard uptake values (SUV) and a qualitative assessment of the images.

The purpose of reducing counts was to simulate a reduction in bed times and also as a surrogate for reduced radiation exposure. To simulate reduced doses of ^{18}F-FDG, the researchers used a phantom to quantify the equivalence of reduced dose and reduced acquisition time.

In the published study,[3] the researchers presented data from 58 patients.

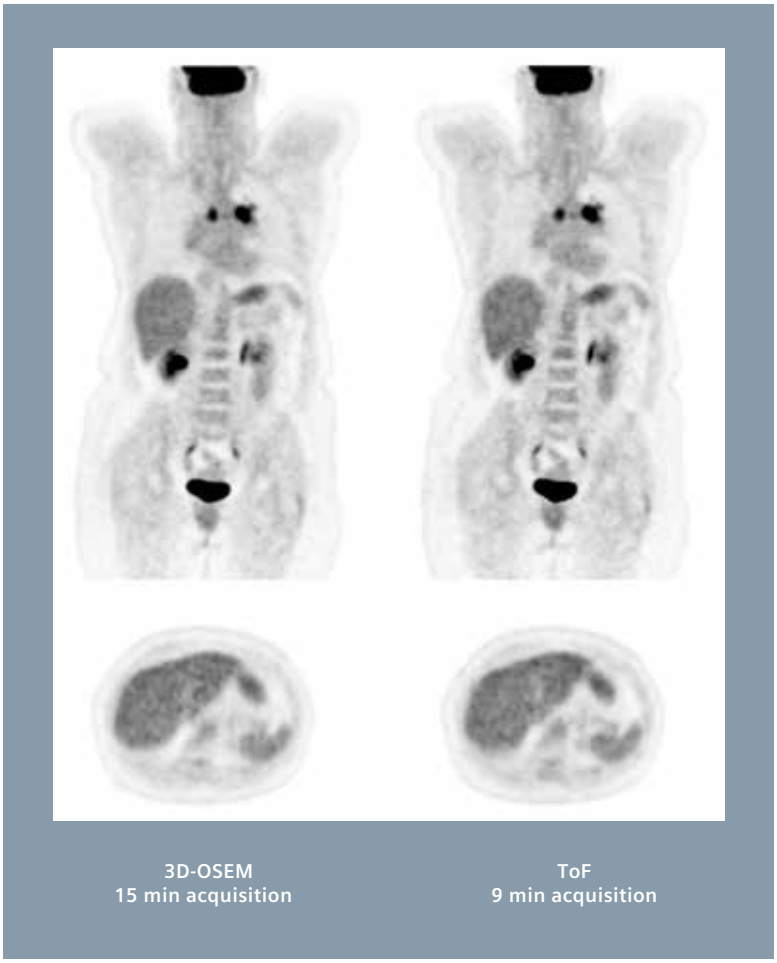

Patient with a BMI of 33 kg/m^2 was administered 365 MBq of ^{18}F-FDG and scanned at 60 minutes post-injection. The SNR measured in the liver is 10.1 for 3D-OSEM and 10.2 for ToF. The comparison between ToF and non-ToF acquisition demonstrates the ability of ToF to not only enable faster scans, but maintain a high lesion contrast. As such, facilities can reduce their levels of dose and still acquire adequate results. Data courtesy of Central Manchester University Hospital, Department of Nuclear Medicine, Manchester, United Kingdom.

Of these, 49 weighed less than 100 kg (220.5 lb); nine weighed more. The members of the lighter cohort were administered 350 MBq of ^{18}F-FDG. Those who weighed more were administered 400 MBq. To test the effect of ToF, the researchers trimmed counts for the lighter cohort by 20 and 40 percent and, for the heavier cohort, by 16 and 30 percent.

The results supported their hypothesis that ToF could be used to substantially reduce dose and/or bed times. Among the 49 patients weighing less than 100 kg, all images with a 20 percent count reduction were considered adequate. Thirty-nine patients with a 40 percent count reduction were considered adequate. Among the nine patients weighing more than 100 kg, all images with a 16 percent count reduction were considered adequate. Five with a 30 percent count reduction were considered adequate.

In the next phase of the study, a new protocol optimized for ToF incorpo-

"Time-of-Flight is a win-win. You can't go wrong with it. Image quality is improved, being more consistent across our patient population, and quantification is preserved."

Ian S. Armstrong, Principal Physicist, Nuclear Medicine
Central Manchester University Hospital, Manchester, United Kingdom

rated the findings of the first phase. Beginning in September 2014, the Manchester team switched from the 350 and 400 MBq doses of ^{18}F-FDG in favor of a 280 MBq dose administered to all patients, a reduction of 20 percent for the lighter cohort and 30 percent for the heavier cohort. In addition, the researchers adjusted scan times per bed positions based on weight or body mass index (BMI). Those weighing less than 85 kg (187.4 lb) and with a BMI of less than 28 spent two minutes per bed position. Those weighing 85 to 115 kg (253.5 lb) or having a BMI of more than 28 spent 2.5 minutes per bed position. Those with a body weight of more than 115 kg spent three minutes per bed position.

Reducing the scan times per bed position to two minutes cut the total time for a six-position scan from 15 to 12 minutes and the time for a seven-position scan from 17.5 to 14 minutes.

The overall result was a significant reduction in radiation exposure to both patients and staff working with PET/CT, the researchers concluded. This is particularly important for patients with certain types of cancer, such as lymphoma. These patients may be relatively young, respond well to treatment, and are likely to undergo multiple PET/CT scans to monitor therapy response (the youngest patient in the study was 25 years old).

Under the reduced dose protocol, there was a marked improvement in the flexibility of scanner scheduling with additional scans such as local views or separate head and neck scans having less of an impact on workflow for the session, according to the researchers.

They also observed fairly uniform gains in image quality (SNR) with ToF across the entire patient group, he said. This was not anticipated.

"Based on Time-of-Flight theory, I was expecting small or negligible gains in the smaller patients, but for our data, that wasn't the case," Armstrong said. "This meant that we could focus further on the smaller patients to develop a weight-based protocol, reducing radiation dose further. Without this information we would have needed to be more conservative."

That finding led to an even more refined ToF ^{18}F-FDG protocol for patients weighing less than 80 kg (176.4 lb). The protocols were tested using 48 routine oncology patients who were given 280 MBq of ^{18}F-FDG (these data have not yet been published). Simulations using reduced counts were employed, as they were in the published study, for patients based on 4.0 or 3.5 MBq per kg (2.205 lb) of weight with measures of image signal to noise used to assess the consistency of image quality over the population. Having concluded that 3.5 MBq per kg was the more effective scheme, they compared SUV_{max} and found the fixed 280 MBq protocol and the 3.5 MBq per kg weight-based protocol produced essentially equivalent quantification. The protocol was adopted in December 2014, establishing the top ^{18}F-FDG administration level at 280 MBq. Bed times are two minutes per segment, but may be increased for larger patients. The weight-based protocol is also used in pediatric cases.

The Manchester team manually administers ^{18}F-FDG with either 3 ml or 5 ml syringes, without the use of an automatic injector. Compliance with the protocol at Central Manchester University Hospital has been very good. "The volumes that are dispensed can be quite small in some cases. The seamless adoption of the weight-based scheme with manual dispensing is a credit to the skills of our technical staff," Armstrong commented.

A look at administration levels for 136 patients following the weight-based protocol found clear reductions in ^{18}F-FDG administration, with smaller patients benefitting considerably. The median ^{18}F-FDG administration was 255.2 MBq, down from 280 MBq under the published protocol.

"There were no real obstacles," Armstrong said. "Time-of-Flight is a win-win. You can't go wrong with it. Image quality is improved, being more consistent across our patient population, and quantification is preserved." ■

References:
[1] Surti, Suleman. "Update on Time-of-Flight PET Imaging." *J Nucl Med*. 2015; 56: 98-105.
[2] Lois, Cristina et al. "An Assessment of the Impact of Incorporating Time-of-Flight Information into Clinical PET/CT Imaging." *J Nucl Med*. 2010; 51(2): 237-245.
[3] Armstrong IS, James, JM, et al. "The assessment of time-of-flight on image quality and quantification with reduced administered activity and scan times in ^{18}F-FDG PET." *Nucl Med Commun*. 2015; 36: 728-737.
[4] "One hundred cancer patients a year in Manchester benefit from new scan technology." *MHS News Hub*. The University of Manchester. Oct 27, 2015. Accessed Feb. 1, 2016.

* The full prescribing information can be found on page 62-64.

The statements by Siemens customers described herein are based on results that were achieved in the customer's unique setting. Since there is no "typical" hospital and many variables exist (e.g., hospital size, case mix, level of IT adoption), there can be no guarantee that other customers will achieve the same results.

Fludeoxyglucose F 18 5-10mCi as an IV injection Indications and Usage

Fludeoxyglucose F 18 Injection is indicated for positron emission tomography (PET) imaging in the following settings:

- **Oncology:** For assessment of abnormal glucose metabolism to assist in the evaluation of malignancy in patients with known or suspected abnormalities found by other testing modalities, or in patients with an existing diagnosis of cancer.
- **Cardiology:** For the identification of left ventricular myocardium with residual glucose metabolism and reversible loss of systolic function in patients with coronary artery disease and left ventricular dysfunction, when used together with myocardial perfusion imaging.
- **Neurology:** For the identification of regions of abnormal glucose metabolism associated with foci of epileptic seizures.

Important Safety Information

- **Radiation Risks:** Radiation-emitting products, including Fludeoxyglucose F 18 Injection, may increase the risk for cancer, especially in pediatric patients. Use the smallest dose necessary for imaging and ensure safe handling to protect the patient and health care worker.
- **Blood Glucose Abnormalities:** In the oncology and neurology setting, suboptimal imaging may occur in patients with inadequately regulated blood glucose levels. In these patients, consider medical therapy and laboratory testing to assure at least two days of normoglycemia prior to Fludeoxyglucose F 18 Injection administration.
- **Adverse Reactions:** Hypersensitivity reactions with pruritus, edema and rash have been reported; have emergency resuscitation equipment and personnel immediately available.

Full prescribing information for Fludeoxyglucose F 18 Injection can be found on pages 62-64.

Dosage Forms and Strengths

Multiple-dose 30 mL and 50 mL glass vial containing 0.74 to 7.40 GBq/mL (20 to 200 mCi/mL) of Fludeoxyglucose F 18 injection and 4.5 mg of sodium chloride with 0.1 to 0.5% w/w ethanolas a stabilizer (approximately 15 to 50 mL volume) for intravenous administration.

Fludeoxyglucose F 18 injection is manufactured by Siemens' PETNET Solutions, 810 Innovation Drive, Knoxville, TN 39732

SPECT Replacement Enables Efficiency and Service Line Expansion

Boice-Willis Clinic, a primary care and multi-specialty practice with seven locations in North Carolina, USA, replaced two aging SPECT scanners with one Symbia Evo™ Excel* SPECT system. Edward O'Neal, MHA, RT(R)(CT), Imaging Manager, and Candie Wachowicz, RT(R)(N), Nuclear Medicine Technologist, talk about the process.

By Rhett Morici, Molecular Imaging Business Line, Siemens Healthcare

Edward O'Neal, MHA, RT(R)(CT), Imaging Manager (left), and Candie Wachowicz, RT(R)(N), Nuclear Medicine Technologist (right).

Boice-Willis Clinic replaced its two SPECT scanners in January 2016. What led to this decision?

Edward O'Neal: Prior to Symbia Evo Excel, we used two older systems from a different vendor. One scanner was installed in 1997, and the other was installed in 2002. When both hit their end of service life, it limited what we could accomplish. For example, if we wanted to add new procedures, it was very costly to do so.

Was there a set of core criteria your new scanner had to have?

Edward O'Neal: Iterative reconstruction was a must-have. Our cardiologists have used systems with iterative reconstruction at other hospitals, so that was especially an interest for them, and we made sure to get it.

"We want the ability and option to grow into different areas, and we want equipment that will enable us to do so."

Edward O'Neal, MHA, RT(R)(CT)
Imaging Manager, Boice-Willis Clinic
North Carolina, USA

Increased weight limit on the patient bed was another must-have. Our older cameras had a 350-pound weight limit, so we looked for options that could accommodate more bariatric patients. Our patient base was limited due to size.

The size of the scanner was another criterion. We are located on the fourth floor in our building, and we have limited available space. Getting the system into place, in our limited space, was important. The small footprint was definitely a benefit.

What questions did you ask during the replacement process?

Edward O'Neal: In addition to our interest in iterative reconstruction and the table weight limit, we looked at system reputation and talked with references about their experiences. We also looked into aspects such as camera life, how long has it been in service, service contracts and the cost of those contracts. One important aspect of Siemens' service contract was non-obsolescence.

Why is non-obsolescence important?

Edward O'Neal: We are a primary care and multi-specialty practice representing 13 clinical specialties including cardiology and oncology. We want the ability and option to grow into different areas, and we want equipment that will enable us to do so.

Have you been able to expand into new services with your new scanner?

Edward O'Neal: Yes. When we went with Symbia Evo Excel, we added, for example, ^{123}I uptake imaging scans without purchasing any additional hardware or software. Boice-Willis Clinic has built a growing endocrinology practice, so we wanted to offer our patients in-house thyroid imaging.

In addition to what was already mentioned, how else has the scanner enabled your department?

Edward O'Neal: We are able to complete cardiac and bone scans much quicker. These account for about 85 percent of our work. We are also in the process of investigating additional types of exams, but have not reached any conclusions yet. Overall, the ability to grow into different practice areas, as well as the previously mentioned options that came with the system, are the biggest benefits for us.

Boice-Willis Clinic replaced two SPECT scanners with only one. After about four months of using the scanner, what does your operational throughput look like?

Candie Wachowicz: We are routinely doing 10-13 heart scans per day, with three additional studies such as gastrointestinal (GI), thyroid or hepatobiliary (HIDA) on this one scanner. Our patient volume has increased since installing the new system.

Edward O'Neal: In the past, we averaged about six cardiac patients per day, with two additional other studies per day. Overall, though, across the entire clinic, patient volume is up. Last month, for instance, between our cardiac and our routine nuclear medicine scans, we did 200 procedures, which is about 50 procedures more than we normally do.

Could you have handled that increased volume on the older scanners?

Edward O'Neal: Not on one camera alone. The iterative reconstruction helps to reduce imaging times.

What is the exam mix at your facility?

Edward O'Neal: Our mix is comprised of about 80 percent cardiology, 10 percent GI, five percent oncology, and five percent in thyroid and endocrinology types of imaging.

At Boice-Willis Clinic, the Symbia Evo Excel scanner is located on the fourth floor at the Rocky Mount Medical Park location in North Carolina, USA. With limited space, it was a requirement that the facility's new SPECT system have a small footprint that fit into the pre-existing space.

Have you found the flexibility of the detector heads, the caudal tilt or the easy gurney bed imaging to be important?

Edward O'Neal: Since we are essentially an outpatient facility, we don't do much gurney imaging. But the flexibility of the camera heads and the ability to move them pretty much in any direction does come in handy, especially with some of the HIDA scans and gastric studies.

Candie Wachowicz: The flexibility is nice, because you can pretty much have the detector heads positioned any way you want.

Describe the learning process for the new scanner?

Candie Wachowicz: I went to the Siemens training and development center in Cary, North Carolina, USA, for training. Once we started using the system at our department, the following week, an applications specialist visited us onsite to train our other technologists. He went through the basics, such as patient handling, and helped set up and customize our protocols.

The applications specialist pulled our protocol books, worked with our providers to better understand our needs and made the protocols specific to those requirements. He went through it all with us and demonstrated how it works. The process was very good. After that initial training, we worked for two weeks on our own, and then the applications specialist returned for a two-day follow-up. That way if we had questions or if any minor issues arose in the meantime, we were able to have those quickly addressed.

Is there a need for you to have standardization in protocols and quality of care at your facility?

Edward O'Neal: Since Boice-Willis Clinic is accredited by the ACR, we are required to operate on standard protocols and reporting.

Does having new technology impact your facility's reputation amongst patients and physicians?

Edward O'Neal: It helps out a great deal, absolutely. Patients feel like we have state-of-the-art equipment and that they are receiving a high level of care. Likewise, when physicians visit us, and see that we have newer equipment, they know we invest resources to help them offer better services to their patients and provide them with the best possible results.

Candie Wachowicz: I think it gives our patients confidence. For example, we have many repeat patients, and when they come in and realize that the scanner is different than from before, they seem to have a confidence boost in that they are getting quality imaging. Also, the study is faster than before, so that helps to increase their overall satisfaction.

Are you measuring patient satisfaction through surveys?

Edward O'Neal: We do clinic-specific, patient satisfaction surveys.

Four Steps to Successful SPECT Replacement

Boice-Willis Clinic, a primary care and multi-specialty practice, replaced two aging SPECT scanners with one Symbia Evo Excel SPECT system. Here are their tips for approaching SPECT scanner replacement.

Define your needs. Identify which capabilities will best address your exam mix now and support growth in the future.

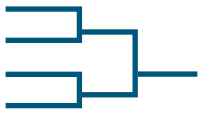

Engage a few vendors. Determine which provider can meet or exceed your needs for the best price without compromising quality.

Talk with users, including technologists. Learn about their experience with the system from both an administrative perspective and in clinical routine.

Evaluate vendor reputation. Confirm equipment and service performance are equally strong.

Have you noticed an increase in the survey scores?

Edward O'Neal: Our surveys account for the department as a whole, and the scores are very positive overall, so it is hard to relay it back to any one piece of equipment. We do receive a lot of verbal feedback from the patients, especially with the cardiac patients when they are here for the better part of the day undergoing a procedure.

What are your top recommendations for departments looking to replace their scanners?

Edward O'Neal: First, define your needs. What do you need out of the system? And then make a list of what you really would want out of a system, but is not necessarily a need. Then choose potential vendors for negotiation.

But I would also call references, talk to the technologists and see how they like the system. People will often say, "Call this administrator." There is nothing wrong with talking to the administrator, but I like talking to the people who are routinely using the system too. Also, look at the reputation of the company and the service history. If a piece of equipment is good, but the service isn't good, then you could have a problem. We believe that we made a very informed decision with this system, and so far, it has met all of our expectations. ■

* Symbia Evo Excel is not commercially available in all countries. Due to regulatory reasons, its future availability cannot be guaranteed. Please contact your local Siemens organization for further details.

The statements by Siemens customers described herein are based on results that were achieved in the customer's unique setting. Since there is no "typical" hospital and many variables exist (e.g., hospital size, case mix, level of IT adoption) there can be no guarantee that other customers will achieve the same results.

Think Whole-body Dynamic PET Imaging is for Research Only?

Perhaps it's Time to Re-evaluate

With the introduction of continuous bed motion technology, whole-body dynamic PET imaging becomes more practical in clinical routine, and less cumbersome in research settings. Recent research undertaken by Koji Murakami, MD, PhD, demonstrates this, which raises the question: Are we at the advent of a paradigm shift?

By Carl von Gall, MD, Molecular Imaging Business Line, Siemens Healthcare

Since the beginning of positron emission tomography (PET), researchers worldwide have tried to understand the processes underlying the uptake, metabolization, trapping and binding of PET tracers. The preferred method of study has been dynamic PET acquisition (dPET), whereby tracer distribution is acquired over time, typically, from a single bed position. From that continuously acquired data, different time frames are then reconstructed.

However, results have been difficult to reproduce, due to individualized approaches to acquisition time, reconstruction methodology and analytical techniques. Thus, dPET has become a heterogeneous field, which limits its feasibility in both clinical routine use and research settings.

From the clinical routine perspective, institutions faced several obstacles, even when incorporating facilitated dynamic approaches. Take dual time-point imaging, for example: Protocol setups varied because they were developed according to the designs of the individual institutions and investigators. Subsequently, none of them fit into daily routine environments because of the high individualization and, therefore, lack of standardization. Without standardization, the complexity of patient handling and imaging made dPET impractical in routine use, especially for institutions with high patient throughput.

From the researcher's perspective, dynamic acquisitions of important lesions or organs were only possible if they all fit in the axial field of view (FoV). For most scanners, the FoV spanned between 15 to 21 cm. Due to this limitation, especially in distant lesions or peripheral foci, dPET acquisition is cumbersome and can sometimes be close to impossible.

This changed with the introduction of Biograph mCT Flow™* with FlowMotion™ technology. Implementing continuous bed motion as its core feature, physicians can acquire dPET in a new way: Whole-body dynamic imaging.

Whole-body dynamic imaging allows the user to overcome the limitations in conventional dPET. It enables dynamic acquisition over the entire scan range by continuously moving the patient in the axial orientation with a defined number of passes until the targeted time period is completed. With this, whole-body dynamic imaging extends the capability of dPET from the FoV to the field of interest. And as such, clinical physicians and researchers may overcome the range limitation and include regions of the body into one dynamic acquisition that used to be out of reach.

Having the capability to consider the bed movements into the acquisition and reconstruction with variable table speed provides a great variety of examination protocols. From shortened dPET protocols and quick time activity curve analysis with *syngo*®.via PET/CT Oncology Engine Pro, to third-party analysis tools. Whether it is tracer distribution in a lesion over time, gathering more inside information of a drug's pathway through the body or tracing the metabolic patterns in multiple organs at the same time over a large FoV, it all becomes easily accessible in a single protocol at the click of a button.

One of the early adopters of whole-body dPET imaging is Koji Murakami, MD, PhD, who is Head of the Division of Nuclear Medicine in the Department of Radiology at Keio University School of Medicine, Tokyo, Japan.

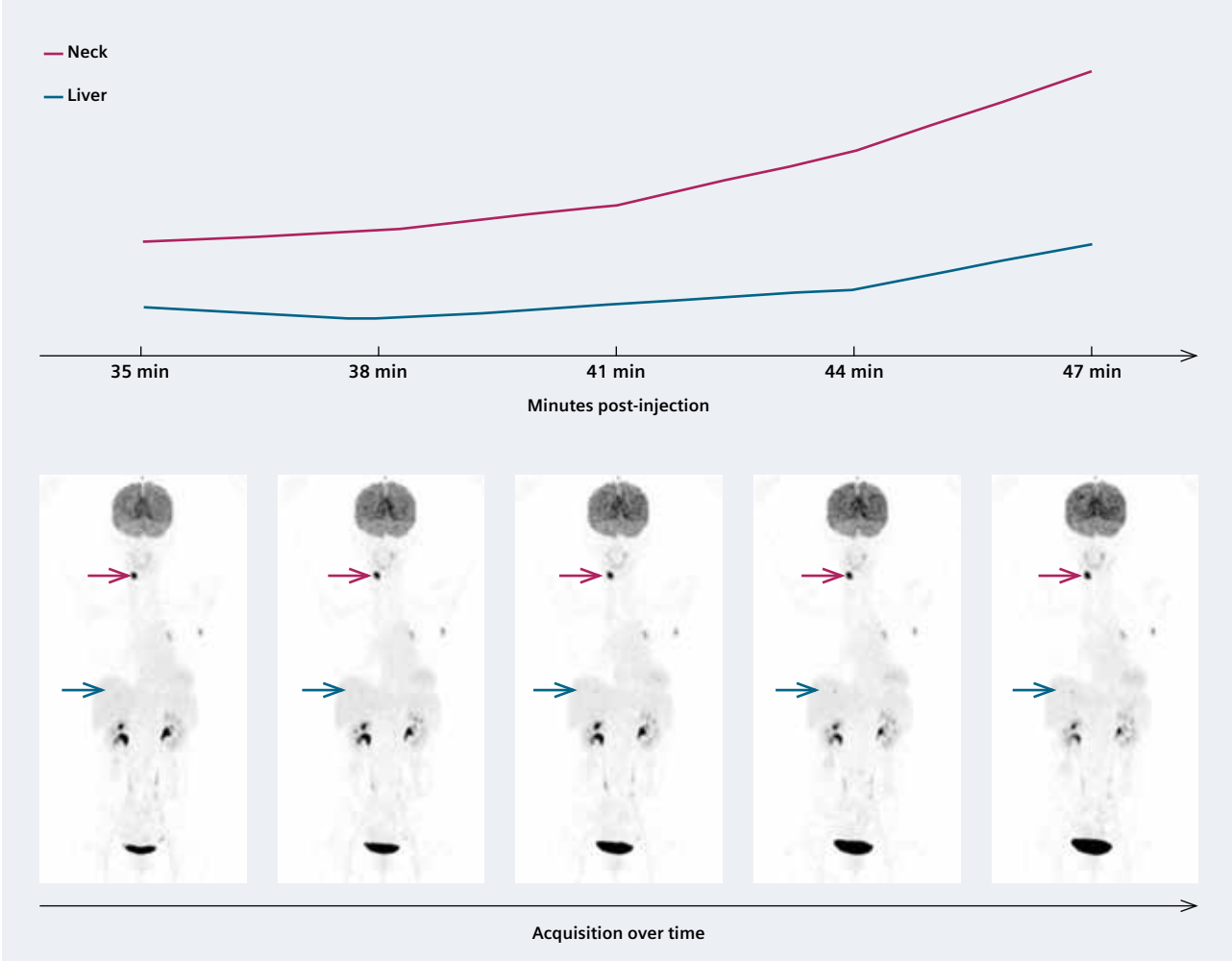

Focally altered metabolism in a patient with malignant disease dynamically acquired 47 minutes post-injection. The graph (top) displays the counts measured in a 1 cm VOI placed over a cervical lesion (*red arrow*) and demarcates liver lesions over time (*blue arrow*). The bottom shows the corresponding whole-body images. Data courtesy of the Department of Radiology, Keio University School of Medicine, Tokyo, Japan.

“With FlowMotion, we obtained a major tool to analyze dynamic studies without limitation to one bed position.”

Koji Murakami, MD, PhD, Head of Nuclear Medicine, Department of Radiology
Keio University School of Medicine, Tokyo, Japan

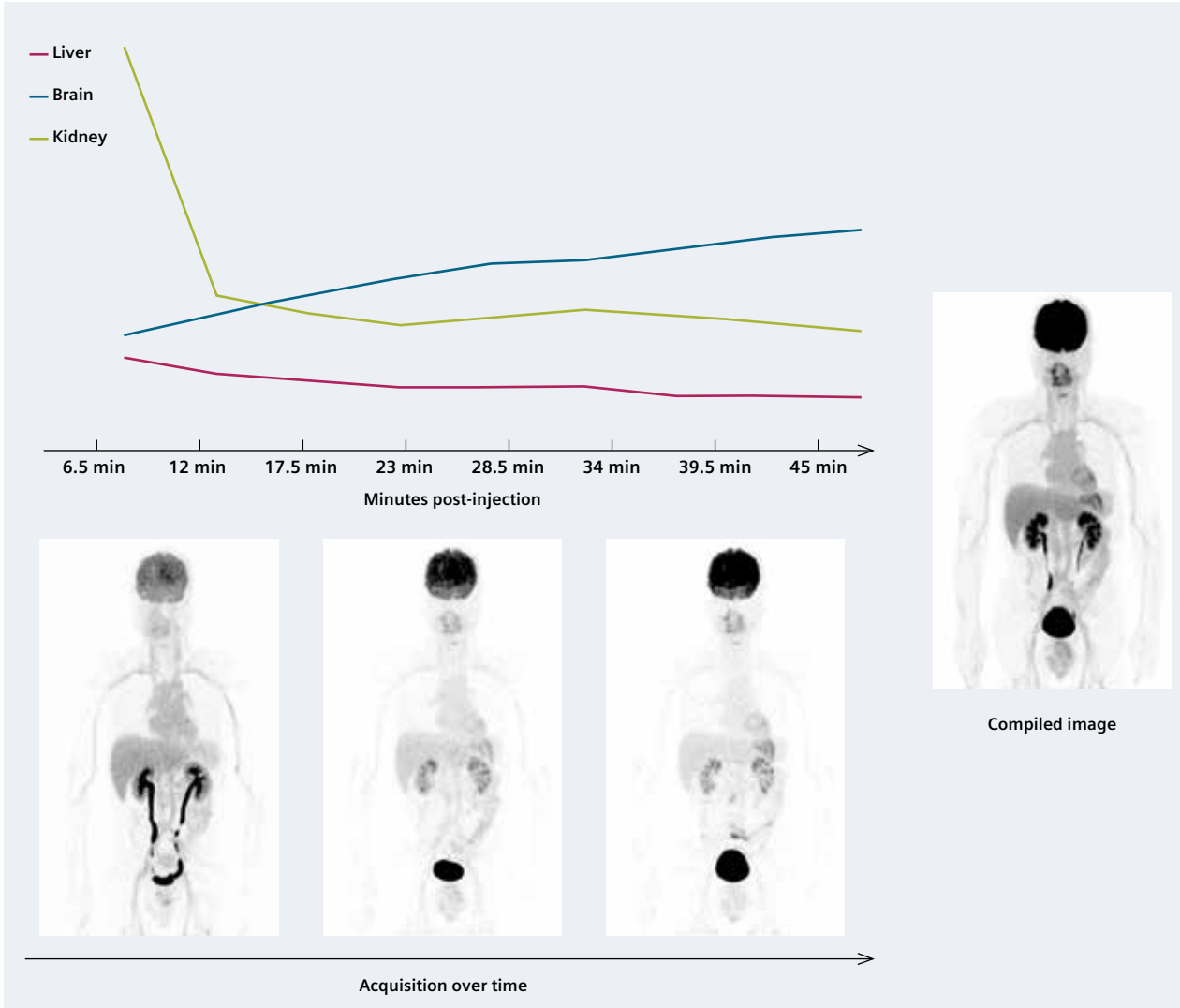

Physiological uptake in a healthy subject dynamically acquired over 45 minutes post-injection. The graph (top) displays the counts measured in a 1 cm VOI placed in the liver, brain and kidney parenchyma on one side. Note the differences in tracer elimination and uptake over time. The bottom shows the corresponding whole-body images with a compiled whole-body of all time frames (*right*). Data courtesy of the Department of Radiology, Keio University School of Medicine, Tokyo, Japan.

Since 2014, Murakami's department has used Biograph mCT Flow and FlowMotion for facilitated respiratory gating and standardized protocols. As a result, Murakami and colleagues have experienced increased uniformity and reduced noise, while maintaining SUV and image quality. Murakami presented the results of his team's work at the European Association of Nuclear Medicine (EANM) Congress 2015 in Hamburg, Germany.

Murakami expanded his use of FlowMotion by taking advantage of the whole-body dynamic feature in his oncological patient setting. Just by the first image series, Murakami felt excited:

"Unlike most CT or MR examinations, the time axis is very important in nuclear medicine. But particular to the field of oncology, sometimes we have to obtain a very long axial field of view to cover all lesions. With FlowMotion, we obtained a major tool to analyze dynamic studies without limitation to one bed position."

Notably his department has experimented with dPET studies of varying length. The researchers have conducted early-series studies, acquiring data soon after injection of the PET tracer, for example, from 30 to 360 seconds post-injection. They have also performed delayed dPET studies spanning 20 minutes.

Recently, the research team has been comparing conventional whole-body PET to compiled whole-body dynamic PET studies. The goal is to document and establish the value of dPET in routine use, and to potentially replace additional static acquisitions in future reporting.

"First we need to determine if we may discriminate additional uptake," Murakami said. "But the objective in the mid-term is to differentiate or improve the diagnosis by analyzing the time-activity curve of a specific disease, and even further, of each individual lesion."

To this end, Murakami has received funding to continue performing research into dynamic PET and expand on studies into compiled imaging as a means to improve routine clinical workflow and further define pathological alterations in glucose metabolism.

Considering Murakami et al.'s promising initial results and acknowledging that, before FlowMotion, whole-body dPET was impractical, there is reason to believe this approach could bring dPET into clinical routine.

Is this the advent of a paradigm shift? We believe the first steps are made. ■

* Biograph mCT Flow is not commercially available in all countries. Due to regulatory reasons, its future availability cannot be guaranteed. Please contact your local Siemens organization for further details.

The statements by Siemens customers described herein are based on results that were achieved in the customer's unique setting. Since there is no "typical" hospital and many variables exist (e.g., hospital size, case mix, level of IT adoption), there can be no guarantee that other customers will achieve the same results.

Setting up dynamic PET protocols

See how easy it is to set up a dynamic PET protocol with FlowMotion.

To watch the video, scan the QR code using the reader app on your smartphone or enter the URL into your internet browser.

siemens.com/dpet-protocol-setup

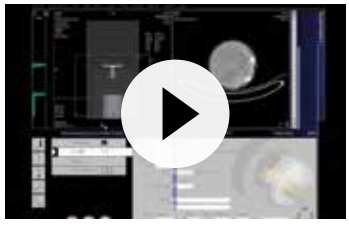

Case 1

Quantitative Infection Imaging with SPECT/CT to Rule Out Presence of Infection in a Patient with Tibial Osteomyelitis Following Surgical Debridement and Arthroplasty

By Partha Ghosh, MD, Molecular Imaging Business Line, Siemens Healthcare

Data courtesy of the Department of Nuclear Medicine, Bundeswehrkrankenhaus Ulm, Ulm, Germany

History

A 74-year-old female, who had a comminuted open fracture of the proximal tibia that was treated with internal fixation, developed osteomyelitis in the fracture area. It was treated with surgical debridement, removal of all metallic internal fixation plates and a resection of the majority of the tibial head—including articular surface with replacement using an antibiotic impregnated cement spacer, along with external fixation of the knee joint. The patient was put on an aggressive antibiotic regime, and a follow-up arthrodesis was planned after the infection was under control. Four months after surgery, the patient underwent SPECT/CT imaging to evaluate for the presence of infection, using ^{99m}Tc-labelled antigranulocyte antibodies to assess the feasibility of arthrodesis.

The study was performed on a Symbia Intevo™* scanner using xSPECT Quant™* technology. 730 MBq (19.73 mCi) of ^{99m}Tc antigranulocyte antibodies (Fab' sulesomab; antigen NCA-90) were injected. Initial dynamic and planar blood pool acquisitions were performed.

SPECT/CT acquisition was performed at 5 and 23 hours following injection. A low-dose diagnostic CT was performed, followed by a SPECT acquisition (32 stops per detector, 5 hours post injection 20 sec/stop; 23 hours post injection 30 sec/stop). xSPECT Quant reconstructions were fused for evaluation. SUV_{max} values were obtained using xSPECT Quant and compared across 5- and 23-hour acquisitions.

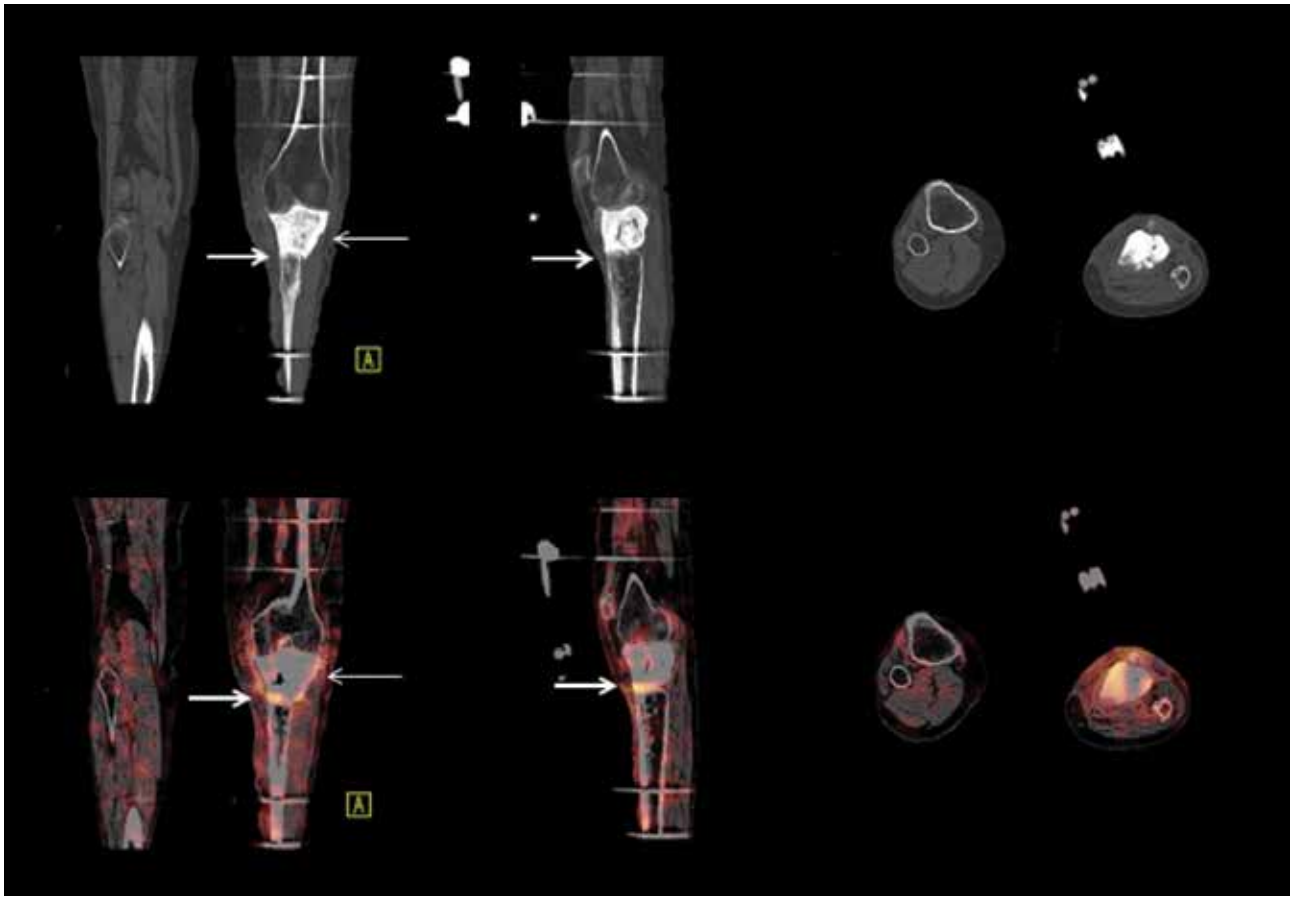

Figure 1: CT and fused SPECT/CT images of the 5-hour post-injection study. CT shows radiodense mass at the proximal end of the tibia (*thin arrow*), which reflects the cement spacer inserted following resection of the majority of the tibial head. The cement fits between the femoral articular surface and the upper end of the tibial shaft. The left knee joint space is eliminated. The tibial tuberosity is still intact and shows osteoporosis, but no sclerosis. The tibial shaft distal to the cement spacer shows cortical thinning with focal calcifications in the marrow. Femoral condyles and shaft appear normal. Fused images show small area of mildly increased uptake at the junction of the dense cement spacer and the tibial shaft (*thick arrows*), as well as mild uptake in the adjacent soft tissue, which is probably related to reactive changes secondary to soft tissue inflammation following surgery and immobilization.

Diagnosis

Figures 1 and 2 showed the irregular junction between the radiodense cement spacer replacing majority of the proximal tibia, except for the tibial tuberosity and the shaft of the tibia below. The irregularity and gaps between the spacer and the margin of the tibial shaft suggested a possibility of pseudoarthrosis. The fused SPECT/CT images showed mild uptake in the anterior part of the junction, which suggested slight accumulation of leucocytes, probably reflecting reactive changes and non-specific inflammation secondary to pseudoarthrosis.

Due to the past history of active infection of the same area, SPECT/CT infection imaging demonstrating mild uptake of ^{99m}Tc-labelled antigranulocyte antibodies at the exact site of pseudoarthrosis strongly suggested the absence of active infection. However, a small focal area of granulocyte accumulation, no matter the size, should be regarded with caution in a situation of prior osteomyelitis. In this context, absolute quantification of tracer uptake performed using xSPECT Quant across 5-hour and 23-hour studies were compared to evaluate if there was a significant increase in leucocyte accumulation in the zone between the cement and tibial shaft.

SUV_{max} in the junction between the radiodense cement spacer and the tibial shaft was 2.00 in the 5-hour study (using OSCG-AC-enhanced datasets for quantification), but changed only slightly to 2.10 in the 23-hour study (*Figure 3*). The stable SUV_{max} over an extended time period suggested the absence of active infection, which is usually associated with accumulation in infected bones. SUV_{max} estimation using xSPECT Quant provided an objective measurement to evaluate granulocyte migration inside the suspected foci.

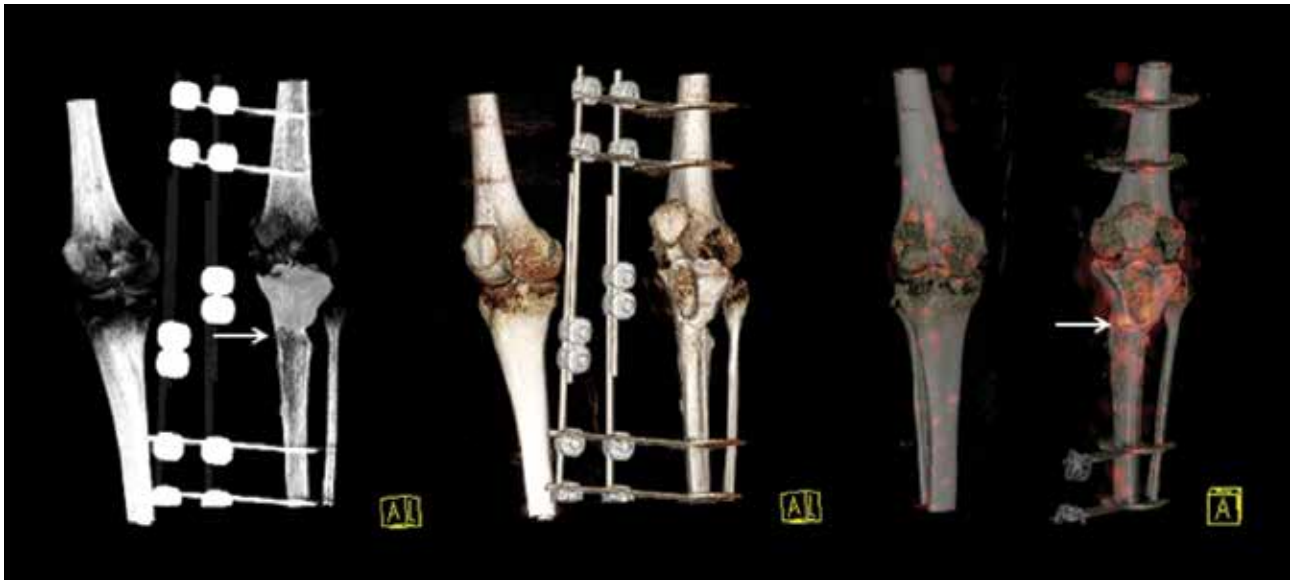

Figure 2: Maximum intensity projection (MIP) and volume rendering of CT of the 5-hour post-injection study show a radiodense cement spacer replacing the proximal tibia articulating with the condylar surface of the left femur. The junction of the cement spacer and the tibial shaft is irregular, suggesting pseudoarthrosis. The external fixation devices are well delineated. The volume rendering of the fused SPECT/CT images show mild increase in uptake of ^{99m}Tc-labelled antigranulocyte antibodies in the line separating the radiodense cement spacer and the tibial shaft (*arrow*), reflecting mild accumulation of leucocytes secondary to reactive changes and secondary to pseudoarthrosis at the bone cement junction.

Moreover, the initial SUV_{max} of 2.00 was also very low, which corresponded to the visual impression of only mild uptake, and reflected reactive changes at the level of pseudoarthrosis. In contrast, the ^{99m}Tc-labelled antigranulocyte antibody SPECT/CT study performed prior to debridement surgery showed an initial SUV_{max} of 2.61 at the point of maximum uptake in the upper end of tibia that increased to 4.56 after 23 hours. The magnitude of increase strongly suggested the presence of active infection, while the mild increase in the present study performed after debridement surgery suggested absence of significant infection.

In the absence of any reference of SUV change in the active infection, the only benchmark for assessment was the earlier study that showed almost 100% increase between 5 and 23 hours. In view of the surgery performed, the stable SUV and the mild uptake based on visual estimate, the diagnosis was to treat the mild uptake as a reactive change and not an infection.

Comments

The increase in uptake intensity with labelled leucocyte scintigraphy between early and late acquisitions reflected progressive accumulation of granulocutes within active infection, especially in osteomyelitis. However, visual impression is often unreliable in presence of low uptake or small foci, especially in count poor 23-hour images when ^{99m}Tc-labelled antigranulocyte antibodies were used. In this clinical example, although the uptake at the focal area of interest was mild, SUV_{max} quantification of uptake radiolabelled antigranulocyte antibodies across multiple time points provided quantifiable evidence of the absence of progression in leucocyte accumulation, thereby confirming absence of active infection in the suspected zone between the cement and tibial shaft. In terms of SUV change, although no reference range for reactive- versus infective-labelled leucocyte accumulation exists, the relatively stable SUV_{max} in the region of mild uptake between 5 and 23 hours was regarded as indicative of reactive change rather than a low-grade infection. Confirmation of absence of infection helped further clinical decision to perform arthrodesis.

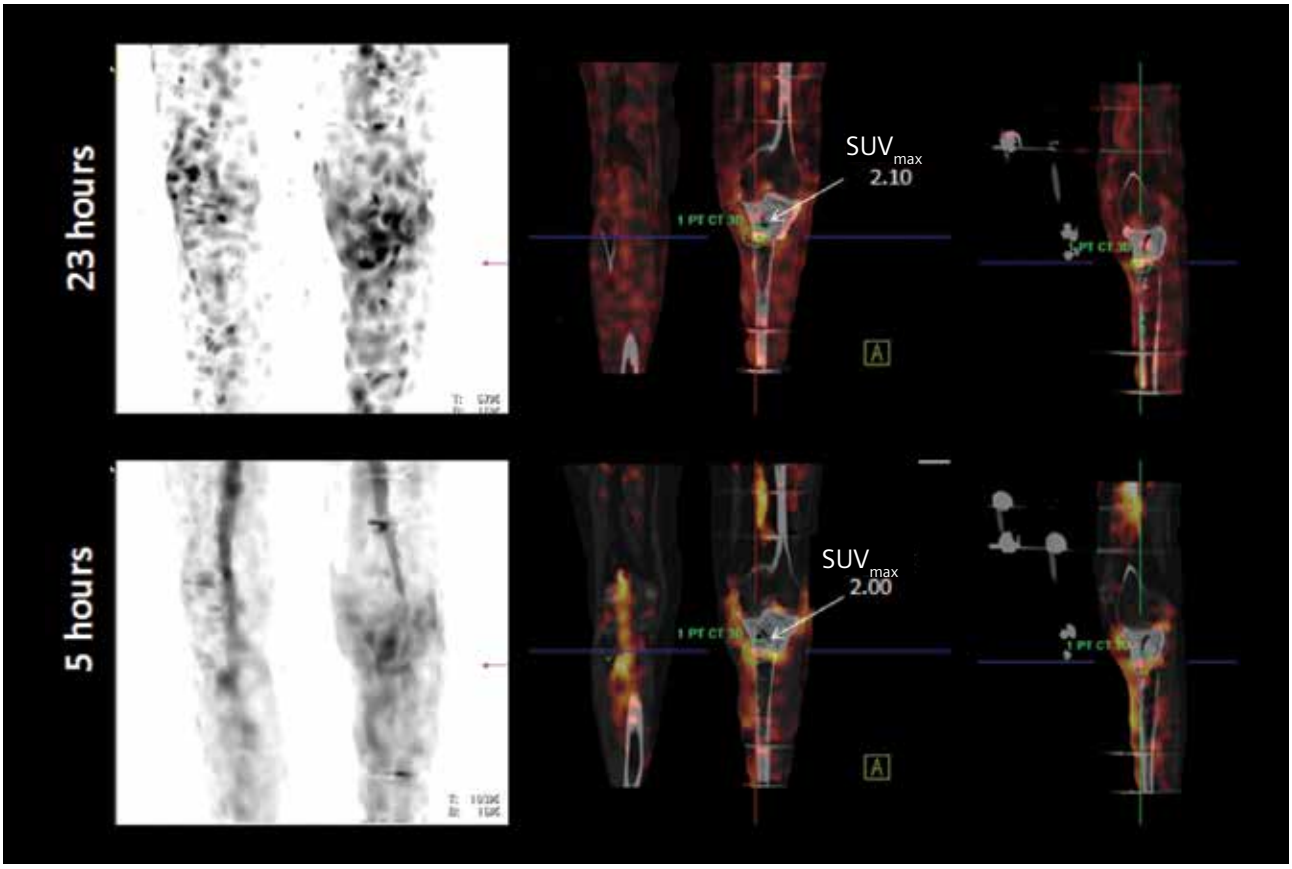

Figure 3: MIP of SPECT and fused images of the sequential 5- and 23-hour SPECT/CT study show slight increase in uptake in the zone separating the cement spacer occupying the region of the proximal tibia and the tibial shaft, with an SUV_{max} of 2.00 in the 5-hour study which remains relatively unchanged to 2.10 at 23 hours, suggesting an absence of active infective foci.

Conclusion

Quantification of SPECT tracer uptake has the potential to support evaluation of suspected infective foci, assess degree of infection and evaluate therapy response. CT helped localize the stable tracer uptake to the region adjacent to the cement spacer likely to show reactive changes, thereby helping accurate evaluation with SPECT/CT. ■

Examination Protocol

Scanner: Symbia Intevo

SPECT	
Injected dose	730 MBq (19.73 mCi) ^{99m}Tc antigranulocyte antibodies
Scan delay	5 and 23 hours post injection
Acquisition	64 projections, 5 hr post injection 20 sec/stop; 23 hr post injection 30 sec/stop
CT	
Tube voltage	130 kV
Tube current	17 eff mAs
Slice collimation	16 x 1.2 mm
Slice thickness	2 mm

* Symbia Intevo and xSPECT Quant are not commercially available in all countries. Due to regulatory reasons their future availability cannot be guaranteed. Please contact your local Siemens organization for further details.

The statements by Siemens customers described herein are based on results that were achieved in the customer's unique setting. Since there is no "typical" hospital and many variables exist (e.g., hospital size, case mix, level of IT adoption) there can be no guarantee that other customers will achieve the same results.

Case 2

Follow-up PET/CT Detects Second Malignancy in Patient with Lung Carcinoma Treated by Radiation Therapy

By Samart Ratchadara, MD, and Ananya Ruangma, MD

Data courtesy of the Department of Nuclear Medicine, Wattanosoth Hospital, Bangkok, Thailand

History
A 66-year-old male presented with a history of a coughing, hemoptysis and evidence of a left hilar lung mass, which was seen on a chest X-ray and diagnosed as squamous cell carcinoma. The patient underwent Fludeoxyglucose F 18 (^{18}F-FDG)* PET/CT for initial staging. The study demonstrated a hypermetabolic left hilar mass without mediastinal or distant metastases. Therefore, the patient underwent radiation therapy for the lung mass, using 60 Gy delivered by 3D conformal radiation therapy at 2 Gy per fraction, 5 fractions per week. Six weeks after completing radiation therapy, the patient underwent a follow-up ^{18}F-FDG PET/CT.

The follow-up PET/CT was performed on Biograph mCT Flow™** 1 hour after an IV injection of 10 mCi (370 MBq) of ^{18}F-FDG. Following a whole-body contrast CT acquisition, PET was acquired using continuous bed motion (FlowMotion™ technology) at a uniform table speed of 1.0 mm/sec. The study was reconstructed using ultraHD•PET [Time-of-Flight (ToF) and point spread function (PSF)].

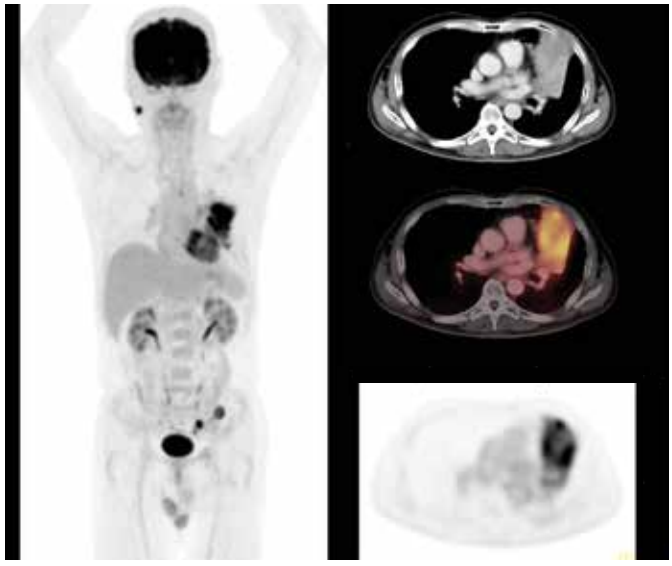

Figure 1: Post-radiation therapy PET/CT shows extensive inflammatory changes in the lung tumor bed in the left hilar region extending to the periphery anteriorly, which is typical of inflammatory infiltrate involving the affected lung lobe in the radiation field. No mediastinal or distal metastatic lesions are visible.

Diagnosis
Demonstrated in Figures 1-2, the post-radiation therapy follow-up PET/CT showed a large area of radiation-induced inflammatory changes leading to lobar consolidation and associated pneumonitis, which explained the CT findings of lobar opacity and hypermetabolism on PET.

Further review of the post-radiation therapy PET/CT revealed focal hypermetabolic lesions in the pelvic bowel, which were initially regarded as physiological uptake. However, careful review of the CT and fused PET/CT transverse slices at the level of the pelvic lesions demonstrated an eccentric mass lesion involving a region of the sigmoid colon, with corresponding hypermetabolism at the

* Indications and important safety information on Fludeoxyglucose F 18 injection can be found on page 41. The full prescribing information can be found on pages 62-64.

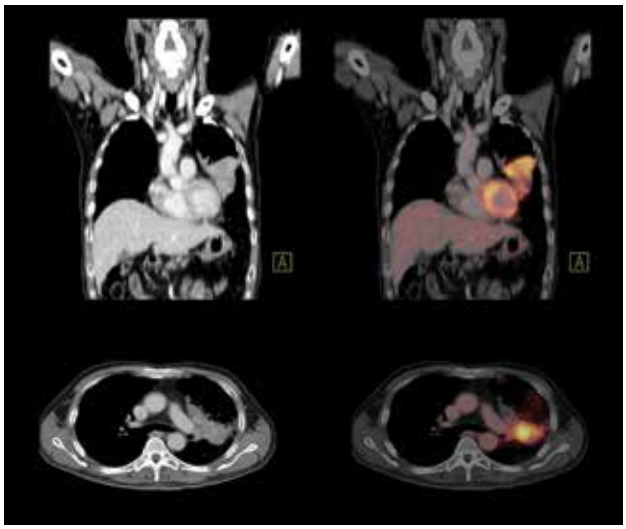

Figure 2: Contrast CT and fused PET/CT images show lobar consolidation with sharp delineation of lobar fissures and pneumonitis at the edges of the consolidation. Patchy hypermetabolism seen on fused PET/CT images reflect inflammation.

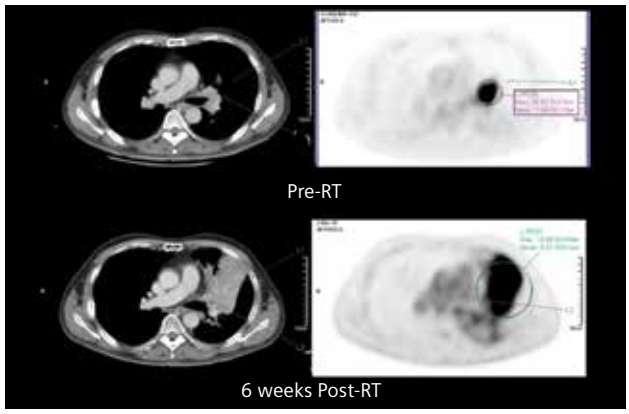

Figure 3: CT and PET transverse slices at the level of the left hilar tumor compared to pre- and post-radiation therapy (RT) PET/CT show a smaller hypermetabolic hilar mass in the pre-therapy PET (SUV_{max} 14.8), with a large area of consolidation and avid glucose uptake (SUV_{max} 10.8) involving the entire lobar segment seen in the post-therapy PET/CT, secondary to post-radiation inflammation. The comparison between the two scans and the uptake suggests resolution of the tumor with superimposition of the uptake related to the post-radiation inflammation.

tumor edge extruding into the colonic cavity (*Figure 4*). The other focal pelvic bowel hypermetabolism lateral to the sigmoid mass lesion appeared to be physiological uptake.

Based on the defined hypermetabolic mass lesion in the sigmoid colon, the pre-therapy PET/CT was reviewed to assess the colonic uptake initially and compare it to the follow-up PET/CT.

The focal bowel lesion was seen in the initial study, but was interpreted as physiological bowel uptake (*Figure 5*). The follow-up study, however, suggested a lesion suspicious for malignancy. A colonoscopy was performed, and a biopsy from the involved segment revealed an adenocarcinoma in the sigmoid colon (*Figure 6*).

Comments

This case illustrates the value of PET/CT for detecting second malignancy in patients with known cancer, and for assessment of tumor metabolism following standard conformal radiation therapy in lung carcinoma in which the inflammation-related hypermetabolism and consolidation may complicate interpretation of the lung tumor's post-radiation response.

Radiation pneumonitis is commonly visible 4 to 12 weeks following completion of radiation therapy involving the lung fields, although the extent of pneumonitis may vary among patients. In a study involving 24 patients with lung cancer who were treated with conformal radiation therapy (mean tumor dose = 55.8 Gy) and who underwent ^{18}F-FDG PET/CT 25-83 days (median = 59 days) post-therapy, PET/CT demonstrated significant radiation pneumonitis in 11 patients.[1] There was a linear correlation between dose to normal lung and level of tracer uptake and SUV with predominant involvement of the volume of lung irradiated >20 Gy. The high tracer uptake related to radiation pneumonitis in the tumor bed may complicate visual and quantitative estimation of tumor response if post-radiation therapy PET/CT is performed following completion of radiation. In this context, studies have shown that PET/CT during the course of radiation therapy, particularly just after delivery of 40-45 Gy to the tumor, may be useful in accurate assessment of tumor response without excess radiation pneumonitis.[2]

A second primary tumor in this patient was detected due to the persistent focal hypermetabolism and eccentric sigmoid colon mass lesion defined by PET/CT and contrast CT. Although the focal hypermetabolism was visualized in the initial staging PET/CT, it was interpreted as physiological uptake in the absence of a significant mass lesion. Findings like these highlight the need for high-quality thin-slice CT with oral and intravenous contrast and good bowel preparation as part of a routine PET/CT study, even in situations where the abdomen is not the primary focus for the tumor or metastases.

Lung cancer is often associated with the presence or development of second primary cancer. In a study involving 860 patients with lung cancer, 44 patients subsequently developed second primary tumors.[3] Of the 44 patients, 31% were second lung

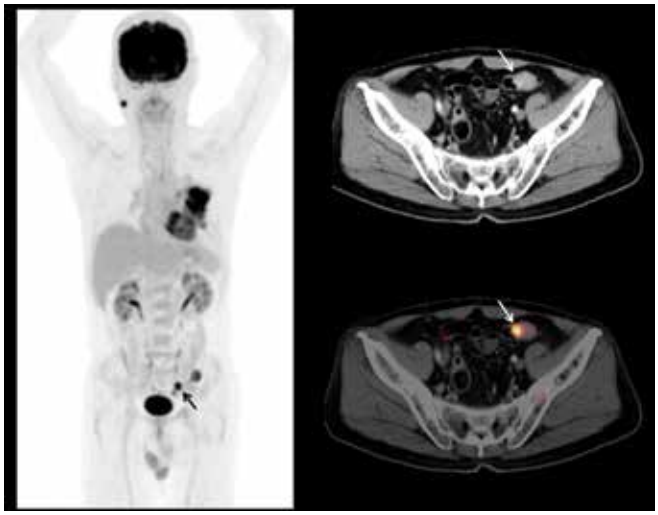

Figure 4: A focal hypermetabolic pelvic lesion (*arrow*) corresponds to eccentric mass encroaching into the cavity in the sigmoid colon, with maximum increase in uptake at the irregular tumor edge eroding into the colonic cavity. The appearance of the colonic mass and the associated hypermetabolism suggests a malignant colonic lesion rather than a benign polyp or physiological colonic uptake.

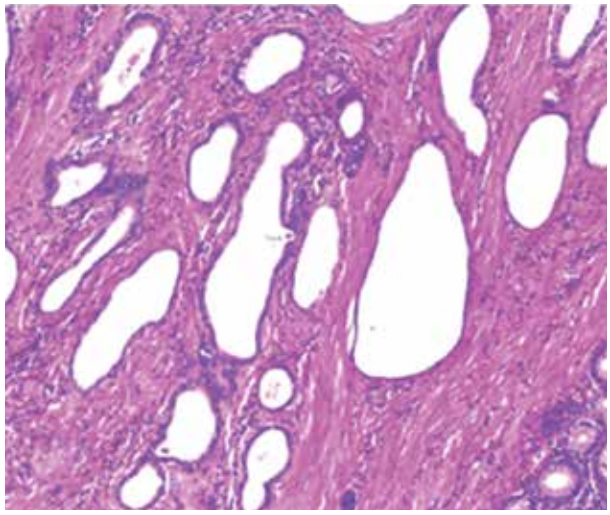

Figure 6: Histopathology of the tubulovillous adenoma in the sigmoid colon detected on PET/CT shows well-differentiated adenocarcinoma with high-grade dysplasia without lymphovascular or perineural invasion.

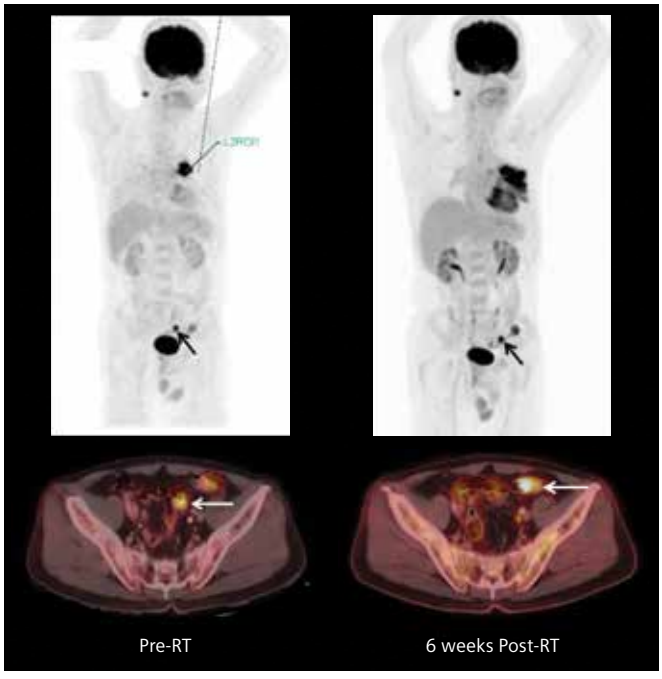

Figure 5: Comparison of PET maximum intensity projection (MIP) images of pre-therapy and 6 weeks post-radiation therapy PET/CT studies show a hypermetabolic primary lung tumor and the extensive radiation-induced inflammation in the tumor base and adjacent lung lobe. The PET images also show hypermetabolic focal colonic uptake in the initial study and in the follow-up study, and there is a slight increase in the degree of hypermetabolism assessed visually in the follow-up. The fused PET/CT images at the same level show a slight shift in the exact location of the affected bowel between the two studies, which is related to the extent of bowel luminal filling and bowel gas. The bowel lumen and associated hypermetabolism in the pre-therapy study was interpreted as physiological uptake since there was no clearly defined mass lesion. However, persistent hypermetabolism in the same colonic focal region with a well-defined mass lesion eroding into the lumen as defined on the follow-up PET/CT suggests a potentially malignant lesion.

tumors, 20% were head and neck cancers, 11% were uroepithelial tumors and only 4.5% were colorectal cancers. The same study also identified 148 patients who developed lung cancer preceded by development of another primary cancer. Of these, 20% were head and neck cancers, 10% were uroepithelial cancers and 6% were colorectal cancers.

Conclusion

This study highlights the need to carefully evaluate PET/CT studies of lung and head and neck cancers for second malignancies. Improved lesion detectability and higher lesion contrast achieved with ToF PET and high-quality CT with contrast and thin slices should help delineation and characterization of such early second malignancies. ■

References:
[1] McCurdy et al. *Radiother Oncol.* July 2012; 104(1): 52-57.
[2] Edet Sanson et al. *Radiotherapy and Oncology.* 102 (2012): 251–257.
[3] Duchateau et al. *Chest.* 2005; 127: 1152–1158.

* The full prescribing information can be found on pages 62-64.

** Biograph mCT Flow is not commercially available in all countries. Due to regulatory reasons its future availability cannot be guaranteed. Please contact your local Siemens organization for further details.

The statements by Siemens customers described herein are based on results that were achieved in the customer's unique setting. Since there is no "typical" hospital and many variables exist (e.g., hospital size, case mix, level of IT adoption) there can be no guarantee that other customers will achieve the same results.

Examination Protocol

Scanner: Biograph mCT Flow

PET	
Injected dose	370 MBq (10 mCi) ^{18}F-FDG
Scan delay	1 hour
Acquisition	Continuous bed motion, uniform table speed (1.0 mm/sec)

CT	*Whole-body contrast*
Tube voltage	120 kV
Tube current	82 eff mAs
Slice collimation	64 x 0.6 mm
Slice thickness	5 mm

Fludeoxyglucose F 18 5-10mCi as an IV injection Indications and Usage

Fludeoxyglucose F 18 Injection is indicated for positron emission tomography (PET) imaging in the following settings:

- **Oncology:** For assessment of abnormal glucose metabolism to assist in the evaluation of malignancy in patients with known or suspected abnormalities found by other testing modalities, or in patients with an existing diagnosis of cancer.
- **Cardiology:** For the identification of left ventricular myocardium with residual glucose metabolism and reversible loss of systolic function in patients with coronary artery disease and left ventricular dysfunction, when used together with myocardial perfusion imaging.
- **Neurology:** For the identification of regions of abnormal glucose metabolism associated with foci of epileptic seizures.

Important Safety Information

- **Radiation Risks:** Radiation-emitting products, including Fludeoxyglucose F 18 Injection, may increase the risk for cancer, especially in pediatric patients. Use the smallest dose necessary for imaging and ensure safe handling to protect the patient and health care worker.
- **Blood Glucose Abnormalities:** In the oncology and neurology setting, suboptimal imaging may occur in patients with inadequately regulated blood glucose levels. In these patients, consider medical therapy and laboratory testing to assure at least two days of normoglycemia prior to Fludeoxyglucose F 18 Injection administration.
- **Adverse Reactions:** Hypersensitivity reactions with pruritus, edema and rash have been reported; have emergency resuscitation equipment and personnel immediately available.

Full prescribing information for Fludeoxyglucose F 18 Injection can be found on pages 62-64.

Dosage Forms and Strengths

Multiple-dose 30 mL and 50 mL glass vial containing 0.74 to 7.40 GBq/mL (20 to 200 mCi/mL) of Fludeoxyglucose F 18 injection and 4.5 mg of sodium chloride with 0.1 to 0.5% w/w ethanolas a stabilizer (approximately 15 to 50 mL volume) for intravenous administration.

Fludeoxyglucose F 18 injection is manufactured by Siemens' PETNET Solutions, 810 Innovation Drive, Knoxville, TN 39732

Case 3

Sequential PET/CT and CT Perfusion Predicting Chemoradiation Therapy Response in a Patient with Multifocal Cervical Carcinoma

By Elizabeth Kidd, MD, Department of Radiation Oncology, Stanford University Hospital, California, USA
Dimitre Hristov, PhD, Department of Radiation Oncology, Stanford University Hospital, California, USA
Partha Ghosh, MD, Molecular Imaging Business Line, Siemens Healthcare

Data courtesy of the Department of Radiation Oncology, Stanford University Hospital, California, Stanford, USA

History
A 70-year-old female with stage IIB cervical carcinoma, a large primary tumor with extension to uterine fundus, was referred for radiation therapy. The patient underwent a PET/CT for evaluation of the primary tumor and for radiation therapy planning. A table-stepping, whole-organ, dynamic CT perfusion study was performed to evaluate the tumor blood flow following the PET/CT study.

The PET/CT study was performed on a Biograph™ mCT 64, following an IV injection of 9.8 mCi (363 MBq) of Fludeoxyglucose F 18 (^{18}F-FDG)*. Following an initial diagnostic CT, whole-body PET was performed in step-and-shoot mode (7 bed positions, acquired in 3 min/position). The study was acquired on a flat table top in treatment position. The study was reconstructed with ultraHD•PET. The CT perfusion study of the pelvis was performed after an IV injection of100 ml of contrast at 5 ml/sec Table-stepping, whole-organ, dynamic CT acquisition was performed for the pelvis (100 kV, 150 mAs, 32 x 1.2 mm slice collimation, 5 mm reconstructed slice thickness).

PET and CT for the pelvis were exported to the Varian Eclipse™ treatment planning system and gross tumor volume (GTV), clinical target volume (CTV) and planning target volume (PTV) were contoured on PET/CT-fused images.

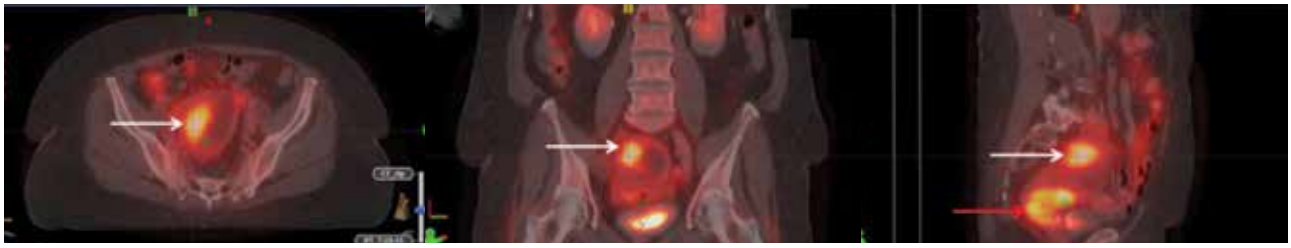

Figure 1: Large primary cervical tumor with extension into the uterine fundus demonstrated on PET/CT as a bi-lobed mass, with a mass in the cervix (*red arrow*) and a mass in the uterine fundus (*white arrows*). No lymph node metastases are identified.

* Indications and important safety information on Fludeoxyglucose F 18 injection can be found on page 41. The full prescribing information can be found on pages 62-64.

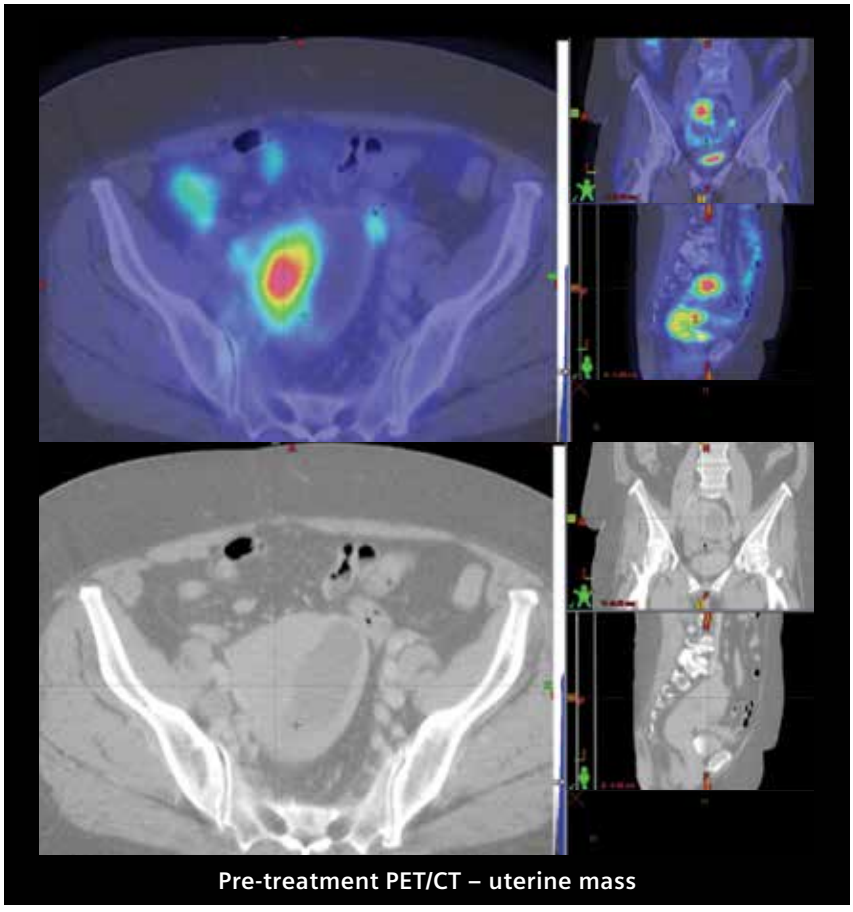

Pre-treatment PET/CT – uterine mass

Figure 2: CT and PET/CT-fused images at the level of the uterine fundus mass showing a large hypermetabolic mass in the upper right uterine wall with dilated uterine cavity.

Figure 3: The CT perfusion study performed prior to initiation of radiation therapy. CT perfusion results shown at the level of the uterine mass demonstrated in Figure 2. The CT transverse slice through the tumor mass at the uterine mass shows contrast enhancement in the entire mass. The CT perfusion parametric maps show high tumor blood flow (165 ml/100 ml/min) in the region with maximum perfusion (*ROI no 5; white arrow*).

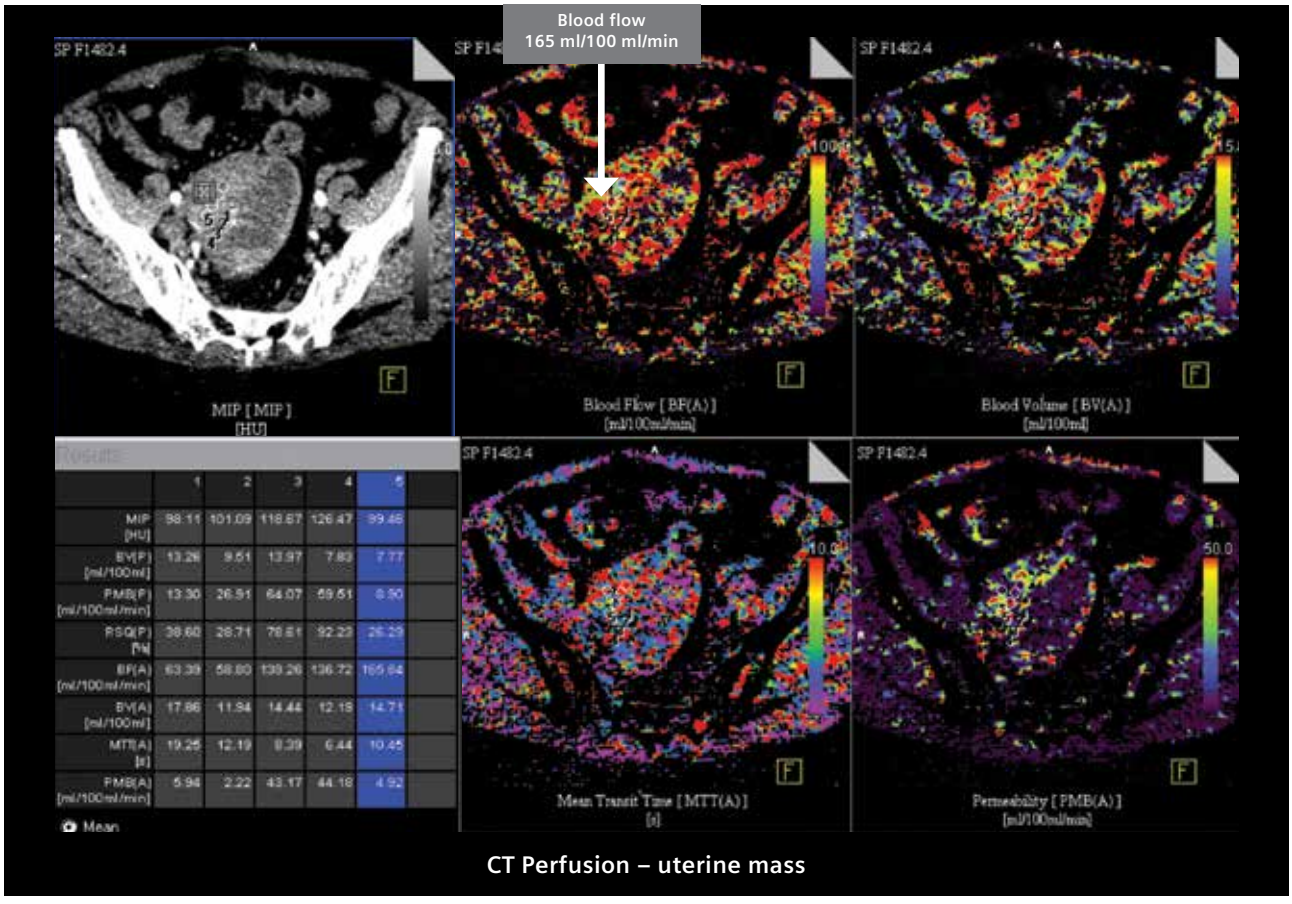

CT Perfusion – uterine mass

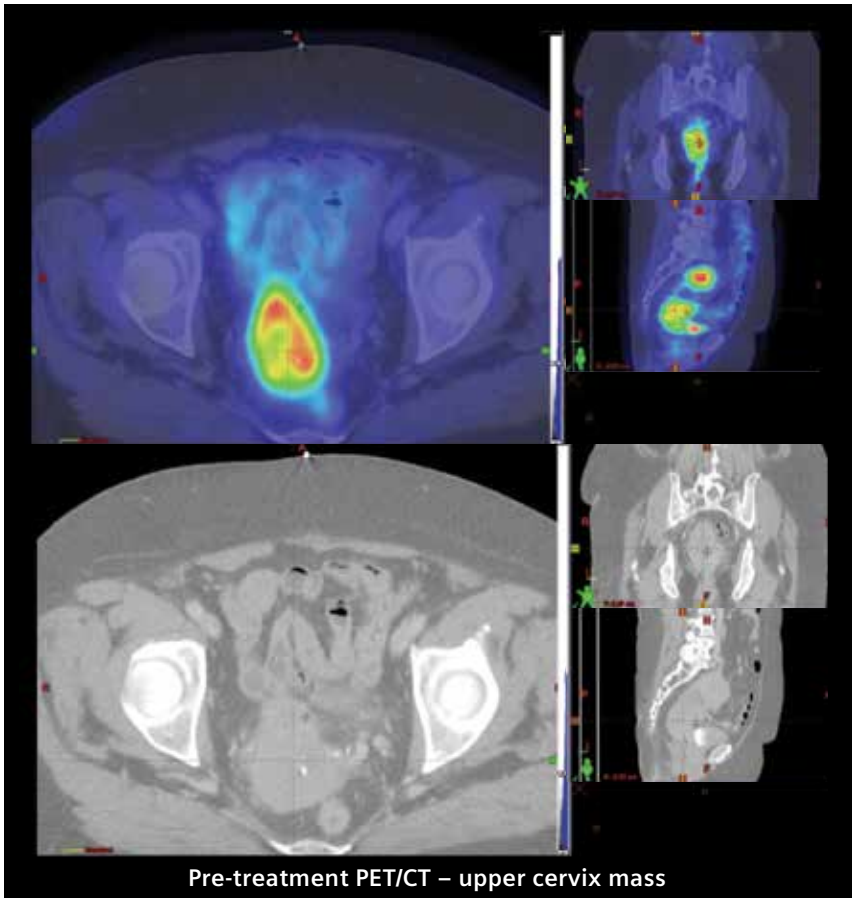

Figure 4: Pre-therapy PET/CT images at the level of the upper cervical tumor mass shows increased tracer uptake in the mass with slightly decreased uptake in the center.

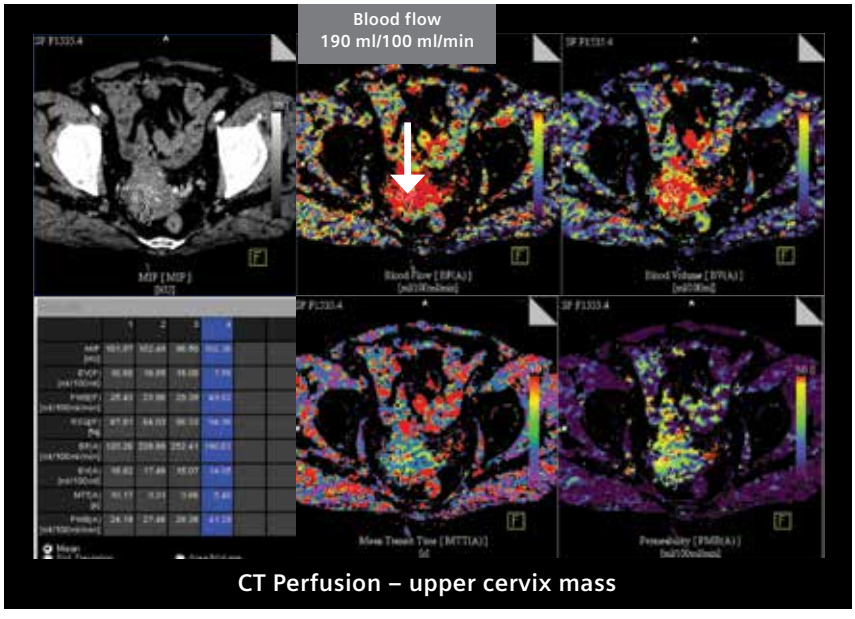

Figure 5: CT perfusion parametric maps show high tumor blood flow, with the highest flow of 190 ml/100 ml/min (*ROI 2, white arrow*).

Diagnosis

As seen in Figures 1-7, the tumor was an elongated mass with two distinct ^{18}F-FDG-avid portions, one in the cervix and another in the uterine fundus. All segments of this multifocal tumor showed high tumor perfusion on the CT perfusion and showed hypermetabolism on the PET/CT.

Comments

Multifocal cervical carcinoma is usually preceded by micro invasive squamous cell carcinoma, which is usually associated with extensive spread of carcinoma in situ (CIS) into the uterine corpus, salpinx and vagina.[1] This kind of tumor is very aggressive and associated with high angiogenetic potential.[2] In this patient, the PET/CT showed high uptake in both the cervical and uterine fundus component of the tumor. High tumor blood flow seen on CT perfusion correlated with high tracer uptake in the cervical and uterine mass, which reflected the high tumor vascularity. The aggressive growth of the tumor reflected the high vascularity and the hypermetabolism with increased tumor blood flow and blood volume, as well as high tracer uptake.

Higher tumor vascularity has shown to be associated with increased risk of recurrence, increased invasiveness and metastatic potential in cervical cancer.[3] However, higher tumor vascularity is associated with improved response to radiation therapy.[4] The complete metabolic response demonstrated by a follow-up PET/CT 6 months after completion of treatment also reflected the excellent response to chemoradiation of the hypervascular tumor.

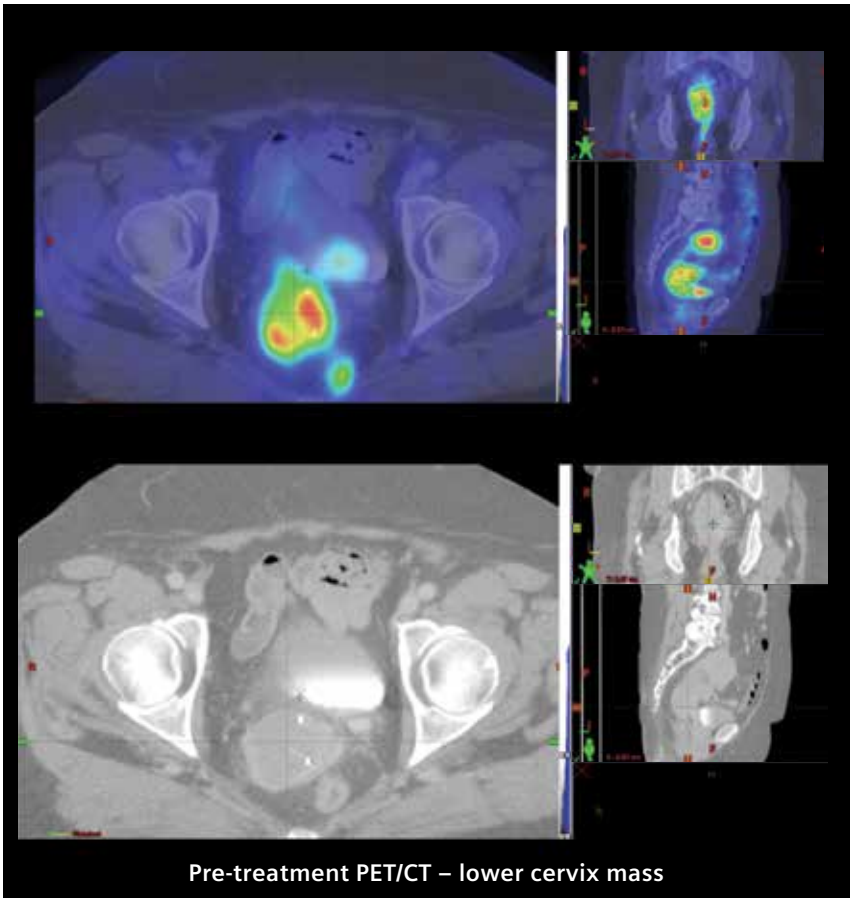

Figure 6: PET/CT at the level of the lower cervical mass also shows high tumoral tracer uptake.

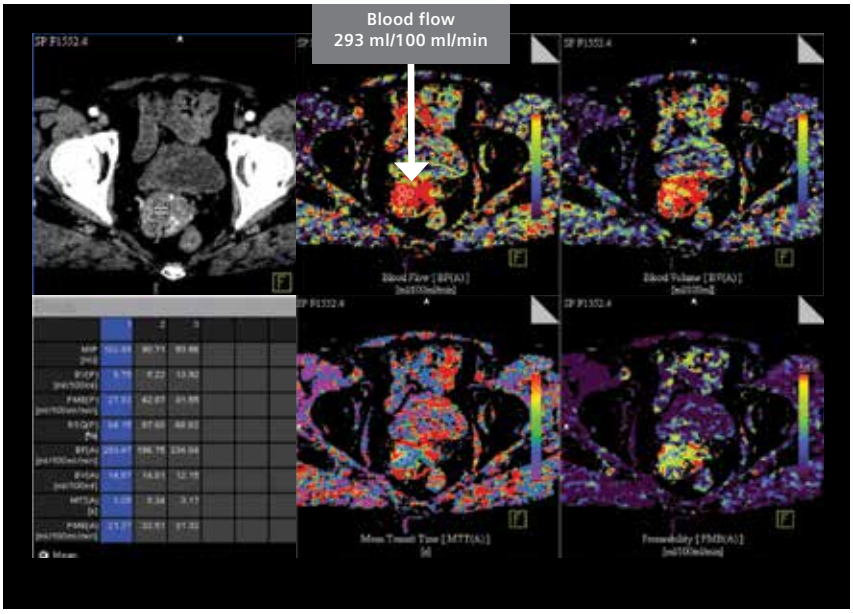

Figure 7: CT perfusion maps at the level of lower cervical mass also show very high blood flow (*highest blood flow value of 293 ml/100 ml/min in ROI 1, white arrow*).

Conclusion

Tumor hypervascularity determined by CT perfusion and tumor metabolism determined by PET/CT can provide prognostic information and guide chemoradiation therapy in patients with locally advanced cervical carcinoma. ■

Examination Protocol

Scanner: Biograph mCT 64

PET	
Injected dose	9.8 mCi (363 MBq) ^{18}F-FDG
Scan delay	1 hour
Acquisition	7 bed positions; 3 min/position
CT	
Tube voltage	100 kV
Tube current	150 mAs
Slice collimation	32 x 1.2 mm
Slice thickness	5 mm

References:
[1] Yang et al. *Eur J Gynaecol Oncol.* 2014; 35(5): 600-603.
[2] Sotiropoulos et al. *Eur J Gynaecol Oncol.* 2004; 25(2): 219-221.
[3] Alcazar et al. *Gynecol Oncol.* 2002 Feb; 84(2): 258-262.
[4] Gasinska et al. *Acta Oncol.* 2002; 41(5): 437-443.

* Indications and important safety information on Fludeoxyglucose F 18 injection can be found on page 41. The full prescribing information can be found on pages 62-64.

The statements by Siemens customers described herein are based on results that were achieved in the customer's unique setting. Since there is no "typical" hospital and many variables exist (e.g., hospital size, case mix, level of IT adoption) there can be no guarantee that other customers will achieve the same results.

Case 4

Femoral Condylar Eminence Impingement in Double Knee Hemiarthroplasty Visualized by xSPECT Bone

By Christian Waldherr, MD, and Martin Sonnenschein, MD

Data courtesy of the Department of Radiology & Nuclear Medicine, Klinik Engeried Bern, Lindenhofgruppe, Bern, Switzerland

History
A 62-year-old male underwent bilateral hemiarthroplasty of the left knee joint for severe arthritis to help preserve the cruciate ligaments. Following surgery, the patient complained of progressive left knee joint pain that was exacerbated during walking. Possibly caused by joint loosening, a periprosthetic fracture or mal-alignment, the patient was referred for a three-phase bone scintigraphy, followed by SPECT/CT of the knee performed on Symbia Intevo™*.

Immediately following an IV injection of 600 MBq (16.22 mCi) of ^{99m}Tc MDP, initial planar dynamic and blood pool images were acquired. Three hours post-injection, planar whole-body and SPECT/CT acquisition were performed on the thigh. After a thin-slice diagnostic CT (110 kV, 120 mAs CareDose), SPECT was acquired with 64 projections at 20 seconds per stop. xSPECT Bone™* reconstruction was performed using CT-based zone information. The xSPECT Bone data was then fused with CT for a final evaluation.

Diagnosis
xSPECT Bone, CT and fused images of the left knee showed focal areas of bone stress in the medial tibial intercondylar eminence adjacent to the tibial component of the medial hemiprosthesis, as well as in the lateral

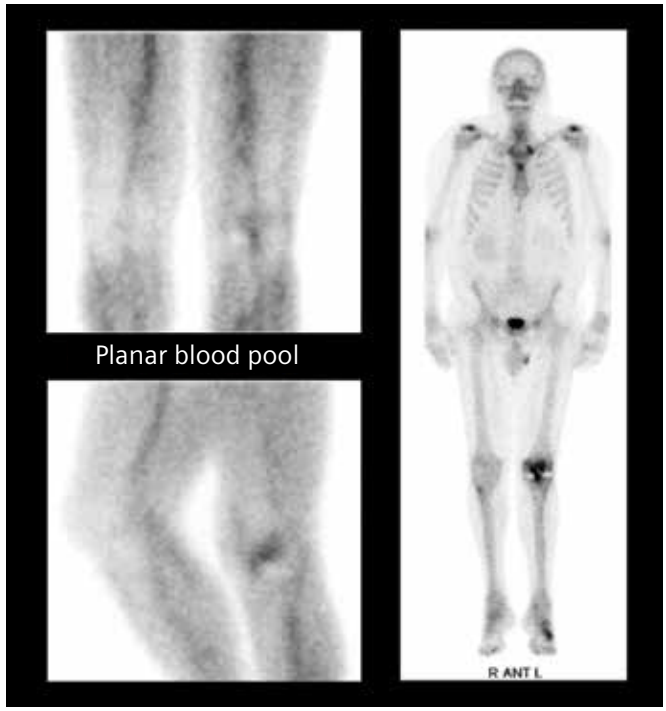

Figure 1: Initial planar blood pool images show hyperemia in the central part of the left knee joint. The delayed whole-body scan shows increased uptake in the left knee around the patella and in the tibial intercondylar eminences between the two tibial plates of the bilateral left knee hemiprosthesis.

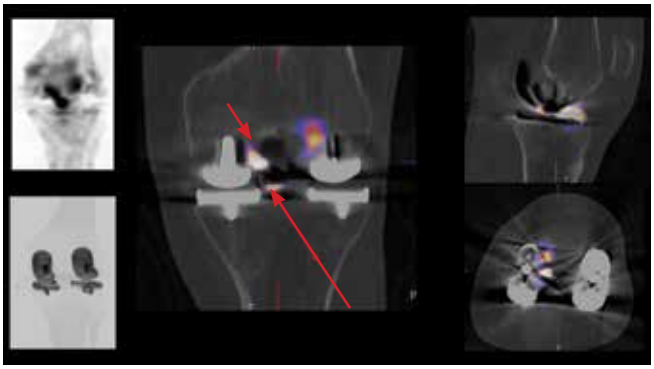

Figure 2: xSPECT Bone maximum intensity projection (MIP) images (*upper left corner*) show focally increased tracer uptake in the tibial intercondylar eminence and in the lateral margin of the medial femoral condyle. xSPECT Bone/CT fusion shows increased uptake in the medial tubercle of the intercondylar eminence of the left tibia located adjacent to the medial tibial plate of the hemiarthroplasty prosthesis (*long red arrow*), which suggests impingement of the medial intercondylar eminence with the edge of the tibial component in the prosthesis. The lateral edge of the medial femoral condyle shows focally increased uptake predominantly in the anterior aspect (*short red arrow*), which suggests impingement of the edge of the femoral component of the medial hemiarthroplasty prosthesis with an osteophyte in the adjacent condylar bone (which demonstrates the highest uptake and is probably the main site of the knee pain).

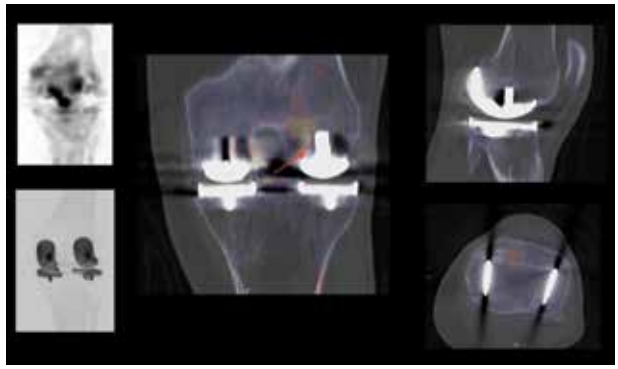

Figure 3: xSPECT Bone and fused images also show mild increases in uptake in the medial margin of the lateral femoral condyle at the junction of the edge of the femoral component of the lateral hemiarthroplasty prosthesis, which suggests stress reaction due to overload at the insertion of the anterior cruciate ligament. The fused images show normal position and alignment of the femoral and tibial components of both hemiarthroplasty prosthesis with no periprosthetic osteolysis or fractures, no lucent zones between the tibial and femoral component stems and the bone. The tibial plates and the femoral condylar component of the prosthetic joints appear properly fixed without dislocation, mal-alignment or subluxation. The CT MIP image (*left lower corner*) also show both hemiprosthesis to be properly positioned and aligned. This suggests an absence of prosthetic loosening, malpositioning or periprosthetic fracture.

margin of the medial femoral condyle in contact with the edge of the medial femoral prosthetic component (*Figure 2-3*). The location and focal nature of the uptake suggested an impingement between the bone and the edges of the prosthesis. And the maximum intensity of the medial femoral condylar uptake suggested that the femoral condylar impingement was the primary driver of the post-bilateral hemiarthroplasty knee pain. CT and fused images also showed proper positioning and alignment of the prosthesis and adjacent bone without any lucent zones, osteolysis or fracture, which excluded loosening, mal-alignment or overload stress.

Comments

Post-hemiarthroplasty knee pain is often caused by the tibial or femoral prosthetic component edges impinging with the adjacent bone, as shown in this example. Prosthetic loosening, infection, stress overload of the prosthetic joint, malposition, mal-alignment and joint component subluxation all may cause pain as well. SPECT/CT is highly accurate in properly characterizing the nature of the bony pathology, especially differentiating from overload stress, periprosthetic fracture, loosening and impingement.

Conclusion

In this case, xSPECT Bone sharply defined the small focal uptake at the impingement sites and provided improved definition of cortical margins, thereby enabling precise localization of the impingement site. ■

* Symbia Intevo and xSPECT Bone are not commercially available in all countries. Due to regulatory reasons their future availability cannot be guaranteed. Please contact your local Siemens organization for further details.

The statements by Siemens customers described herein are based on results that were achieved in the customer's unique setting. Since there is no "typical" hospital and many variables exist (e.g., hospital size, case mix, level of IT adoption) there can be no guarantee that other customers will achieve the same results.

Examination Protocol

Scanner: Symbia Intevo

SPECT	
Injected dose	600 MBq (16.22 mCi) ^{99m}Tc MDP
Scan delay	3 hours
Acquisition	64 projections, 20 sec/stop

CT	
Tube voltage	110 kV
Tube current	120 eff mAs
Slice collimation	16 x 2.5 mm
Slice thickness	3 mm

Case 5

xSPECT Bone Delineates Vertebral End Plate Fracture in Lumbar Spine in a Patient with Lumbar Interbody Fusion

By Christian Waldherr, MD, and Martin Sonnenschein, MD

Data courtesy of the Department of Radiology & Nuclear Medicine, Klinik Engeried Bern, Lindenhofgruppe, Bern, Switzerland

History
A 61-year-old female, who underwent a fusion of the facets of L5-S1 more than 10 years ago, followed by a more recent lumbar interbody fusion of L2-L4, presented with lower back pain that she had for a month. A fracture of the fused facets (L4-S1) was suspected. The CT study was equivocal due to metal artifacts. MR of the lumbar spine was also inconclusive due to metal artifacts. The patient was referred for a ^{99m}Tc MDP SPECT/CT study to evaluate for facet fracture or loosening, or fracture of the spinal stabilization screws.

The study was performed three hours following an IV injection of 600 MBq (16.22 mCi) of ^{99m}Tc MDP. The initial planar study was followed by SPECT/CT acquisition. A non-contrast diagnostic CT was performed followed by SPECT acquisition (64 projections, 20 sec/stop). xSPECT Bone™* reconstruction was performed using CT-based zone information.

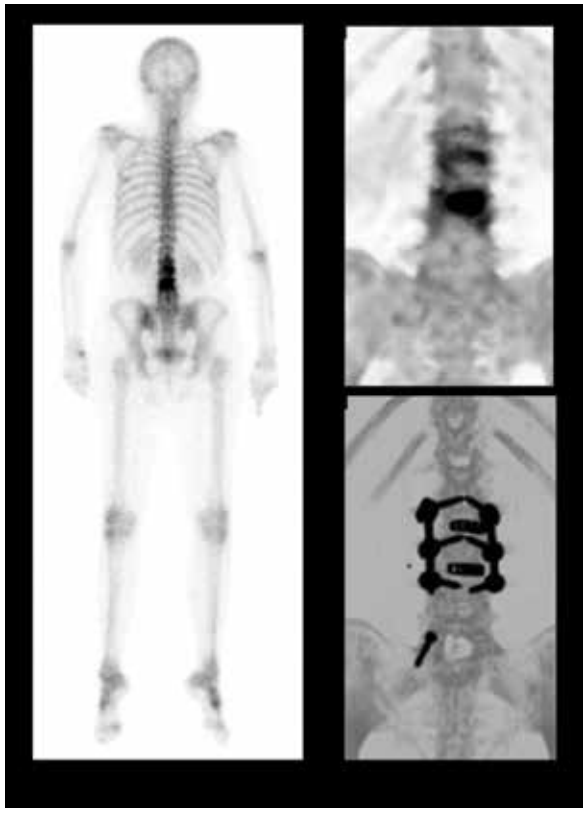

Figure 1: Planar bone scan shows increased uptake in the bodies of L4 and L3 vertebrae. xSPECT Bone maximum intensity projection (MIP) shows gross increase in tracer uptake in the upper part of the body of the L4 vertebrae and the L3-L4 intervertebral disc level, as well as mildly increased uptake in the L2-L3 intervertebral disc space. MIP of CT shows the orientation of the lumbar interbody fusion screws and end plates through the facets and bodies of L2, L3 and L4 vertebrae, as well as interbody cages in L2-L3 and L3-L4 intervertebral disc spaces. The solitary screw fusing right L5 facet to S1 reflects past surgery without evidence of any osseous stress.

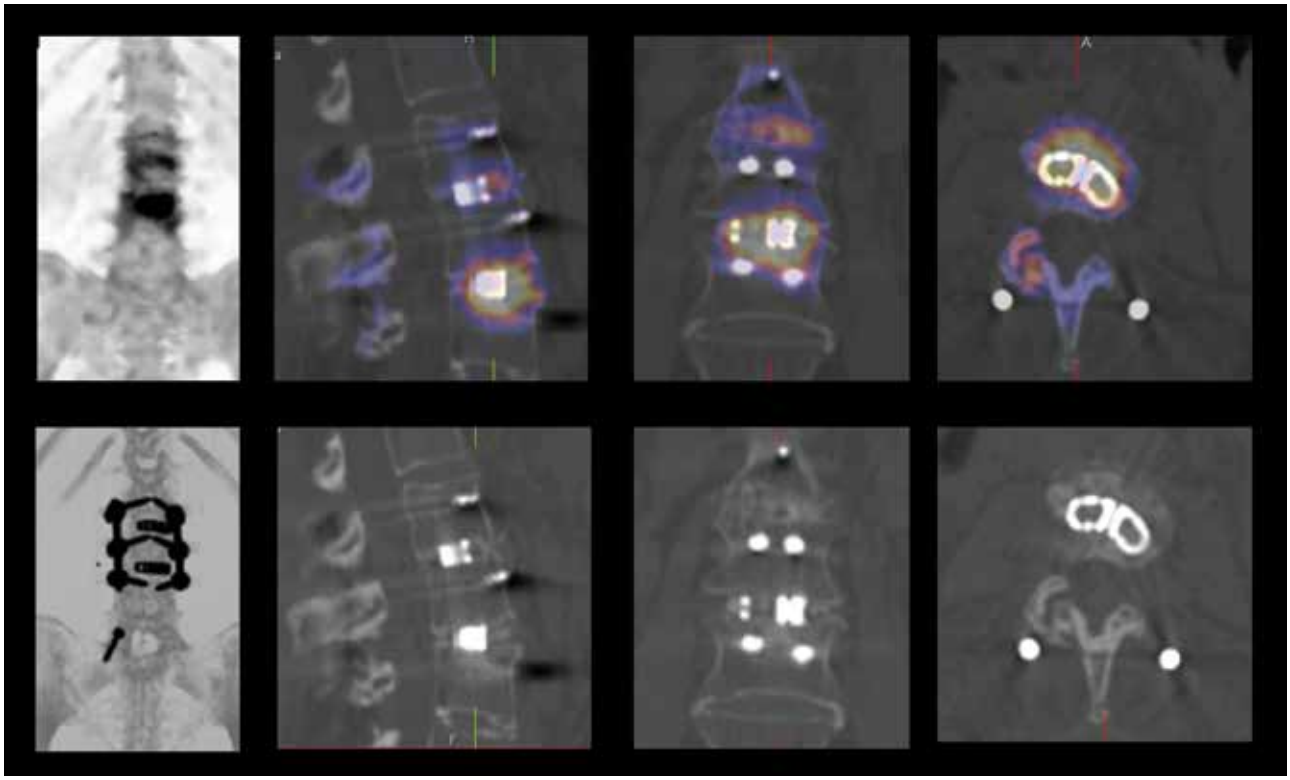

Figure 2: Fusion of xSPECT Bone and CT shows increased tracer uptake in the upper end plate and adjacent body of the L4 vertebrae and the L3-L4 intervertebral disc space. There is also mild uptake in the L2-L3 intervertebral disc space. CT images at the level of the upper end plate of the L4 vertebrae show irregularity in the surface of the upper end plate, which reflects impression fracture along with subchondral sclerosis. The right upper intra-articular facet of the L4 vertebrae shows increased uptake probably reflecting increased shear stress due to instability of lumbar fusion.

Diagnosis

Demonstrated in Figures 1-5, xSPECT Bone and CT findings revealed an impression fracture of the upper end plate of the L4 vertebrae with resultant instability leading to hypermetabolism in the intervertebral disc spaces and right-sided intra-articular facet joints. The study showed no evidence of pedicle screw loosening or interbody cage displacement. The older L5-S1 screw appeared stable, as well. The L4 upper end plate impression fracture may have been precipitated by osteoporosis or sudden weight-bearing stress.

Comments

CT and MR, in this case, were not helpful in defining the actual cause of the back pain. Although CT demonstrated the end plate irregularities, the metal in the interbody cages and pedicle screws made the interpretation difficult. It was not possible to establish the main cause of the pain since the body of the L2-L3 and L3-L4 vertebrae had similar levels of end plate erosion. With xSPECT Bone, the sharp

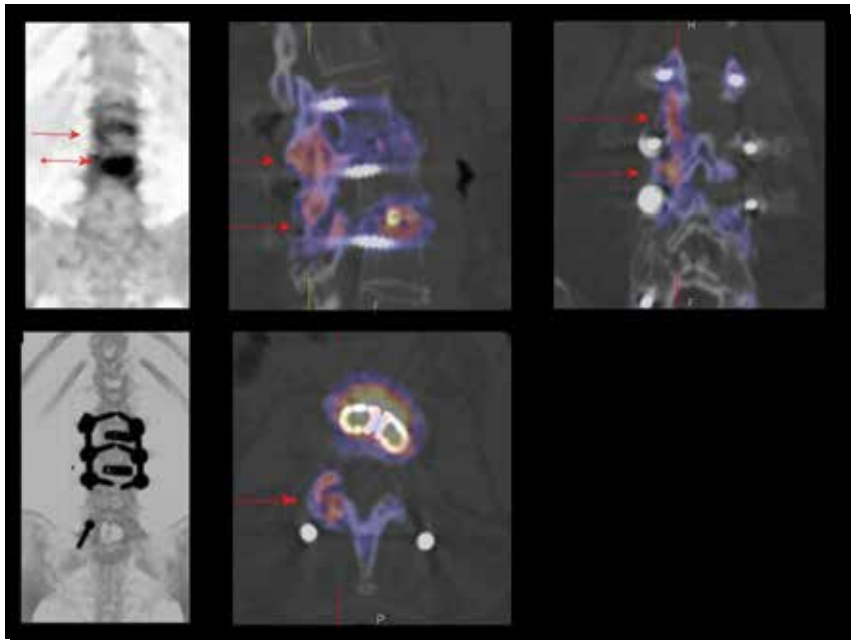

Figure 3: CT and fused images at the level of the body of the L3 vertebrae show increased uptake in the right intra-articular facets of the L2, L3 and L4 vertebrae (*arrows*), which reflects osseous stress related to vertebral instability secondary to impression fracture of upper end plate of the L4 vertebrae. The facet uptakes are not related to the path of the pedicle screws, and no evidence of loosening of the lumber fixations screws are evident on CT or fused images.

Figure 4: Fused images at the level of the lumbar interbody fusion screws and fixation plates show mild uptake in the laminar bone adjacent to the right pedicle screw, which reflects minor shear stress. There is no evidence on CT or xSPECT Bone of loosening of the pedicle screws.

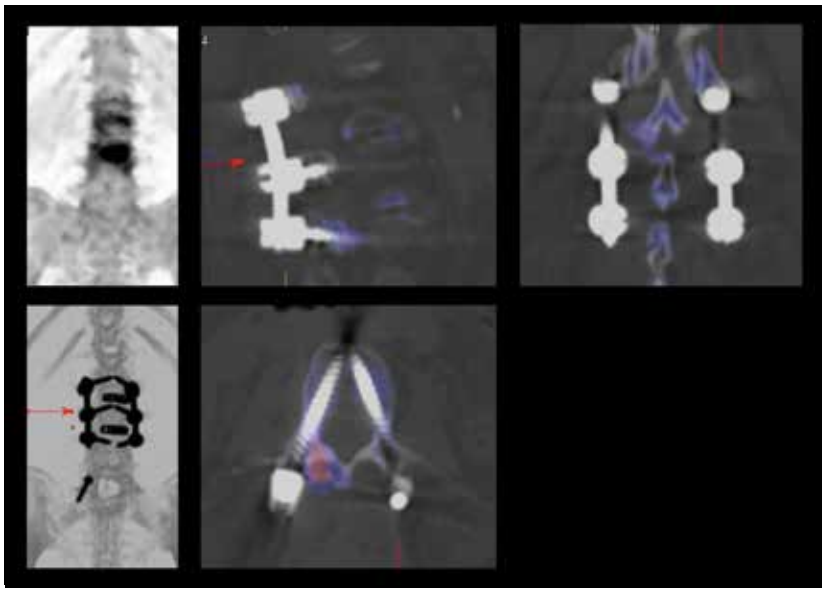

Figure 5: Fused images at the level of pedicle screw fusing right L5 and S1 facets shows absence of abnormal tracer uptake and no CT evidence of loosening or fracture.

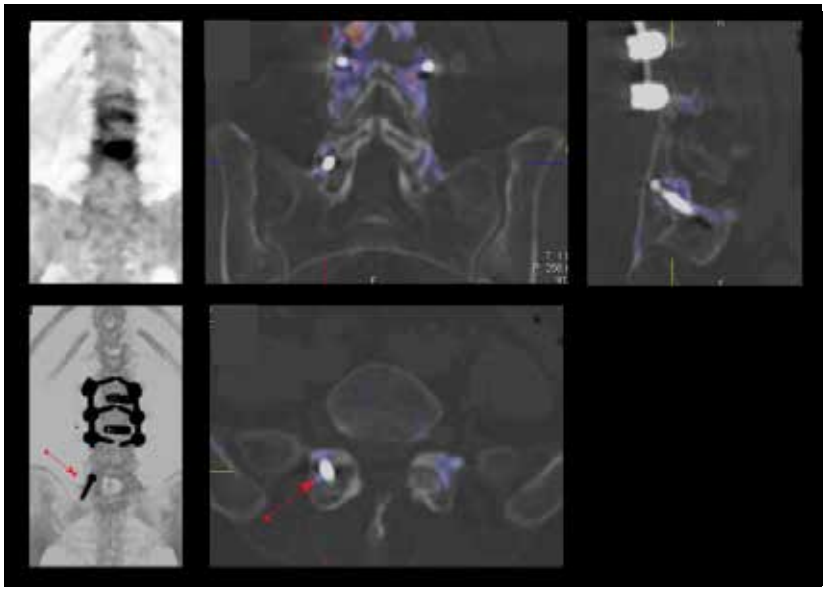

Figure 6: Thin-slice diagnostic CT with sharp kernel to define bony details shows irregular surface of the upper end plate of the L4 vertebrae (*red arrows*). The upper end plate of the L3 vertebrae also shows significant irregularities (*white arrow*). However, due to xSPECT Bone, the increased uptake in the upper end plate of the L4 vertebrae is clearly defined as the cause of the pain due to the osseous stress related to impression fracture and related instability. Although the upper end plate of the L3 vertebrae also shows irregularity, the degree of hypermetabolism is mild and suggests insignificant relevance to the pain. The artifacts due to metal in the pedicle screws and interbody cages hinder the true assessment of the bony abnormalities and disc space erosion. The CT also shows significant bone loss, loss of trabeculae, suggestive of osteoporosis, which may have been instrumental in the impression fracture of the L4 upper end plate.

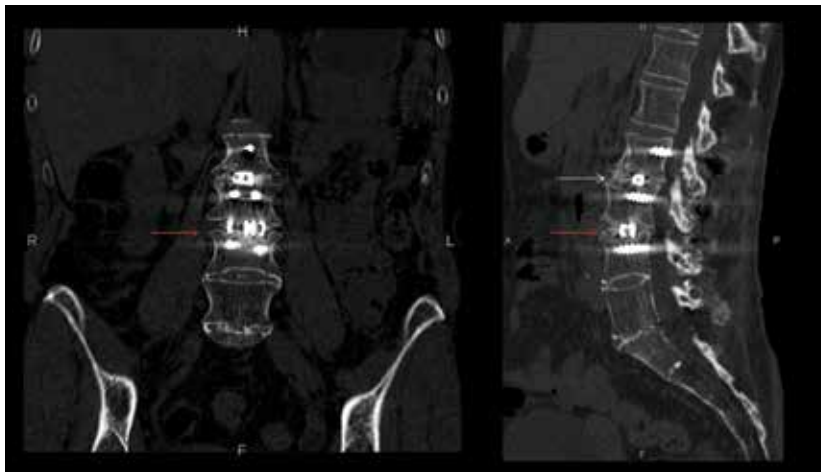

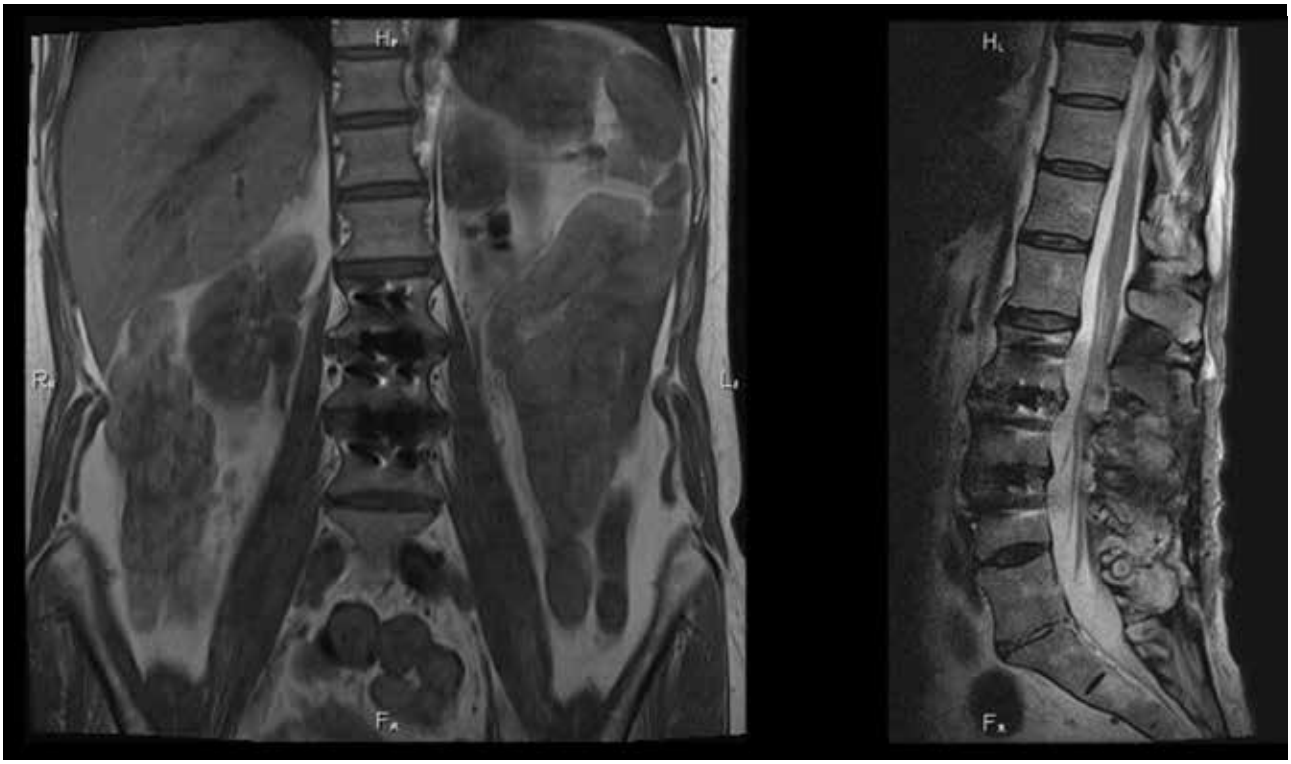

Figure 7: Corresponding T1 MR images show severe signal loss in the L2-L3 and L3-L4 intervertebral disc spaces and adjacent vertebral bodies due to metal artifacts which makes the study non diagnostic.

definition of the hypermetabolism in the L4 upper end plate and adjacent intervertebral disc space was conclusive of the diagnosis of impression fracture. There was no focal uptake typical of pedicular screw loosening and CT also did not show any periprosthetic resorption.

Conclusion

xSPECT Bone sharply defined the vertebral body and facet margins. It also showed high intensity and clear margins of the abnormal uptake, especially in the end plates, which improved the appreciation of skeletal hypermetabolism in the periprosthetic zones, facet joints and intervertebral discs when fused with CT. As a result, xSPECT Bone helped physicians corroborate the suspicion of an impression fracture and provide a conclusive diagnosis. ■

Examination Protocol

Scanner: Symbia Intevo™*

SPECT	
Injected dose	600 MBq (16.22 mCi) ^{99m}Tc MDP
Scan delay	3 hours
Acquisition	64 projections, 20 sec/stop
CT	Non-contrast diagnostic
Tube voltage	110 kV
Tube current	120 eff mAs
Slice collimation	16 x 2.5 mm
Slice thickness	3 mm

* Symbia Intevo and xSPECT Bone are not commercially available in all countries. Due to regulatory reasons their future availability cannot be guaranteed. Please contact your local Siemens organization for further details.

The statements by Siemens customers described herein are based on results that were achieved in the customer's unique setting. Since there is no "typical" hospital and many variables exist (e.g., hospital size, case mix, level of IT adoption) there can be no guarantee that other customers will achieve the same results.

Case 6

PET/CT-guided Ablation of Liver Metastases in a Patient with Breast Carcinoma

By Paul B. Shyn, MD

Data courtesy of Brigham & Women's Hospital, Boston, Massachusetts, USA

History

A 65-year-old woman with right breast carcinoma and axillary lymph node metastases diagnosed in 1999 was treated with surgery followed by chemotherapy. Recurrence in the lung, bone and mediastinal lymph nodes was diagnosed in 2009, and the patient was prescribed chemotherapy with Taxol®, Herceptin® and Avastin®. New liver metastases were detected in 2012 and chemotherapy was restarted. Chemotherapy with Taxol was stopped due to neuropathy. In view of a solitary liver metastasis amenable to percutaneous ablation, the patient was admitted for image-guided microwave ablation.

Diagnosis

Microwave ablation was planned to include PET/CT metabolic imaging guidance and Ammonia N 13 (^{13}N-NH_3)* PET perfusion imaging to confirm complete tumor ablation with an adequate margin. On the day of ablation therapy, the patient was injected with 5 mCi (185 MBq) of Fludeoxyglucose F 18 (^{18}F-FDG)**.

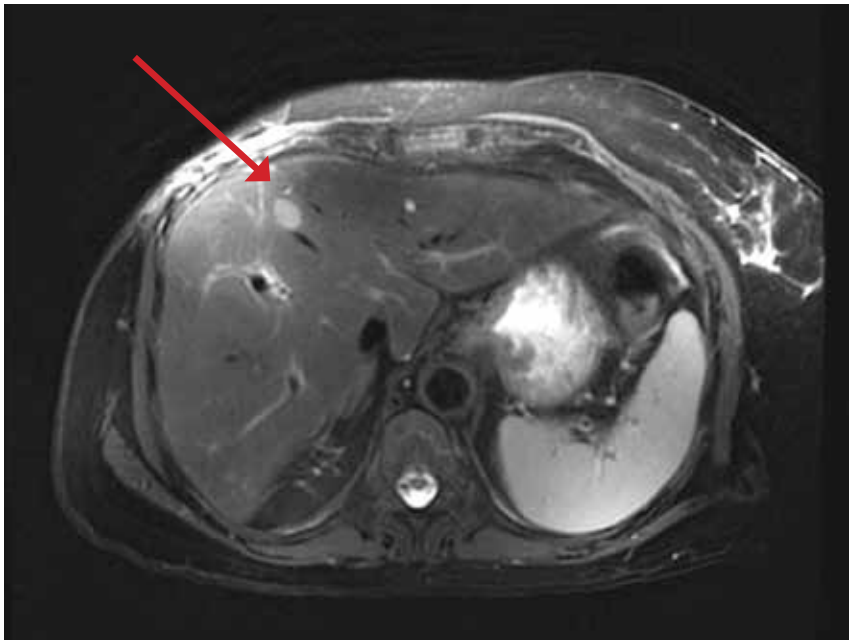

Figure 1: Fat-suppressed breath-hold MRI image acquired before ablation therapy shows hyperintense solitary liver metastases.

* Indications and important safety information on Ammonia N 13 injection can be found on page 55. The full prescribing information can be found on pages 65-66.

** Indications and important safety information on Fludeoxyglucose F 18 injection can be found on page 41. The full prescribing information can be found on pages 62-64.

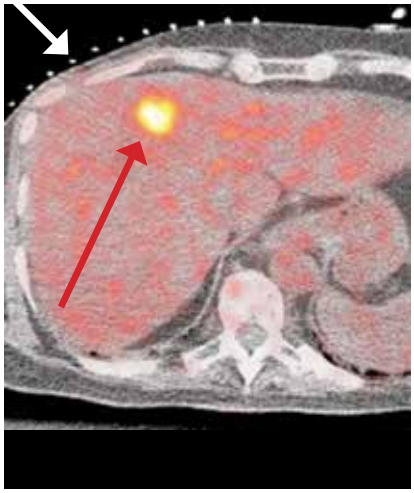

Figure 2: Planning PET/CT performed with 30-second breath hold by suspending ventilation during the general anesthesia. Fused PET/CT image shows hypermetabolic solitary liver metastases (*red arrow*) corresponding to the hyperintense lesion seen on MRI. The opaque skin markers (*white arrow*) represent a grid attached to the patient's skin over the liver for determining the coordinates for insertion of the ablation probe.

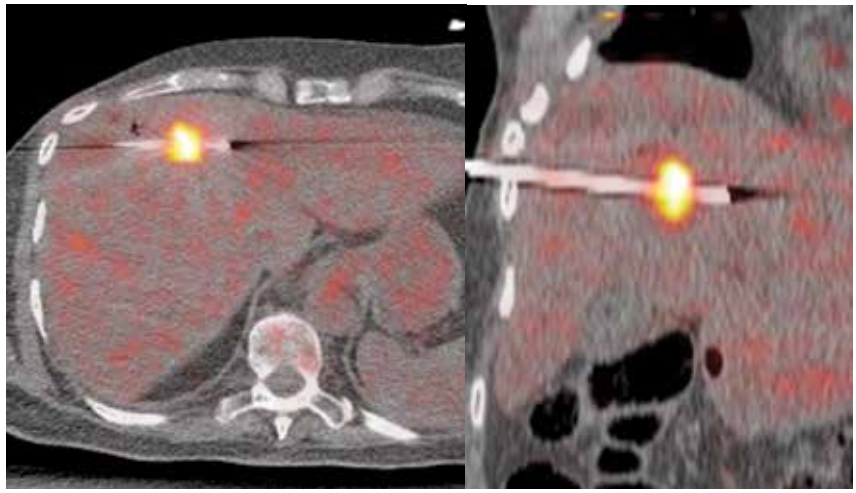

Figure 3: Axial- and coronal-fused PET/CT images acquired with suspended ventilation confirm excellent microwave ablation probe placement through tumor in two planes.

about 1 hour prior to ablation therapy. The patient was brought into the advanced multi-modality image-guided operating (AMIGO) suite equipped with a Biograph™ mCT PET/CT (configured with CT fluoroscopy). The patient was placed under general anesthesia. An initial planning PET/CT was performed with the patient supine in the treatment position. Both CT and PET acquisitions were acquired at a single bed position over the liver during suspended respiration under the general anesthesia. The CT and PET images were both acquired during a single 30-second breath hold.

Following the planning PET/CT, the fused PET/CT images were used to plan the insertion location for the microwave ablation probe, its direction and distance to the tumor. A single microwave probe was inserted following a small skin incision and advanced to the planned depth based on the PET/CT. Following the insertion, another PET/CT similar to the initial one using another 30-second suspension of ventilation to eliminate respiratory motion was performed. Following the acquisition, the fused images of the second PET/CT were checked to assess the position of the tip of the microwave probe.

The microwave ablation was performed following confirmation of accurate probe placement by PET/CT. Following the procedure, a PET perfusion study was performed to demonstrate the perfusion of the unablated liver surrounding the ablation zone. Ten mCi (370 MBq) of ^{13}N-NH_3 were infused intravenously into the patient. Three minutes after initiation of infusion, a single bed position PET/CT study was acquired during a 60-second breath hold with suspended ventilation in order to eliminate respiratory motion.

The trapped ^{18}F-FDG within the tumor after ablation enabled persistent visualization of the entire tumor. Perfusion PET imaging with ^{13}N-NH_3 demonstrated the unablated normal liver. The "cold" band between the "hot" tumor and the "warm" perfused liver represents the ablation margin. The ablation margin is the amount of normal liver tissue ablated beyond the tumor. Decisions regarding further microwave ablation were based on the extent of the halo around the ^{18}F-FDG-avid tumor. As demonstrated in Figure 4, the entire tumor is surrounded by the halo and appeared to have been ablated completely with the desired minimum 1 cm ablation margin. It is important to avoid microwave damage to normal liver tissue as much as possible, and to limit the halo to a few centimeters around the tumor. Based on the PET image following ^{13}N-NH_3 infusion, the microwave procedure was concluded.

The patient was discharged from hospital and underwent a follow-up CT after 4 months.

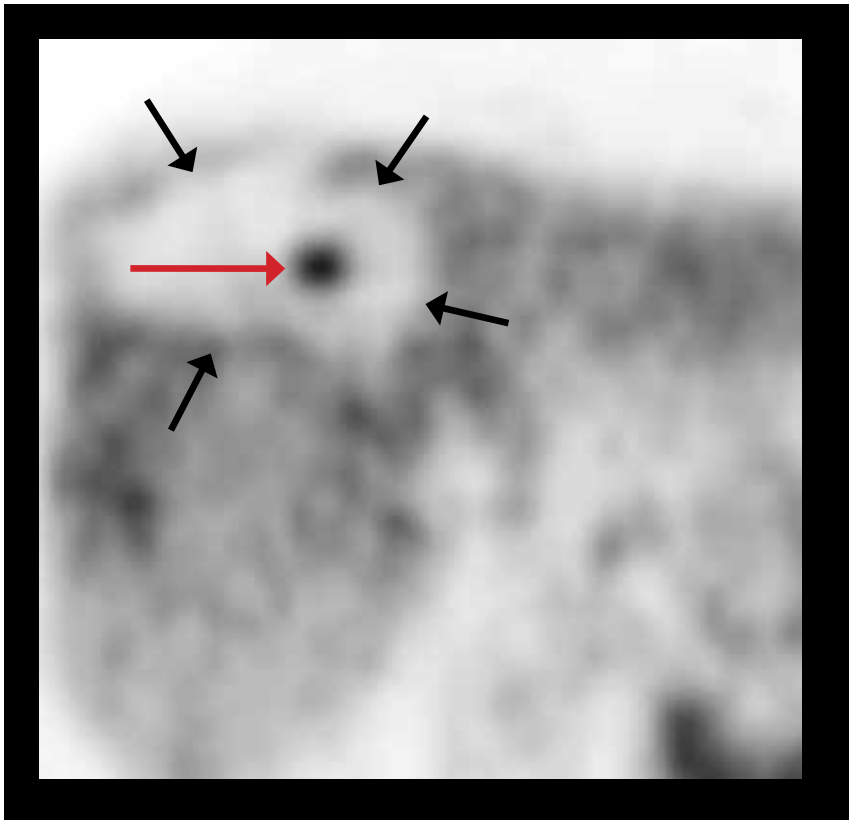

Figure 4: PET-only image acquired after infusion of ^{13}N-NH_3 shows perfusion activity surrounding the non-perfused hypometabolic ablation margin (*black arrows*), which in turn surrounds the tumor (*red arrow*) (containing persistent high activity due to trapped ^{18}F-FDG within the tumor despite microwave ablation).

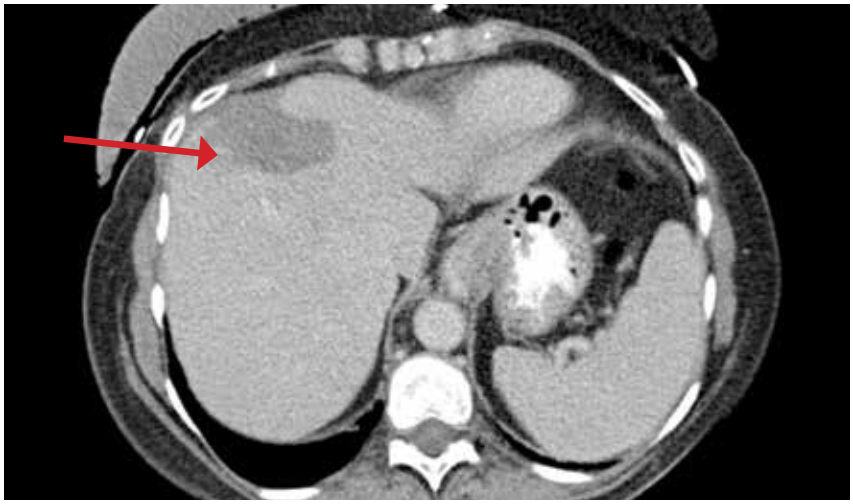

Figure 5: Follow-up CT shows hypo-intensity in the entire ablation zone (*red arrow*) correlating well with the zone of hypo-perfusion delineated by the ^{13}N-NH_3 perfusion PET, but with some involution. No tumor recurrence in the tumor bed or elsewhere in the liver is visible.

Comments

Microwave ablation is a technique that achieves tumor cell killing by heating of tissues through agitation of water molecules, ultimately leading to coagulation necrosis. Tracer uptake within the tumor does not dissipate following microwave ablation as evident from the persistent ^{18}F-FDG uptake within the tumor immediately after the microwave ablation, as demonstrated by the PET image acquired during ^{13}N-NH_3 infusion following ablation. Sainani et al.[1] demonstrated dissipation of ^{18}F-FDG activity in liver and lung tumors following radiofrequency or cryoablation. Dissipation of ^{18}F-FDG activity within the tumor following microwave ablation cannot be used to indicate the extent of tumor ablation. Proper delineation of the extent of ablation is important in assessing the completeness of ablation coverage of the tumor.

In this context, perfusion imaging with ^{13}N-NH_3 PET/CT is useful, since it highlighted the perfused, unablated liver surrounding the ablation zone. The ablation zone was then characterized by the photopenic band (ablation margin) surrounding the persistently "hot" tumor, as seen in the clinical example. Follow-up CT after 4 months from the procedure showed an excellent result with no evidence of tumor bed recurrence.

Conclusion

Breath-hold PET/CT is helpful during such ablation procedures since it helps eliminate respiratory motion-related artifacts both in PET and CT, and ensures accurate coregistration of PET and CT so determination of the tumor size and extent of perfusion abnormality is possible. A 30- to 60-second breath-hold

PET/CT is easily accomplished using suspended ventilation during general anesthesia. Although count statistics for 30- or 60-second PET acquisitions are low, particularly with an injected dose of only 5 mCi, the high sensitivity of the PET/CT system and the lack of respiratory motion enables adequate image quality as required for the ablation procedure. ■

Examination Protocol

Scanner: Biograph mCT

PET	
Injected dose	5 mCi (185 MBq) ^{18}F-FDG
Scan delay	1 hour
Acquisition	30-sec suspended ventilation
CT	
Tube voltage	120 kV
Tube current	30 mAs
Slice collimation	32 x 1.2 mm
Slice thickness	5 mm

References:
[1] Sainani et al. *J Vasc Interv Radiol.* 2011 Mar; 22(3): 354-360.

* The full prescribing information can be found on pages 65-66.

** Indications and important safety information on Fludeoxyglucose F 18 injection can be found on page 41. The full prescribing information can be found on pages 62-64.

The statements by Siemens customers described herein are based on results that were achieved in the customer's unique setting. Since there is no "typical" hospital and many variables exist (e.g., hospital size, case mix, level of IT adoption) there can be no guarantee that other customers will achieve the same results.

Ammonia N 13 Injection for Intravenous Use
Indications and Usage

Ammonia N 13 Injection is a radioactive diagnostic agent for Positron Emission Tomography (PET) indicated for diagnostic PET imaging of the myocardium under rest or pharmacologic stress conditions to evaluate myocardial perfusion in patients with suspected or existing coronary artery disease.

Important Safety Information

- **Radiation Risks:** Ammonia N 13 Injection may increase the risk of cancer. Use the smallest dose necessary for imaging and ensure safe handling to protect the patient and health care worker.
- **Adverse R\eactions:** No adverse reactions have been reported for Ammonia N 13 Injection based on a review of the published literature, publicly available reference sources and adverse drug reaction reporting systems. However, the completeness of these sources is not known.

Siemens' PETNET Solutions is a manufacturer of Ammonia N 13 Injection. Indication and important safety information as approved by the US Food and Drug Administration can be found at the links below for Ammonia N 13, adult dose 8-12 mCi, administered by intravenous injection.

Full Prescribing Information for Ammonia N 13 Injection can be found on pages 65-66.

Ammonia N 13 Injection is manufactured by Siemens' PETNET Solutions, 810 Innovation Drive, Knoxville, TN 39732

Case 7

PET/CT-guided Cryoablation of Perisplenic Metastases in a Patient with Uterine Cancer

By Paul B. Shyn, MD

Data courtesy of Brigham & Women's Hospital, Boston, Massachusetts, USA

History

A 57-year-old female was diagnosed with endometrial adenocarcinoma in December 2013, and was treated with total laparoscopic hysterectomy, bilateral salpingo-oophorectomy, and complete pelvic and limited peri-aortic lymphadenectomy. Histopathology revealed carcinosarcoma of the uterus. The patient subsequently received chemotherapy including carboplatin and Taxol®. In October 2014, a recurrent pelvic mass was detected on CT and the patient underwent a pelvic tumor resection, including resection of the terminal ileum and anterior rectum. This was followed by pelvic external beam radiation therapy and concurrent cisplatin.

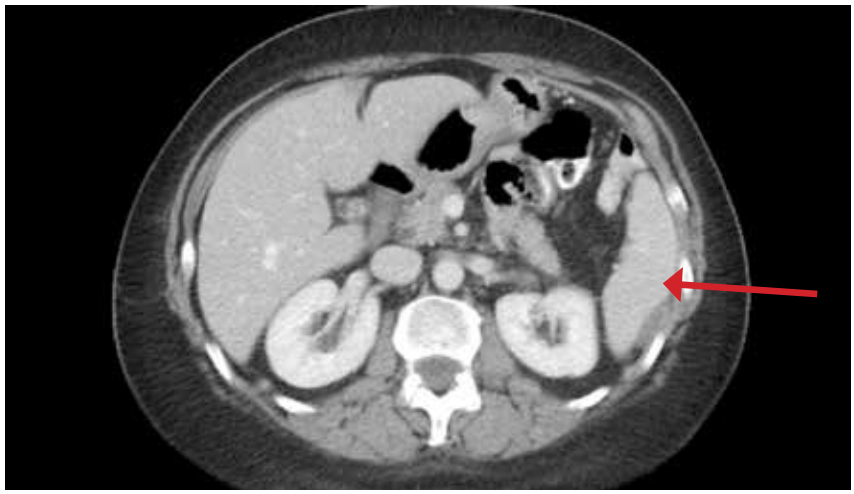

Figure 1: Contrast-enhanced CT performed in June 2015, shows the hypodense mass along the posterolateral border of the spleen (*red arrow*) confirming a solitary peritoneal metastases. No other tumor foci identified.

A follow-up Fludeoxyglucose F 18 (^{18}F-FDG)* PET/CT was performed in February 2015, to evaluate for residual pelvic metastases and new lesions. The PET/CT revealed a markedly ^{18}F-FDG-avid lesion, hypodense on CT, along the posterolateral border of the spleen, which suggested metastatic peritoneal disease. Pelvic metastases were not visualized. Chemotherapy with doxorubicin was initiated, but the patient could not tolerate more than 2 doses.

In view of the presence of a solitary peritoneal metastases located at the posterolateral border of the spleen, which was reconfirmed by another follow-up contrast CT performed in June 2015 (*Figure 1*), it was considered approachable for a percutaneous ablation procedure, the patient was offered ^{18}F-FDG PET/CT-guided percutaneous cryoablation in August 2015.

Diagnosis

The patient was injected with 5 mCi (185 MBq) of ^{18}F-FDG 1 hour prior to initiation of the procedure. The cryoablation procedure was carried out in an AMIGO (Advanced Multimodality Image-Guided Operating) suite, a state-of-the-art operating room that includes PET/CT (Biograph™ mCT) equipped with CT fluoroscopy**. The procedure was performed using

* Indications and important safety information on Fludeoxyglucose F 18 injection can be found on page 41. The full prescribing information can be found on pages 62-64.

general anesthesia and cryoablation technology. The patient was placed prone on the PET/CT table in order to approach the lesion from a posterior and lateral low-intercostal space.

A limited planning PET/CT was performed covering one bed position during a single breath-hold period of 35 seconds, which was achieved by suspending ventilation during general anesthesia. Both the CT and PET acquisitions are obtained during this single suspended respiration. The PET acquisition time was limited to only 15 seconds of this 35-second PET/CT acquisition. Suspended ventilation eliminates respiratory motion of both CT and PET, thereby eliminating motion-related blurring that would otherwise degrade tumor definition and ablation device depiction. The resulting fused PET/CT images were also adequately co-registered.

The perisplenic metastasis had considerably increased in size in the 2 months interval between the CT scan in June 2015, and the ablation procedure in August 2015 (*Figures 2-3*). The position and size of the lesion presented several challenges for cryoablation. The presence of the bowel so close to the anterior margin of the tumor in the prone treatment position presented a risk of injuring the bowel during cryoablation, which could lead to bowel perforation. In order to avoid that complication, infusion of saline with iodinated contrast in the space between the tumor and the bowel was planned, so as to displace the bowel wall away from the tumor and avoid the bowel contact with the cryoablation ice ball. The kidney that was present at the medial margin of the tumor is more tolerant of cryoablation, but care was needed to avoid freezing too much renal parenchyma.

Based on the fused PET/CT images, a plan was made for the cryoablation procedure, including selection of the entry point, as well as the direction and depth of cryoablation probe insertions to achieve complete ablation of the entire tumor with margins. Needle placement for instillation of saline with contrast for bowel displacement was also determined from the planning PET/CT.

Following a small skin incision, the saline infusion needle was inserted under CT fluoroscopic guidance to reach the space between the anterior margin of the tumor and the bowel wall, and a small volume of saline mixed with CT contrast was infused. CT fluoroscopy was used to check the position of the instilled saline.

Following the instillation of saline and the CT fluoroscopic confirmation of increased separation of the bowel wall from the tumor, two cryoablation probes were inserted into the superior and inferior parts of the tumor using fluoroscopic guidance and the PET/CT-based plan. Following probe placement and prior to cryoablation, a single bed position PET/CT was performed using a 35-second suspension of ventilation to acquire both CT and PET without respiratory motion-related blurring or mis-registration.

After PET/CT helped confirm the proper placement of both the cryoablation probes and hydro-displacement needle, the cryoablation was started. PET/CT performed during the cryoablation showed growth of the hypo-dense ice ball encompassing the entire tumor. Cryoablation was followed by thawing and re-freezing of the tumor, which enhances cellular damage/death within a tumor. Immediately after the initial cryoablation, another single bed position PET/CT was performed using a suspended respiration for 35 seconds.

The patient was discharged the following day after an uneventful recovery. She underwent a follow-up MRI the next day to assess the results of the cryoablation and to provide a baseline for future follow-ups. There was a follow-up CT scan after 2 weeks for restaging.

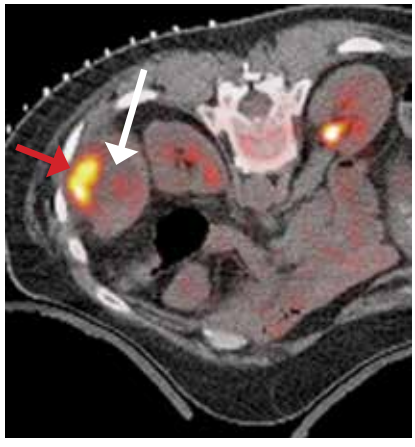

Figure 2: Fused PET/CT image acquired using 35-second suspended ventilation prior to probe placement shows the perisplenic peritoneal mass positioned posterior and lateral to the spleen (*red arrow*). The metastatic mass appears partially necrotic in the medial part of the tumor and indents the spleen (*white arrow*). Compared to the previous CT (June 2015), the metastatic mass appears to have grown significantly in size. Note the radio-opaque skin markers overlying the spleen that are placed in order to help plan the exact coordinates for the placement of the cryoablation probes.

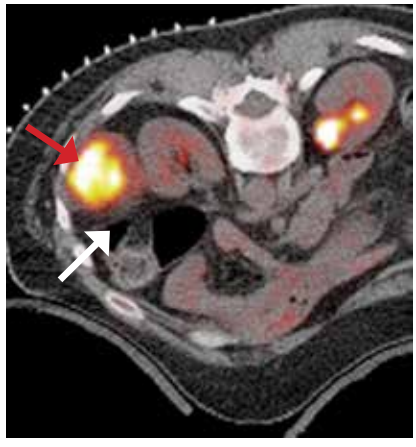

Figure 3: Another slice level of the fused planning PET/CT positioned slightly inferior to that in Figure 2 showing large ^{18}F-FDG-avid perisplenic peritoneal metastasis (*red arrow*) with its medial surface in close proximity to the left kidney and the anterior surface adjacent to the splenic flexure of the colon (*white arrow*).

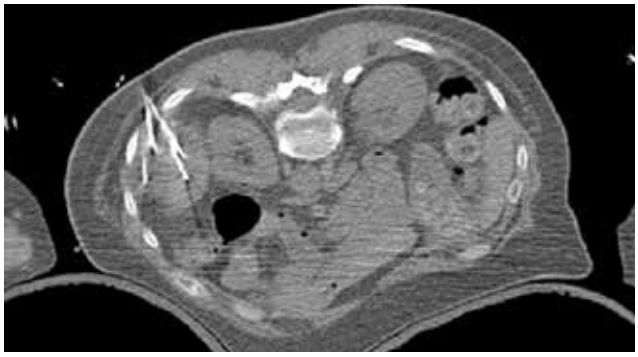

Figure 4: CT Fluoroscopy images show placement of the needles and probes into the tumor.

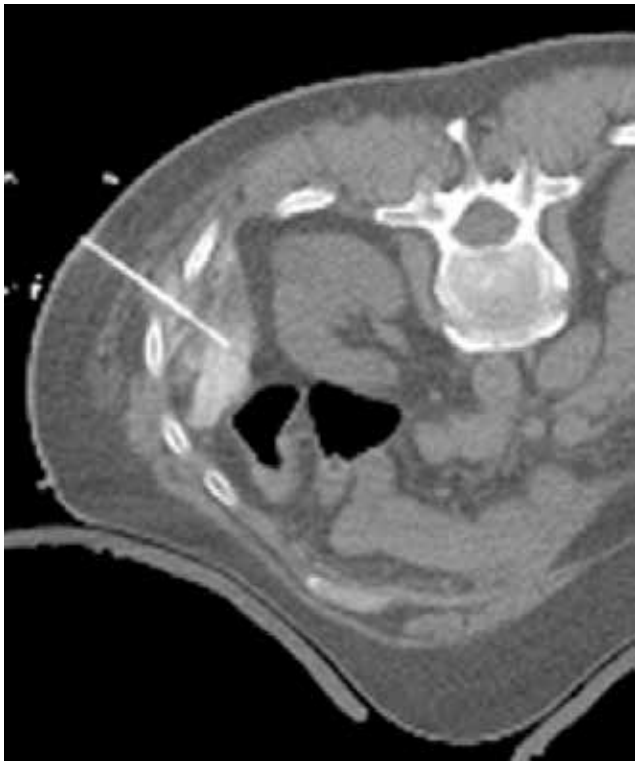

Figure 5: CT Fluoroscopy shows placement of a 20G Chiba needle for hydro-displacement of the splenic flexure of colon with instillation of dilute iodinated contrast into the space between the tumor and colonic wall. This maneuver prevents cryoablation injury of the bowel.

Comments

Cryoablation uses extreme cold to freeze and destroy diseased tissue, including cancer cells. During cryotherapy, liquid nitrogen or argon gas flows into a needle-like applicator (cryoprobe) creating intense cold that ablates diseased tissue. Image-guidance, commonly with CT or MRI helps guide the insertion of cryoprobes to treatment sites. PET/CT also helps guide the cryoprobe placements into the viable tumor and ensures proper coverage of the tumor by the cryoablation procedure. Precise image-guidance helps avoid missing a part of the tumor and reduces local tumor bed recurrences. Since ^{18}F-FDG does not leave the tumor during or immediately following cryoablation, the ^{18}F-FDG-avid tumor remains clearly discernable even in the minutes to hours following the cryoablation procedure. As a result, the cryoablation ice ball defined by CT and the tumor defined by tracer uptake on PET can be compared on fused PET/CT and the adequacy of ice ball coverage and margin beyond the tumor edge can be determined.

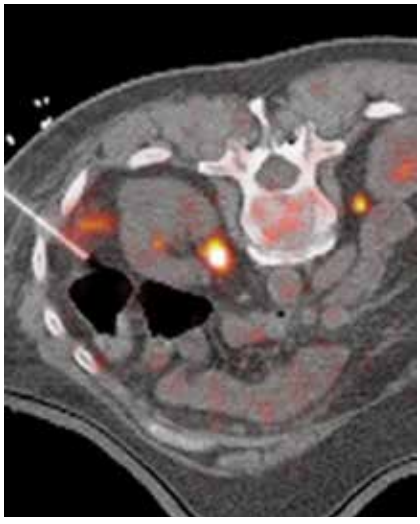

Figure 6: Fused PET/CT image shows placement of the hydro-displacement needle between tumor and bowel wall.

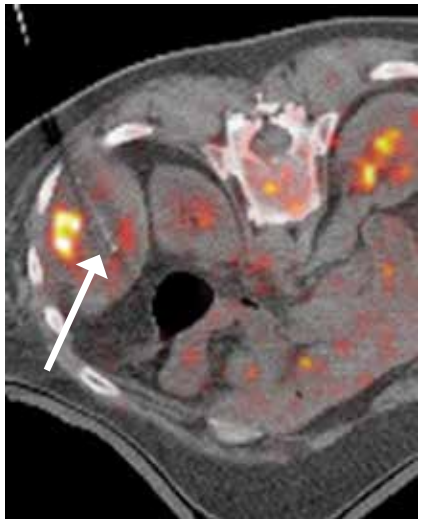

Figure 7: Fused PET/CT demonstrating the superior cryoablation probe (*white arrow*) placed within the necrotic medial part of the tumor.

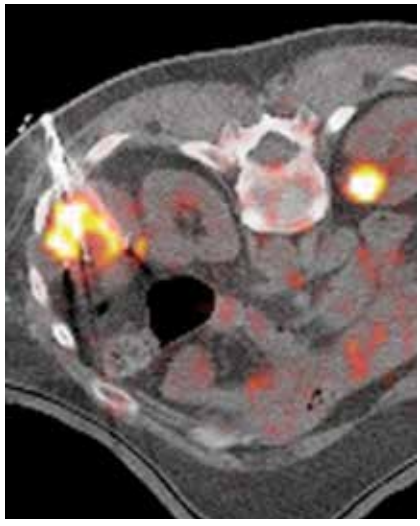

Figure 8: Fused PET/CT image demonstrates inferior cryoablation probes placed within the tumor mass.

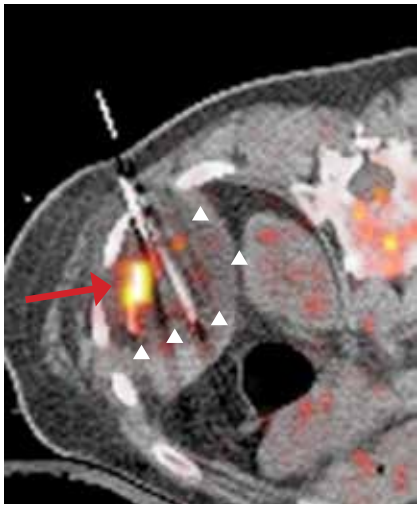

Figure 9: Fused PET/CT at the level of the upper cryoablation probe performed after initial cryoablation shows a hypo-intense region encompassing the tumor (*white arrowheads*), which represents the cryoablation ice ball. The area of uptake (*red arrow*) remains unchanged as compared to initial planning PET/CT since ^{18}F-FDG does not dissipate from the tumor during or following cryoablation. Cryoablation freezes the tumor and creates an ice ball involving the tumor and adjacent tissues; the tracer within the tumor remains trapped, even after ablation. This helps confirm that the cryoablation ice ball, represented by the hypodense zone on CT extends beyond the ^{18}F-FDG-avid tumor, thus ensuring adequate coverage of the tumor and a safety margin with cryoablation.

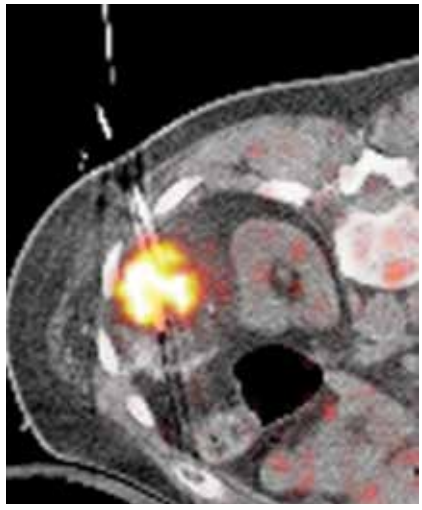

Figure 10: Fused PET/CT performed towards the end of the cryoablation at the level of lower cryoablation probes shows persistent tracer uptake within the tumor and a hypodense ice ball on CT extending beyond the ^{18}F-FDG avid tumor. This confirms an adequate ablation margin including and extending beyond the entire tumor. Note the bowel wall is at a significant distant from the cryoablation zone, which has been achieved by hydro-displacement.

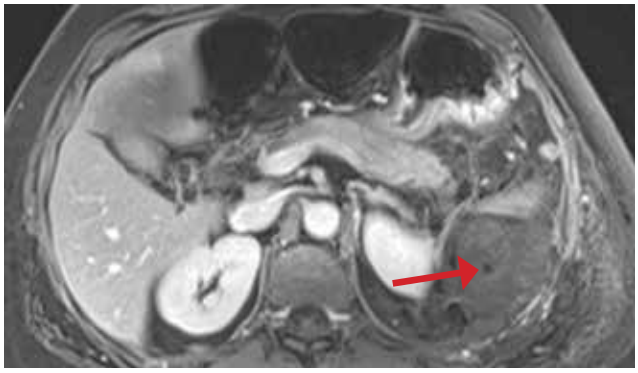

Figure 11: 3D VIBE breath hold, contrast-enhanced MRI shows the hypo-enhancing ablation zone (*red arrow*). No enhancing residual tumor is visualized.

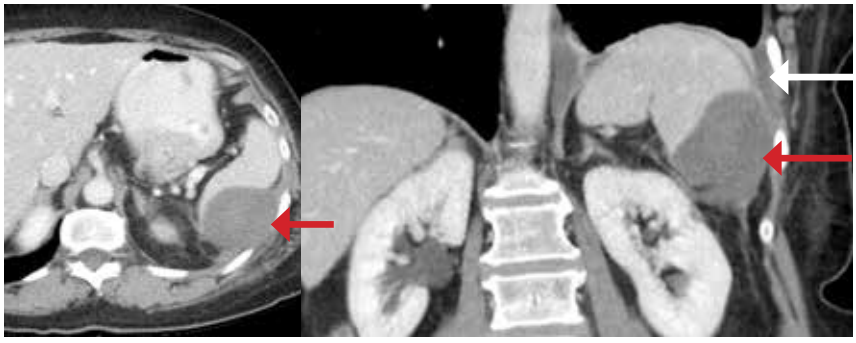

Figure 12: Follow-up contrast-enhanced CT (axial and coronal) shows the hypo-enhancing ablation zone without an enhancing residual tumor (*red arrows*). There is a small area of reactive left pleural effusion (*white arrow*) that is expected, following ablations adjacent to the diaphragm. The left renal margin adjacent to the ablation zone in the coronal image does not show significant cryoablation-related hypo-density, thus ensuring lack of significant renal parenchymal damage.

Conclusion

Breath-hold PET and CT using suspended ventilation under general anesthesia eliminated respiratory motion-related blurring and ensured motion-free images with fusion of PET and CT. Although the count statistics of a 15-second breath hold PET may be low, the high sensitivity PET system with Time-of-Flight acquisition and elimination of respiratory motion during PET enabled adequate image quality for the purposes of planning, targeting and assessment during ablation procedures. ■

Examination Protocol

Scanner: Biograph mCT

PET	
Injected dose	5 mCi (185 MBq) ^{18}F-FDG
Scan delay	1 hour
Acquisition	30 sec suspended ventilation
CT	
Tube voltage	120 kV
Tube vurrent	30 mAs
Slice vollimation	32 x 1.2 mm
Slice thickness	5 mm

* Indications and important safety information on Fludeoxyglucose F 18 injection can be found on page 41. The full prescribing information can be found on pages 62-64.

** Intervention Pro with i-Fluoro.

The statements by Siemens customers described herein are based on results that were achieved in the customer's unique setting. Since there is no "typical" hospital and many variables exist (e.g., hospital size, case mix, level of IT adoption) there can be no guarantee that other customers will achieve the same results.

Imaging Life

Imaging Life is your resource for molecular imaging innovation. Read about the latest trends, best practices, news and more from leading healthcare professionals around the world.

Regular updates online

siemens.com/
imaginglife

Scan and subscribe!

For current and past issues and to order magazines, please visit **siemens.com/ healthcare-magazine**

Connect with us on Twitter **@SiemensHealth** and **#ImagingLife**

Our Family of Customer Magazines

Specialty publications offering best practices and background information for a variety of clinical fields.

SOMATOM Sessions
Everything from the world of computed tomography.

AXIOM Innovations
Everything from the world of interventional radiology, cardiology and surgery.

MAGNETOM Flash
Everything from the world of magnetic resonance imaging.

Heartbeat
Everything from the world of sustainable cardiovascular care.

Medical Solutions
Innovations and trends in healthcare.

Imaging Life
Everything from the world of molecular imaging innovations.

Publisher:
Siemens Medical Solutions USA, Inc.
Molecular Imaging
2501 North Barrington Road
Hoffman Estates, IL 60192
USA
Phone: +1 847 304-7700
siemens.com/mi

Editor: Rhett Morici
rhett.morici@siemens.com

Content and journalistic network, p. 14-25:
The Freiherr Group, Wisconsin, USA
Greg Freiherr

Content and journalistic network, p. 6-13:
Primafila AG, Hornbachstrasse 50,
8034 Zurich, Switzerland
Viviane Egli, Roman Elsener

Design consulting:
Clint Poy Design, Georgia, USA
Clint Poy

Infographics, p. 12:
Independent Medien-Design,
Widenmayerstrasse 16,
80538 Munich, Germany

Printer:
Sheridan Press, USA

Cover photo:
Courtesy of Radiology Center

Photo credit:
p. 6 & 8 courtesy of Radiology Center

p. 10 & 11 courtesy of Alliance HealthCare Radiology

p. 19 courtesy of Halifax Health

p. 26 & 28 courtesy of Boice-Willis Clinic

p. 32 courtesy of Kat Swystun

We welcome your questions and comments about the editorial content of *Imaging Life*. Please contact the editor.

***Imaging Life* is available online: siemens.com/imaginglife**

Some of the imaging biomarkers in this publication are not currently recognized by the U.S. Food and Drug Administration (FDA) or other regulatory agencies as being safe and effective, and Siemens does not make any claims regarding their use.

DISCLAIMERS: *Imaging Life*: "The information presented in this magazine is for illustration only and is not intended to be relied upon by the reader for instruction as to the practice of medicine. Healthcare practitioners reading this information are reminded that they must use their own learning, training and expertise in dealing with their individual patients. This material does not substitute for that duty and is not intended by Siemens Healthcare GmbH to be used for any purpose in that regard." Contrast agents: "The drugs and doses mentioned herein are consistent with the approved labeling for uses and/or indications of the drug. The treating physician bears the sole responsibility for the diagnosis and treatment of patients, including drugs and doses prescribed in connection with such use. The operating instructions must always be strictly followed when operating your Siemens system. The source for the technical data is the corresponding data sheets." Trademarks: "All trademarks mentioned in this document are property of their respective owners." Results: "The outcomes achieved by the Siemens customers described herein were achieved in the customer's unique setting. Since there is no "typical" hospital and many variables exist (e.g., hospital size, case mix, level of IT adoption), there can be no guarantee that others will achieve the same results."

HIGHLIGHTS OF PRESCRIBING INFORMATION

These highlights do not include all the information needed to use Fludeoxyglucose F 18 Injection safely and effectively. See full prescribing information for Fludeoxyglucose F 18 Injection.

Fludeoxyglucose F 18 Injection, USP
For intravenous use
Initial U.S. Approval: 2005

RECENT MAJOR CHANGES

Warnings and Precautions (5.1, 5.2)	7/2010
Adverse Reactions (6)	7/2010

INDICATIONS AND USAGE

Fludeoxyglucose F18 Injection is indicated for positron emission tomography (PET) imaging in the following settings:

- Oncology: For assessment of abnormal glucose metabolism to assist in the evaluation of malignancy in patients with known or suspected abnormalities found by other testing modalities, or in patients with an existing diagnosis of cancer.
- Cardiology: For the identification of left ventricular myocardium with residual glucose metabolism and reversible loss of systolic function in patients with coronary artery disease and left ventricular dysfunction, when used together with myocardial perfusion imaging.
- Neurology: For the identification of regions of abnormal glucose metabolism associated with foci of epileptic seizures (1).

DOSAGE AND ADMINISTRATION

Fludeoxyglucose F 18 Injection emits radiation. Use procedures to minimize radiation exposure. Screen for blood glucose abnormalities.

- In the oncology and neurology settings, instruct patients to fast for 4 to 6 hours prior to the drug's injection. Consider medical therapy and laboratory testing to assure at least two days of normoglycemia prior to the drug's administration (5.2).
- In the cardiology setting, administration of glucose-containing food or liquids (e.g., 50 to 75 grams) prior to the drug's injection facilitates localization of cardiac ischemia (2.3).

Aseptically withdraw Fludeoxyglucose F 18 Injection from its container and administer by intravenous injection (2).

The recommended dose:

- for adults is 5 to 10 mCi (185 to 370 MBq), in all indicated clinical settings (2.1).
- for pediatric patients is 2.6 mCi in the neurology setting (2.2).

Initiate imaging within 40 minutes following drug injection; acquire static emission images 30 to 100 minutes from time of injection (2).

DOSAGE FORMS AND STRENGTHS

Multi-dose 30mL and 50mL glass vial containing 0.74 to 7.40 GBq/mL (20 to 200 mCi/mL) Fludeoxyglucose F 18 Injection and 4.5mg of sodium chloride with 0.1 to 0.5% w/w ethanol as a stabilizer (approximately 15 to 50 mL volume) for intravenous administration (3).

CONTRAINDICATIONS

None (4)

WARNINGS AND PRECAUTIONS

- Radiation risks: use smallest dose necessary for imaging (5.1).
- Blood glucose abnormalities: may cause suboptimal imaging (5.2).

ADVERSE REACTIONS

Hypersensitivity reactions have occurred; have emergency resuscitation equipment and personnel immediately available (6).

To report SUSPECTED ADVERSE REACTIONS, contact PETNET Solutions, Inc. at 877-473-8638 or FDA at 1-800-FDA-1088 or www.fda.gov/medwatch.

USE IN SPECIFIC POPULATIONS

Pregnancy Category C: No human or animal data. Consider alternative diagnostics; use only if clearly needed (8.1).

- Nursing mothers: Use alternatives to breast feeding (e.g., stored breast milk or infant formula) for at least 10 half-lives of radioactive decay, if Fludeoxyglucose F 18 Injection is administered to a woman who is breast-feeding (8.3).
- Pediatric Use: Safety and effectiveness in pediatric patients have not been established in the oncology and cardiology settings (8.4).

See 17 for PATIENT COUNSELING INFORMATION

Revised: 1/2016

FULL PRESCRIBING INFORMATION: CONTENTS*

* Sections or subsections omitted from the full prescribing information are not listed.

FULL PRESCRIBING INFORMATION

1 INDICATIONS AND USAGE

Fludeoxyglucose F 18 Injection is indicated for positron emission tomography (PET) imaging in the following settings:

1.1 Oncology

For assessment of abnormal glucose metabolism to assist in the evaluation of malignancy in patients with known or suspected abnormalities found by other testing modalities, or in patients with an existing diagnosis of cancer.

1.2 Cardiology

For the identification of left ventricular myocardium with residual glucose metabolism and reversible loss of systolic function in patients with coronary artery disease and left ventricular dysfunction, when used together with myocardial perfusion imaging.

1.3 Neurology

For the identification of regions of abnormal glucose metabolism associated with foci of epileptic seizures.

2 DOSAGE AND ADMINISTRATION

Fludeoxyglucose F 18 Injection emits radiation. Use procedures to minimize radiation exposure. Calculate the final dose from the end of synthesis (EOS) time using proper radioactive decay factors. Assay the final dose in a properly calibrated dose calibrator before administration to the patient [see Description (11.2)].

2.1 Recommended Dose for Adults

Within the oncology, cardiology and neurology settings, the recommended dose for adults is 5 to 10 mCi (185 to 370 MBq) as an intravenous injection.

2.2 Recommended Dose for Pediatric Patients

Within the neurology setting, the recommended dose for pediatric patients is 2.6 mCi, as an intravenous injection. The optimal dose adjustment on the basis of body size or weight has not been determined [see *Use in Special Populations (8.4)*].

2.3 Patient Preparation

- To minimize the radiation absorbed dose to the bladder, encourage adequate hydration. Encourage the patient to drink water or other fluids (as tolerated) in the 4 hours before their PET study.
- Encourage the patient to void as soon as the imaging study is completed and as often as possible thereafter for at least one hour.
- Screen patients for clinically significant blood glucose abnormalities by obtaining a history and/or laboratory tests [see *Warnings and Precautions (5.2)*]. Prior to Fludeoxyglucose F 18 PET imaging in the oncology and neurology settings, instruct patient to fast for 4 to 6 hours prior to the drug's injection.
- In the cardiology setting, administration of glucose-containing food or liquids (e.g., 50 to 75 grams) prior to Fludeoxyglucose F18 Injection facilitates localization of cardiac ischemia

2.4 Radiation Dosimetry

The estimated human absorbed radiation doses (rem/mCi) to a newborn (3.4 kg), 1-year old (9.8 kg), 5-year old (19 kg), 10-year old (32 kg), 15-year old (57 kg), and adult (70 kg) from intravenous administration of Fludeoxyglucose F 18 Injection are shown in Table 1. These estimates were calculated based on human[2] data and using the data published by the International Commission on Radiological Protection[4] for Fludeoxyglucose ^{18}F. The dosimetry data show that there are slight variations in absorbed radiation dose for various organs in each of the age groups. These dissimilarities in absorbed radiation dose are due to developmental age variations (e.g., organ size, location, and overall metabolic rate for each age group). The identified critical organs (in descending order) across all age groups evaluated are the urinary bladder, heart, pancreas, spleen, and lungs.

Table 1. Estimated Absorbed Radiation Doses (rem/mCi) After Intravenous Administration of Fludeoxyglucose F-18 Injection[a]

Organ	Newborn (3.4 kg)	1-year old (9.8 kg)	5-year old (19 kg)	10-year old (32 kg)	15-year old (57 kg)	Adult (70 kg)
Bladder wall[b]	4.3	1.7	0.93	0.60	0.40	0.32
Heart wall	2.4	1.2	0.70	0.44	0.29	0.22
Pancreas	2.2	0.68	0.33	0.25	0.13	0.096
Spleen	2.2	0.84	0.46	0.29	0.19	0.14
Lungs	0.96	0.38	0.20	0.13	0.092	0.064
Kidneys	0.81	0.34	0.19	0.13	0.089	0.074
Ovaries	0.80	0.8	0.19	0.11	0.058	0.053
Uterus	0.79	0.35	0.19	0.12	0.076	0.062
LLI wall *	0.69	0.28	0.15	0.097	0.060	0.051
Liver	0.69	0.31	0.17	0.11	0.076	0.058
Gallbladder wall	0.69	0.26	0.14	0.093	0.059	0.049
Small intestine	0.68	0.29	0.15	0.096	0.060	0.047
ULI wall **	0.67	0.27	0.15	0.090	0.057	0.046
Stomach wall	0.65	0.27	0.14	0.089	0.057	0.047
Adrenals	0.65	0.28	0.15	0.095	0.061	0.048
Testes	0.64	0.27	0.14	0.085	0.052	0.041
Red marrow	0.62	0.26	0.14	0.089	0.057	0.047
Thymus	0.61	0.26	0.14	0.086	0.056	0.044
Thyroid	0.61	0.26	0.13	0.080	0.049	0.039
Muscle	0.58	0.25	0.13	0.078	0.049	0.039
Bone surface	0.57	0.24	0.12	0.079	0.052	0.041
Breast	0.54	0.22	0.11	0.068	0.043	0.034
Skin	0.49	0.20	0.10	0.060	0.037	0.030
Brain	0.29	0.13	0.09	0.078	0.072	0.070
Other tissues	0.59	0.25	0.13	0.083	0.052	0.042

[a] MIRDOSE 2 software was used to calculate the radiation absorbed dose. Assumptions on the biodistribution based on data from Gallagher et al.[1] and Jones et al.[2]

[b] The dynamic bladder model with a uniform voiding frequency of 1.5 hours was used. *LLI = lower large intestine; **ULI = upper large intestine

2.5 Radiation Safety – Drug Handling

- Use waterproof gloves, effective radiation shielding, and appropriate safety measures when handling Fludeoxyglucose F 18 Injection to avoid unnecessary radiation exposure to the patient, occupational workers, clinical personnel and other persons.
- Radiopharmaceuticals should be used by or under the control of physicians who are qualified by specific training and experience in the safe use and handling of radionuclides, and whose experience and training have been approved by the appropriate governmental agency authorized to license the use of radionuclides.
- Calculate the final dose from the end of synthesis (EOS) time using proper radioactive decay factors. Assay the final dose in a properly calibrated dose calibrator before administration to the patient [see *Description (11.2)*].
- The dose of Fludeoxyglucose F 18 used in a given patient should be minimized consistent with the objectives of the procedure, and the nature of the radiation detection devices employed.

2.6 Drug Preparation and Administration

- Calculate the necessary volume to administer based on calibration time and dose.
- Aseptically withdraw Fludeoxyglucose F 18 Injection from its container.
- Inspect Fludeoxyglucose F 18 Injection visually for particulate matter and discoloration before administration, whenever solution and container permit.
- Do not administer the drug if it contains particulate matter or discoloration; dispose of these unacceptable or unused preparations in a safe manner, in compliance with applicable regulations.
- Use Fludeoxyglucose F 18 Injection within 12 hours from the EOS.

2.7 Imaging Guidelines

- Initiate imaging within 40 minutes following Fludeoxyglucose F 18 Injection administration.
- Acquire static emission images 30 to 100 minutes from the time of injection.

3 DOSAGE FORMS AND STRENGTHS

Multiple-dose 30 mL and 50 mL glass vial containing 0.74 to 7.40 GBq/mL (20 to 200 mCi/mL) of Fludeoxyglucose F 18 Injection and 4.5 mg of sodium chloride with 0.1 to 0.5% w/w ethanol as a stabilizer (approximately 15 to 50 mL volume) for intravenous administration.

4 CONTRAINDICATIONS

None

5 WARNINGS AND PRECAUTIONS

5.1 Radiation Risks

Radiation-emitting products, including Fludeoxyglucose F 18 Injection, may increase the risk for cancer, especially in pediatric patients. Use the smallest dose necessary for imaging and ensure safe handling to protect the patient and health care worker [see *Dosage and Administration (2.5)*].

5.2 Blood Glucose Abnormalities

In the oncology and neurology setting, suboptimal imaging may occur in patients with inadequately regulated blood glucose levels. In these patients, consider medical therapy and laboratory testing to assure at least two days of normoglycemia prior to Fludeoxyglucose F 18 Injection administration.

6 ADVERSE REACTIONS

Hypersensitivity reactions with pruritus, edema and rash have been reported in the post-marketing setting. Have emergency resuscitation equipment and personnel immediately available.

7 DRUG INTERACTIONS

The possibility of interactions of Fludeoxyglucose F 18 Injection with other drugs taken by patients undergoing PET imaging has not been studied.

8 USE IN SPECIFIC POPULATIONS

8.1 Pregnancy

Pregnancy Category C

Animal reproduction studies have not been conducted with Fludeoxyglucose F 18 Injection. It is also not known whether Fludeoxyglucose F 18 Injection can cause fetal harm when administered to a pregnant woman or can affect reproduction capacity. Consider alternative diagnostic tests in a pregnant woman; administer Fludeoxyglucose F 18 Injection only if clearly needed.

8.3 Nursing Mothers

It is not known whether Fludeoxyglucose F 18 Injection is excreted in human milk. Consider alternative diagnostic tests in women who are breast-feeding. Use alternatives to breast feeding (e.g., stored breast milk or infant formula) for at least 10 half-lives of radioactive decay, if Fludeoxyglucose F 18 Injection is administered to a woman who is breast-feeding.

8.4 Pediatric Use

The safety and effectiveness of Fludeoxyglucose F 18 Injection in pediatric patients with epilepsy is established on the basis of studies in adult and pediatric patients. In pediatric patients with epilepsy, the recommended dose is 2.6 mCi. The optimal dose adjustment on the basis of body size or weight has not been determined. In the oncology or cardiology settings, the safety and effectiveness of Fludeoxyglucose F 18 Injection have not been established in pediatric patients.

11 DESCRIPTION

11.1 Chemical Characteristics

Fludeoxyglucose F 18 Injection is a positron emitting radiopharmaceutical that is used for diagnostic purposes in conjunction with positron emission tomography (PET) imaging. The active ingredient 2-deoxy-2-[^{18}F]fluoro-D-glucose has the molecular formula of $C_6H_{11}{}^{18}FO_5$ with a molecular weight of 181.26, and has the following chemical structure:

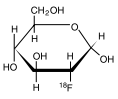

Fludeoxyglucose F 18 Injection is provided as a ready to use sterile, pyrogen free, clear, colorless solution. Each mL contains between 0.740 to 7.40GBq (20.0 to 200 mCi) of 2-deoxy-2-[^{18}F]fluoro-D-glucose at the EOS, 4.5 mg of sodium chloride and 0.1 to 0.5% w/w ethanol as a stabilizer. The pH of the solution is between 4.5 and 7.5. The solution is packaged in a multiple-dose glass vial and does not contain any preservative.

11.2 Physical Characteristics

Fluorine F 18 decays by emitting positron to Oxygen O 16 (stable) and has a physical half-life of 109.7 minutes. The principal photons useful for imaging are the dual 511 keV gamma photons, that are produced and emitted simultaneously in opposite direction when the positron interacts with an electron (Table 2).

Table 2. Pricipal Radiation Emission Data for Fluorine F18

Radiation/Emission	% Per Disintegration	Mean Energy
Positron (b+)	96.73	249.8 keV
Gamma (±)*	193.46	511.0 keV

*Produced by positron annihilation

From: Kocher, D.C. Radioactive Decay Tables DOE/TIC-I 1026, 89 (1981)

The specific gamma ray constant (point source air kerma coefficient) for fluorine F 18 is 5.7 R/hr/mCi (1.35 x 10^{-6} Gy/hr/kBq) at 1 cm. The half-value layer (HVL) for the 511 keV photons is 4 mm lead (Pb). The range of attenuation coefficients for this radionuclide as a function of lead shield thickness is shown in Table 3. For example, the interposition of an 8 mm thickness of Pb, with a coefficient of attenuation of 0.25, will decrease the external radiation by 75%.

Table 3. Radiation Attenuation of 511 keV Photons by lead (Pb) shielding

Shield thickness (Pb) mm	Coefficient of attenuation
0	0.00
4	0.50
8	0.25
13	0.10
26	0.01
39	0.001
52	0.0001

For use in correcting for physical decay of this radionuclide, the fractions remaining at selected intervals after calibration are shown in Table 4.

Table 4. Physical Decay Chart for Fluorine F18

Minutes	Fraction Remaining
0*	1.000
15	0.909
30	0.826
60	0.683
110	0.500
220	0.250

*calibration time

12 CLINICAL PHARMACOLOGY

12.1 Mechanism of Action

Fludeoxyglucose F 18 is a glucose analog that concentrates in cells that rely upon glucose as an energy source, or in cells whose dependence on glucose increases under pathophysiological conditions. Fludeoxyglucose F 18 is transported through the cell membrane by facilitative glucose transporter proteins and is phosphorylated within the cell to [^{18}F] FDG-6-phosphate by the enzyme hexokinase. Once phosphorylated it cannot exit until it is dephosphorylated by glucose-6-phosphatase. Therefore, within a given tissue or pathophysiological process, the retention and clearance of Fludeoxyglucose F 18 reflect a balance involving glucose transporter, hexokinase and glucose-6-phosphatase activities. When allowance is made for the kinetic differences between glucose and Fludeoxyglucose F 18 transport and phosphorylation (expressed as the ‚lumped constant" ratio), Fludeoxyglucose F 18 is used to assess glucose metabolism.

In comparison to background activity of the specific organ or tissue type, regions of decreased or absent uptake of Fludeoxyglucose F 18 reflect the decrease or absence of glucose metabolism. Regions of increased uptake of Fludeoxyglucose F 18 reflect greater than normal rates of glucose metabolism.

12.2 Pharmacodynamics

Fludeoxyglucose F 18 Injection is rapidly distributed to all organs of the body after intravenous administration. After background clearance of Fludeoxyglucose F 18 Injection, optimal PET imaging is generally achieved between 30 to 40 minutes after administration.

In cancer, the cells are generally characterized by enhanced glucose metabolism partially due to (1) an increase in activity of glucose transporters, (2) an increased rate of phosphorylation activity, (3) a reduction of phosphatase activity or, (4) a dynamic alteration in the balance among all these processes. However, glucose metabolism of cancer as reflected by Fludeoxyglucose F 18 accumulation shows considerable variability. Depending on tumor type, stage, and location, Fludeoxyglucose F 18 accumulation may be increased, normal, or decreased. Also, inflammatory cells can have the same variability of uptake of Fludeoxyglucose F 18.

In the heart, under normal aerobic conditions, the myocardium meets the bulk of its energy requirements by oxidizing free fatty acids. Most of the exogenous glucose taken up by the myocyte is converted into glycogen. However, under ischemic conditions, the oxidation of free fatty acids decreases, exogenous glucose becomes the preferred myocardial sub strate, glycolysis is stimulated, and glucose taken up by the myocyte is metabolized immediately instead of being converted into glycogen. Under these condi-

tions, phosphorylated Fludeoxyglucose F 18 accumulates in the myocyte and can be detected with PET imaging.

In the brain, cells normally rely on aerobic metabolism. In epilepsy, the glucose metabolism varies. Generally, during a seizure, glucose metabolism increases. Interictally, the seizure focus tends to be hypometabolic.

12.3 Pharmacokinetics

Distribution: In four healthy male volunteers, receiving an intravenous administration of 30 seconds induration, the arterial blood level profile for Fludeoxyglucose F 18 decayed triexponentially. The effective half-life ranges of the three phases were 0.2 to 0.3 minutes, 10 to 13 minutes with a mean and standard deviation (STD) of 11.6 (±) 1.1 min, and 80 to 95 minutes with a mean and STD of 88 (±) 4 min.

Plasma protein binding of Fludeoxyglucose F 18 has not been studied.

Metabolism: Fludeoxyglucose F 18 is transported into cells and phosphorylated to [^{18}F]-FDG-6- phosphate at a rate proportional to the rate of glucose utilization within that tissue. [F18]-FDG-6-phosphate presumably is metabolized to 2-deoxy-2-[F18]fluoro-6-phospho-D-mannose([F 18]FDM-6-phosphate).

Fludeoxyglucose F 18 Injection may contain several impurities (e.g., 2-deoxy-2-chloro-D-glucose (ClDG)). Biodistribution and metabolism of ClDG are presumed to be similar to Fludeoxyglucose F 18 and would be expected to result in intracellular formation of 2-deoxy-2-chloro-6-phospho-D-glucose (ClDG-6-phosphate) and 2-deoxy-2-chloro-6-phospho-D-mannose (ClDM-6-phosphate). The phosphorylated deoxyglucose compounds are dephosphorylated and the resulting compounds (FDG, FDM, ClDG, and ClDM) presumably leave cells by passive diffusion. Fludeoxyglucose F 18 and related compounds are cleared from non-cardiac tissues within 3 to 24 hours after administration. Clearance from the cardiac tissue may require more than 96 hours. Fludeoxyglucose F 18 that is not involved in glucose metabolism in any tissue is then excreted in the urine.

Elimination: Fludeoxyglucose F 18 is cleared from most tissues within 24 hours and can be eliminated from the body unchanged in the urine. Three elimination phases have been identified in the reviewed literature. Within 33 minutes, a mean of 3.9% of the administrated radioactive dose was measured in the urine. The amount of radiation exposure of the urinary bladder at two hours post-administration suggests that 20.6% (mean) of the radioactive dose was present in the bladder.

Special Populations:

The pharmacokinetics of Fludeoxyglucose F 18 Injection have not been studied in renally-impaired, hepatically impaired or pediatric patients. Fludeoxyglucose F 18 is eliminated through the renal system. Avoid excessive radiation exposure to this organ system and adjacent tissues.

The effects of fasting, varying blood sugar levels, conditions of glucose intolerance, and diabetes mellitus on Fludeoxyglucose F 18 distribution in humans have not been ascertained [*see Warnings and Precautions (5.2)*].

13 NONCLINICAL TOXICOLOGY

13.1 Carcinogenesis, Mutagenesis, Impairment of Fertility

Animal studies have not been performed to evaluate the Fludeoxyglucose F 18 Injection carcinogenic potential, mutagenic potential or effects on fertility.

14 CLINICAL STUDIES

14.1 Oncology

The efficacy of Fludeoxyglucose F 18 Injection in positron emission tomography cancer imaging was demonstrated in 16 independent studies. These studies prospectively evaluated the use of Fludeoxyglucose F 18 in patients with suspected or known malignancies, including non-small cell lung cancer, colo-rectal, pancreatic, breast, thyroid, melanoma, Hodgkin's and non-Hodgkin's lymphoma, and various types of metastatic cancers to lung, liver, bone, and axillary nodes. All these studies had at least 50 patients and used pathology as a standard of truth. The Fludeoxyglucose F 18 Injection doses in the studies ranged from 200 MBq to 740 MBq with a median and mean dose of 370 MBq.

In the studies, the diagnostic performance of Fludeoxyglucose F 18 Injection varied with the type of cancer, size of cancer, and other clinical conditions. False negative and false positive scans were observed. Negative Fludeoxyglucose F 18 Injection PET scans do not exclude the diagnosis of cancer. Positive Fludeoxyglucose F 18 Injection PET scans can not replace pathology to establish a diagnosis of cancer. Non-malignant conditions such as fungal infections, inflammatory processes and benign tumors have patterns of increased glucose metabolism that may give rise to false-positive scans. The efficacy of Fludeoxyglucose F 18 Injection PET imaging in cancer screening was not studied.

14.2 Cardiology

The efficacy of Fludeoxyglucose F 18 Injection for cardiac use was demonstrated in ten independent, prospective studies of patients with coronary artery disease and chronic left ventricular systolic dysfunction who were scheduled to undergo coronary revascularization. Before revascularization, patients underwent PET imaging with Fludeoxyglucose F 18 Injection (74 to 370 MBq, 2 to 10 mCi) and perfusion imaging with other diagnostic radiopharmaceuticals. Doses of Fludeoxyglucose F 18 Injection ranged from 74 to 370 MBq (2 to 10 mCi). Segmental, left ventricular, wall-motion assessments of asynergic areas made before revascularization were compared in a blinded manner to assessments made after successful revascularization to identify myocardial segments with functional recovery.

Left ventricular myocardial segments were predicted to have reversible loss of systolic function if they showed Fludeoxyglucose F 18 accumulation and reduced perfusion (i.e., flow-metabolism mismatch). Conversely, myocardial segments were predicted to have irreversible loss of systolic function if they showed reductions in both Fludeoxyglucose F 18 accumulation and perfusion (i.e., matched defects).

Findings of flow-metabolism mismatch in a myocardial segment may suggest that successful revascularization will restore myocardial function in that segment. However, false-positive tests occur regularly, and the decision to have a patient undergo revascularization should not be based on PET findings alone. Similarly, findings of a matched defect in a myocardial segment may suggest that myocardial function will not recover in that segment, even if it is successfully revascularized. However, false-negative tests occur regularly, and the decision to recommend against coronary revascularization, or to recommend a cardiac transplant, should not be based on PET findings alone. The reversibility of segmental dysfunction as predicted with Fludeoxyglucose F 18 PET imaging depends on successful coronary revascularization. Therefore, in patients with a low likelihood of successful revascularization, the diagnostic usefulness of PET imaging with Fludeoxyglucose F 18 Injection is more limited.

14.3 Neurology

In a prospective, open label trial, Fludeoxyglucose F 18 Injection was evaluated in 86 patients with epilepsy. Each patient received a dose of Fludeoxyglucose F 18 Injection in the range of 185 to 370 MBq (5 to 10 mCi). The mean age was 16.4 years (range: 4 months to 58 years; of these, 42 patients were less than 12 years and 16 patients were less than 2 years old). Patients had a known diagnosis of complex partial epilepsy and were under evaluation for surgical treatment of their seizure disorder. Seizure foci had been previously identified on ictal EEGs and sphenoidal EEGs. Fludeoxyglucose F 18 Injection PET imaging confirmed previous diagnostic findings in 16% (14/87) of the patients; in 34% (30/87) of the patients, Fludeoxyglucose F 18 Injection PET images provided new findings. In 32% (27/87), imaging with Fludeoxyglucose F 18 Injection was inconclusive. The impact of these imaging findings on clinical outcomes is not known.

Several other studies comparing imaging with Fludeoxyglucose F 18 Injection results to subsphenoidal EEG, MRI and/or surgical findings supported the concept that the degree of hypometabolism corresponds to areas of confirmed epileptogenic foci. The safety and effectiveness of Fludeoxyglucose F 18 Injection to distinguish idiopathic epileptogenic foci from tumors or other brain lesions that may cause seizures have not been established.

15 REFERENCES

1. Gallagher B.M., Ansari A., Atkins H., Casella V., Christman D.R., Fowler J.S., Ido T., MacGregor R.R., Som P., Wan C.N., Wolf A.P., Kuhl D.E., and Reivich M. "Radiopharmaceuticals XXVII. ^{18}F-labeled 2-deoxy-2-fluoro-d-glucose as a radiopharmaceutical for measuring regional myocardial glucose metabolism in vivo: tissue distribution and imaging studies in animals," J Nucl Med, 1977; 18, 990-6.
2. Jones S.C., Alavi, A., Christman D., Montanez, I., Wolf, A.P., and Reivich M. "The radiation dosimetry of 2 [F-18] fluoro-2-deoxy-D-glucose in man," J Nucl Med, 1982; 23, 613-617.
3. Kocher, D.C. "Radioactive Decay Tables: A handbook of decay data for application to radiation dosimetry and radiological assessments," 1981, DOE/TIC-I 1026, 89.
4. ICRP Publication 53, Volume 18, No. I-4,1987, pages 75-76.

16 HOW SUPPLIED/STORAGE AND DRUG HANDLING

Fludeoxyglucose F 18 Injection is supplied in a multi-dose, capped 30 mL and 50 mL glass vial containing between 0.740 to 7.40GBq/mL (20 to 200 mCi/mL), of no carrier added 2deoxy-2-[F 18] fluoro-D-glucose, at end of synthesis, in approximately 15 to 50 mL. The contents of each vial are sterile, pyrogen-free and preservative-free.

NDC 40028-511-30; 40028-511-50

Receipt, transfer, handling, possession, or use of this product is subject to the radioactive material regulations and licensing requirements of the U.S. Nuclear Regulatory Commission, Agreement States or Licensing States as appropriate.

Store the Fludeoxyglucose F 18 Injection vial upright in a lead shielded container at 25°C (77°F); excursions permitted to 15-30°C (59-86°F).

Store and dispose of Fludeoxyglucose F 18 Injection in accordance with the regulations and a general license, or its equivalent, of an Agreement State or a Licensing State.

The expiration date and time are provided on the container label. Use Fludeoxyglucose F 18 Injection within 12 hours from the EOS time.

17 PATIENT COUNSELING INFORMATION

Instruct patients in procedures that increase renal clearance of radioactivity. Encourage patients to:

- drink water or other fluids (as tolerated) in the 4 hours before their PET study.
- void as soon as the imaging study is completed and as often as possible thereafter for at least one hour.

Manufactured by: PETNET Solutions Inc.
810 Innovation Drive
Knoxville, TN 37932

Distributed by: PETNET Solutions Inc.
810 Innovation Drive
Knoxville, TN 37932

PETNET Solutions

HIGHLIGHTS OF PRESCRIBING INFORMATION

These highlights do not include all the information needed to use Ammonia N 13 Injection safely and effectively. See full prescribing information for Ammonia N 13 Injection.

Ammonia N 13 Injection for intravenous use
Initial U.S. Approval: 2007

INDICATIONS AND USAGE

Ammonia N 13 Injection is a radioactive diagnostic agent for Positron Emission Tomography (PET) indicated for diagnostic PET imaging of the myocardium under rest or pharmacologic stress conditions to evaluate myocardial perfusion in patients with suspected or existing coronary artery disease (1).

DOSAGE AND ADMINISTRATION

Rest Imaging Study (2.1):

- Aseptically withdraw Ammonia N 13 Injection from its container and administer 10 mCi – 20 mCi (0.368 GBq – 0.736 GBq) as a bolus through a catheter inserted into a large peripheral vein.
- Start imaging 3 minutes after the injection and acquire images for a total of 10 minutes – 20 minutes.

Stress Imaging Study (2.2):

- If a rest imaging study is performed, begin the stress imaging study 40 minutes or more after the first Ammonia N13 injection to allow sufficient isotope decay.
- Administer a pharmacologic stress-inducing drug in accordance with its labeling.
- Aseptically withdraw Ammonia N 13 Injection from its container and administer 10 mCi – 20 mCi (0.368 GBq – 0.736 GBq) of Ammonia N 13 Injection as a bolus at 8 minutes after the administration of the pharmacologic stress-inducing drug.
- Start imaging 3 minutes after the Ammonia N 13 Injection and acquire images for a total of 10 minutes – 20 minutes.

Patient Preparation (2.3):

- To increase renal clearance of radioactivity and to minimize radiation dose to the bladder, hydrate the patient before the procedure and encourage voiding as soon as each image acquisition is completed and as often as possible thereafter for at least one hour.

DOSAGE FORMS AND STRENGTHS

Glass vial containing 0.138 GBq/mL – 1.387 GBq/mL (3.75 mCi/mL –37.5 mCi/mL) of Ammonia N 13 Injection in aqueous 0.9% sodium chloride solution (approximately 7 mL volume) (3).

CONTRAINDICATIONS

None (4)

WARNINGS AND PRECAUTIONS

Ammonia N 13 Injection may increase the risk of cancer. Use the smallest dose necessary for imaging and ensure safe handling to protect the patient and health care worker (5).

ADVERSE REACTIONS

No adverse reactions have been reported for Ammonia N 13 Injection based on a review of the published literature, publicly available reference sources, and adverse drug reaction reporting system (6).

To report SUSPECTED ADVERSE REACTIONS, contact PETNET Solutions, Inc. at 877-473-8638 or FDA at 1-800-FDA-1088 or www.fda.gov/medwatch.

USE IN SPECIFIC POPULATIONS

- It is not known whether this drug is excreted in human milk. Alternatives to breastfeeding (e.g. using stored breast milk or infant formula) should be used for 2 hours (>10 half-lives of radioactive decay for N 13 isotope) after administration of Ammonia N 13 Injection (8.3).
- The safety and effectiveness of Ammonia N 13 Injection has been established in pediatric patients (8.4).

See 17 for PATIENT COUNSELING INFORMATION

Revised: 1/2016

FULL PRESCRIBING INFORMATION: CONTENTS*

* Sections or subsections omitted from the full prescribing information are not listed.

FULL PRESCRIBING INFORMATION

1 INDICATIONS AND USAGE

Ammonia N 13 Injection is indicated for diagnostic Positron Emission Tomography (PET) imaging of the myocardium under rest or pharmacologic stress conditions to evaluate myocardial perfusion in patients with suspected or existing coronary artery disease.

2 DOSAGE AND ADMINISTRATION

2.1 Rest Imaging Study

- Aseptically withdraw Ammonia N 13 Injection from its container and administer 10 mCi – 20 mCi (0.368 GBq – 0.736 GBq) as a bolus through a catheter inserted into a large peripheral vein.
- Start imaging 3 minutes after the injection and acquire images for a total of 10 minutes – 20 minutes.

2.2 Stress Imaging Study

- If a rest imaging study is performed, begin the stress imaging study 40 minutes or more after the first Ammonia N 13 injection to allow sufficient isotope decay.
- Administer a pharmacologic stress-inducing drug in accordance with its labeling.
- Aseptically withdraw Ammonia N 13 Injection from its container and administer 10 mCi – 20 mCi (0.368 GBq – 0.736 GBq) of Ammonia N 13 Injection as a bolus at 8 minutes after the administration of the pharmacologic stress-inducing drug.
- Start imaging 3 minutes after the Ammonia N 13 Injection and acquire images for a total of 10 minutes – 20 minutes.

2.3 Patient Preparation

To increase renal clearance of radioactivity and to minimize radiation dose to the bladder, ensure that the patient is well hydrated before the procedure and encourage voiding as soon as a study is completed and as often as possible thereafter for at least one hour.

2.4 Radiation Dosimetry

The converted radiation absorbed doses in rem/mCi are shown in Table 1. These estimates are calculated from the Task Group of Committee 2 of the International Commission on Radiation Protection.[1]

Table 1: N 13 Absorbed Radiation Dose Per Unit Activity (rem/mCi) for Adults and Pediatric Groups .

Organ	Adult	15-year old	10-year old	5-year old	1-year old
Adrenals	0.0085	0.0096	0.016	0.025	0.048
Bladder wall	0.030	0.037	0.056	0.089	0.17
Bone surfaces	0.0059	0.0070	0.011	0.019	0.037
Brain	0.016	0.016	0.017	0.019	0.027
Breast	0.0067	0.0067	0.010	0.017	0.033
Stomach wall	0.0063	0.0078	0.012	0.019	0.037
Small intestine	0.0067	0.0081	0.0013	0.021	0.041
*ULI	0.0067	0.0078	0.013	0.021	0.037
**LLI	0.0070	0.0078	0.013	0.020	0.037
Heart	0.0078	0.0096	0.015	0.023	0.041
Kidneys	0.017	0.021	0.031	0.048	0.089
Liver	0.015	0.018	0.029	0.044	0.085
Lungs	0.0093	0.011	0.018	0.029	0.056
Ovaries	0.0063	0.0085	0.014	0.021	0.041
Pancreas	0.0070	0.0085	0.014	0.021	0.041
Red marrow	0.0063	0.0078	0.012	0.020	0.037
Spleen	0.0093	0.011	0.019	0.030	0.056
Testes	0.0067	0.0070	0.011	0.018	0.035
Thyroid	0.0063	0.0081	0.013	0.021	0.041
Uterus	0.0070	0.0089	0.014	0.023	0.041
Other tissues	0.0059	0.0070	0.011	0.018	0.035

* Upper large intestine, **Lower large intestine

2.5 Drug Handling

- Inspect Ammonia N 13 Injection visually for particulate matter and discoloration before administration, whenever solution and container permit.
- Do not administer Ammonia N 13 Injection containing particulate matter or discoloration; dispose of these unacceptable or unused preparations in a safe manner, in compliance with applicable regulations.
- Wear waterproof gloves and effective shielding when handling Ammonia N 13 Injection.
- Use aseptic technique to maintain sterility during all operations involved in the manipulation and administration of Ammonia N 13 Injection. The contents of each vial are sterile and non-pyrogenic.
- Use appropriate safety measures, including shielding, consistent with proper patient management to avoid unnecessary radiation exposure to the patient, occupational workers, clinical personnel, and other persons.
- Radiopharmaceuticals should be used by or under the control of physicians who are qualified by specific training and experience in the safe use and handling of radionuclides, and whose experience and training have been approved by the appropriate governmental agency authorized to license the use of radionuclides.
- Before administration of Ammonia N 13 Injection, assay the dose in a properly calibrated dose calibrator.

3 DOSAGE FORMS AND STRENGTHS

Glass vial (30 mL) containing 0.138 GBq/mL – 1.387 GBq/mL (3.75 mCi/mL – 37.5 mCi/mL) of Ammonia N 13 Injection in aqueous 0.9% sodium chloride solution (approximately 7 mL volume) that is suitable for intravenous administration.

4 CONTRAINDICATIONS

None

5 WARNINGS AND PRECAUTIONS

5.1 Radiation Risks

Ammonia N 13 Injection may increase the risk of cancer. Use the smallest dose necessary for imaging and ensure safe handling to protect the patient and health care worker [*see Dosage and Administration (2.4)*].

6 ADVERSE REACTIONS

No adverse reactions have been reported for Ammonia N 13 Injection based on a review of the published literature, publicly available reference sources, and adverse drug reaction reporting systems. However, the completeness of these sources is not known.

7 DRUG INTERACTIONS

The possibility of interactions of Ammonia N 13 Injection with other drugs taken by patients undergoing PET imaging has not been studied.

8 USE IN SPECIFIC POPULATIONS

8.1 Pregnancy

Pregnancy Category C

Animal reproduction studies have not been conducted with Ammonia N 13 Injection. It is also not known whether Ammonia N 13 Injection can cause fetal harm when administered to a pregnant woman or can affect reproduction capacity. Ammonia N 13 Injection should be given to a pregnant woman only if clearly needed.

8.3 Nursing Mothers

It is not known whether this drug is excreted in human milk. Because many drugs are excreted in human milk and because of the potential for radiation exposure to nursing infants from Ammonia N 13 Injection, use alternative infant nutrition sources (e.g. stored breast milk or infant formula) for 2 hours (>10 halflives of radioactive decay for N 13 isotope) after administration of the drug or avoid use of the drug, taking into account the importance of the drug to the mother.

8.4 Pediatric Use

The safety and effectiveness of Ammonia N 13 Injection has been established in pediatric patients based on known metabolism of ammonia, radiation dosimetry in the pediatric population, and clinical studies in adults [see Dosage and Administration (2.4)].

11 DESCRIPTION

11.1 Chemical Characteristics

Ammonia N 13 Injection is a positron emitting radiopharmaceutical that is used for diagnostic purposes in conjunction with positron emission tomography (PET) imaging. The active ingredient, [^{13}N] ammonia, has the molecular formula of NH with a molecular weight of 16.02, and has the following chemical structure:

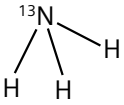

Ammonia N 13 Injection is provided as a ready to use sterile, pyrogen-free, clear and colorless solution. Each mL of the solution contains between 0.138 GBq to 1.387 GBq (3.75 mCi to 37.5 mCi) of [^{13}N] ammonia, at the end of synthesis (EOS) reference time, in 0.9% aqueous sodium chloride. The pH of the solution is between 4.5 to 7.5. The recommended dose of radioactivity (10 mCi – 20 mCi) is associated with a theoretical mass dose of 0.5 picomoles – 1.0 picomoles (8.47 picograms – 16.94 picograms) of ammonia.

11.2 Physical Characteristics

Nitrogen N13 decays by emitting positron to Carbon C13 (stable) and has a physical half-life of 9.96 minutes. The principal photons useful for imaging are the dual 511 keV gamma photons that are produced and emitted simultaneously in opposite direction when the positron interacts with an electron (Table 2).

Table 2. Principal Radiation Emission Data for Nitrogen 13

Radiation/Emission	% Per Disintegration	Energy
Positron (β+)	100	1190 keV (Max.)
Gamma (±)*	200	511 keV

*Produced by positron annihilation

The specific gamma ray constant (point source air kerma coefficient) for nitrogen N13 is 5.9 R/hr/mCi (1.39 x 10-6 Gy/hr/kBq) at 1 cm. The half-value layer (HVL) of lead (Pb) for 511 keV photons is 4 mm. Selected coefficients of attenuation are listed in Table 3 as a function of lead shield thickness. For example, the use of 39 mm thickness of lead will attenuate the external radiation by a factor of about 1000.

Table 3. Radiation Attenuation of 511 keV Photons by lead (Pb) shielding

Shield thickness (Pb) mm	Coefficient of attenuation
4	0.50
8	0.25
13	0.10
26	0.01
39	0.001
52	0.0001

Table 4 lists fractions remaining at selected time intervals from the calibration time. This information may be used to correct for physical decay of the radionuclide.

Table 4. Physical Decay Chart for Nitrogen N 13

Minutes	Fraction Remaining
0*	1.000
5	0.706
10	0.499
15	0.352
20	0.249
25	0.176
30	0.124

*calibration time

12 CLINICAL PHARMACOLOGY

12.1 Mechanism of Action

Ammonia N 13 Injection is a radiolabeled analog of ammonia that is distributed to all organs of the body after intravenous administration. It is extracted from the blood in the coronary capillaries into the myocardial cells where it is metabolized to glutamine N 13 and retained in the cells. The presence of ammonia N 13 and glutamine N 13 in the myocardium allows for PET imaging of the myocardium.

12.2 Pharmacodynamics

Following intravenous injection, ammonia N 13 enters the myocardium through the coronary arteries. The PET technique measures myocardial blood flow based on the assumption of a three-compartmental disposition of intravenous ammonia N 13 in the myocardium. In this model, the value of the rate constant, which represents the delivery of blood to myocardium, and the fraction of ammonia N 13 extracted into the myocardial cells, is a measure of myocardial blood flow. Optimal PET imaging of the myocardium is generally achieved between 10 minutes to 20 minutes after administration.

12.3 Pharmacokinetics

Following intravenous injection, Ammonia N 13 Injection is cleared from the blood with a biologic half-life of about 2.84 minutes (effective half-life of about 2.21 minutes). In the myocardium, its biologic half-life has been estimated to be less than 2 minutes (effective half-life less than 1.67 minutes).

The mass dose of Ammonia N 13 Injection is very small as compared to the normal range of ammonia in the blood (0.72 mg – 3.30 mg) in a healthy adult man [*see Description (11.1)*].

Plasma protein binding of ammonia N 13 or its N 13 metabolites has not been studied.

Ammonia N 13 undergoes a five-enzyme step metabolism in the liver to yield urea N 13 (the main circulating metabolite). It is also metabolized to glutamine N 13 (the main metabolite in tissues) by glutamine synthesis in the skeletal muscles, liver, brain, myocardium, and other organs. Other metabolites of ammonia N 13 include small amounts of N 13 amino acid anions (acidic amino acids) in the forms of glutamate N 13 or aspartate N 13.

Ammonia N 13 is eliminated from the body by urinary excretion mainly as urea N 13.

The pharmacokinetics of Ammonia N 13 Injection have not been studied in renally impaired, hepatically impaired, or pediatric patients.

13 NONCLINICAL TOXICOLOGY

13.1 Carcinogenesis, Mutagenesis, Impairment of Fertility

Long term animal studies have not been performed to evaluate the carcinogenic potential of Ammonia N 13 Injection. Genotoxicity assays and impairment of male and female fertility studies with Ammonia N 13 Injection have not been performed.

14 CLINICAL STUDIES

In a descriptive, prospective, blinded image interpretation study of adult patients with known or suspected coronary artery disease[2], myocardial perfusion deficits in stress and rest PET images obtained with Ammonia N 13 (N=111) or Rubidium 82 (N=82) were compared to changes in stenosis flow reserve (SFR) as determined by coronary angiography. The principal outcome of the study was the evaluation of PET defect severity relative to SFR.

PET perfusion defects at rest and stress for seven cardiac regions(anterior, apical, anteroseptal, posteroseptal, anterolateral, posterolateral, and inferior walls) were graded on a 0 to 5 scale defined as normal (0), possible (1), probable (2), mild (3), moderate (4), and severe (5) defects. Coronary angiograms were used to measure absolute and relative stenosis dimensions and to calculate stenosis flow reserve defined as the maximum value of flow at maximum coronary vasodilatation relative to rest flow under standardized hemodynamic conditions. SFR scores ranged from 0 (total occlusion) to 5 (normal).

With increasing impairment of flow reserve, the subjective PET defect severity increased. A PET defect score of 2 or higher was positively correlated with flow reserve impairment (SFR<3).

15 REFERENCES

1. Annals of the ICRP. Publication 53. Radiation dose to patients from radiopharmaceuticals. New York: Pergamon Press, 1988.
2. Demer, L.L.K.L.Gould, R.A.Goldstein, R.L.Kirkeeide, N.A.Mullani, R.W. Smalling, A.Nishikawa, and M.E.Merhige. Assessment of coronary artery disease severity by PET: Comparison with quantitative arteriography in 193 patients. Circulation 1989; 79: 825-35..

16 HOW SUPPLIED/STORAGE AND DRUG HANDLING

Ammonia N 13 Injection is packaged in 30 mL multiple dose glass vial containing between 1.11 GBq to 11.1 GBq (30 mCi to 300 mCi) of [N] ammonia, at the end of synthesis (EOS) reference time, in 0.9% sodium chloride injection solution in approximately 7 mL volume. The recommended dose of radioactivity (10 mCi – 20 mCi) is associated with a theoretical mass dose of 0.5 picomoles – 1.0 picomoles (8.47 picograms – 16.94 picograms) of Ammonia.

Storage

Store at 25°C (77°F); excursions permitted to 15°C – 30°C (59°F – 86°F). Use the solution within 30 minutes of the End of Synthesis (EOS) calibration.

17 PATIENT COUNSELING INFORMATION

17.1 Pre-study Hydration

Instruct patients to drink plenty of water or other fluids (as tolerated) in the 4 hours before their PET study.

17.2 Post-study Voiding

Instruct patients to void after completion of each image acquisition session and as often as possible for one hour after the PET scan ends.

17.3 Post-study Breastfeeding Avoidance

Instruct nursing patients to substitute stored breast milk or infant formula for breast milk for 2 hours after administration of Ammonia N 13 Injection.

Manufactured and distributed by: PETNET Solutions Inc.
810 Innovation Drive
Knoxville, TN 37932

Revised: 1/2016

PETNET Solutions

On account of certain regional limitations of sales rights and service availability, we cannot guarantee that all products included in this brochure are available through the Siemens sales organization worldwide. Availability and packaging may vary by country and is subject to change without prior notice. Some/all of the features and products described herein may not be available in the United States.

The information in this document contains general technical descriptions of specifications and options as well as standard and optional features which do not always have to be present in individual cases.

Siemens reserves the right to modify the design, packaging, specifications and options described herein without prior notice.

Please contact your local Siemens sales representative for the most current information.

Note: Any technical data contained in this document may vary within defined tolerances. Original images always lose a certain amount of detail when reproduced.

Siemens Healthcare Headquarters
Siemens Healthcare GmbH
Henkestr. 127
91052 Erlangen
Germany
Phone: +49 9131 84-0
siemens.com/healthcare

Global Business Line
Siemens Medical Solutions USA, Inc.
Molecular Imaging
2501 North Barrington Road
Hoffman Estates, IL 60192
USA
Phone: +1 847 304-7700
siemens.com/mi

Order No. A91MI-10437-1M-7600 | Printed in USA | MI-2954.RM.CP.SNM.13M

siemens.com/imaginglife